One Dimensional 4-Component Alkali Fermions

Von der Fakultät für Mathematik und Physik
der Gottfried Wilhelm Leibniz Universität Hannover

zur Erlangung des Grades

Doktor der Naturwissenschaften
Dr. rer. nat.

genehmigte Dissertation

von

B.Sc. Juan Diego Jaramillo Salazar

geboren am 28. März 1983 in Tuluá, Colombia

2014

Schlüsselwörter: Ultrakalte Atome, Alkalimetalle, Starke Korrelationen
Keywords: Ultracold Atoms, Alkali Metals, Strong Correlations

Referent: Jun.-Prof. Dr. Temo Vekua
Korreferent: Prof. Dr. Luis Santos

Tag der Promotion: 16. April 2014

"In learning a language, when from mere words we reach the laws of words, we have gained a great deal. But if we stop at that point and concern ourselves only with the marvels of the formation of a language, seeking the hidden reason of all its apparent caprices, we do not reach that end, for grammar is not literature... When we come to literature, we find that, though it conforms to the rules of grammar, it is yet a thing of joy; it is freedom itself. The beauty of a poem is bound by strict laws, yet it transcends them. The laws are its wings. They do not keep it weighed down. They carry it to freedom. Its form is in law, but its spirit is in beauty. Law is the first step toward freedom, and beauty is the complete liberation which stands on the pedestal of law. Beauty harmonizes in itself the limit and the beyond –the law and the liberty."

– Rabindranath Tagore, *Sadhana*.

GOTTFRIED WILHELM LEIBNIZ UNIVERSITÄT HANNOVER

Abstract

Fakultät für Mathematik und Physik
Institut für Theoretische Physik

Doktor der Naturwissenschaft

One Dimensional 4-Component Alkali Fermions

by B.Sc. Juan Diego Jaramillo Salazar

In this Thesis we examine the ground state of one dimensional 4-component alkali atoms. Optical lattices provides an environment to control with high precision many of the parameters ruling the stability and dynamics of ultracold gases. In particular, it allows the dimensional reduction of effective space and control of the scattering length between atoms (Chapter 1). The interest in low dimensional quantum systems derives from the highly collective nature of its interacting ground states. Powerful analytical tools have been developed to describe the universal features of their phase diagram. In 1D, one of these techniques is bosonization, where low energy interacting fermionic excitations are mapped into free bosons (Chapter 2). In this Thesis it is systematically used to study interacting 4-component spinors. Starting from the highly symmetric spin-3/2 Hamiltonian, it is shown how attractive interactions leads to pairing and quartetting instabilities controllable by an external magnetic field (Chapter 3). Finally it is shown (Chapter 4) that in the lesser symmetric case of a 4-component projection of alkali metal ^{40}K new phases arise via a Gaussian phase transition in the strong coupling regime: a Néel magnetic phase and in the presence of an external magnetic field a Haldane insulator. Relevant for experiments is the observation that both of these phases are located within the scale of scattering length of present experiments [1], that the strong coupling regime can be reached without the need of selective control of interactions and that the Haldane insulator in ^{40}K lies near a band insulator, a naturally stable phase. Chapter 5 presents a different topic, a collaboration in [2] studying the effect of unidirectional spin-orbit coupling (USOC) of fermions in a ladderlike optical lattice at half filling. In particular we show the strong rung-coupling limit where Dzyaloshinskii-Moriya term associated to the USOC gives rise to a Néel phase located between a rung singlet (RS) order and a ferromagnetic phase.

GOTTFRIED WILHELM LEIBNIZ UNIVERSITÄT HANNOVER

Zusammenfassung

Fakultät für Mathematik und Physik

Institut für Theoretische Physik

Doktor der Naturwissenschaft

Eindimensionaler 4-komponentiger Alkali Fermionen

by B.Sc. Juan Diego Jaramillo Salazar

Diese Arbeit widmet sich der Untersuchung des Grundzustandes eindimensionaler 4-komponentiger Alkali Atome. Optische Gitter stellen eine Umgebung zur Verfügung in der sich viele der die Stabilität und Dynamik ultrakalter Gase beeinflussenden Parameter mit hoher Präzision kontrollieren lassen. Insbesondere ermöglichen sie die effektive räumliche Dimension der Gase zu einzuschränken und die Streulängen von Atomen einzustellen (Kapitel 1). Das Interesse an eindimensionalen Systemen rührt von der hoch-kollektiven Natur ihrer Grundzustände her. Mächtige Analysewerkzeuge wurden entwickelt, um die universellen Eigenschaften ihrer Phasen-Diagramme zu beschreiben. In einer räumlichen Dimension ist eine dieser Techniken die sogenannte Bosonisierung, wobei die Niedrigenergie-Anregungen der wechselwirkenden Fermionen auf nicht-wechselwirkende freie Bosonen abgebildet werden (Kapitel 2). In dieser Arbeit wird diese Technik systematisch genutzt um wechselwirkende 4-komponentige Spinorgase zu studieren. Ausgehend von einem hoch-symmetrischen Spin 3/2 Hamiltonian, wird beschrieben, wie attraktive Wechselwirkungen zu Paar- und Quartett-Instabilitäten führen, welche durch eine äusseres Magnetfeld kontrollierbar sind (Kapitel 3). Schliesslich wird gezeigt (Kapitel 4) dass für den weniger symmetrischen Fall von Alkali-Atomen im stark wechselwirkenden Regime neue Phasen und ein gaussschen Phasenübergang beobachtet werden können: Eine Néel-magnetische Phase und in Gegenwart eines externen Magnetfeldes ein Haldane Isolator. Hierbei ist experimentell relevant, dass beide Phasen für die Gröenordnung der Streulänge aktueller Experimente realisiert werden können, das stark wechselwirkende Regime ohne die Notwendigkeit einer expliziten Kontrolle der Wechselwirkungen erreicht werden kann und dass sich der Haldane Isolator für ^{40}K in der Nähe eines Band-Isolators befindet, der auf natürliche Weise eine sehr stabile Phase ist. In Kapitel 5 wird ein anderes Thema präsentiert, eine Zusammenarbeit [2], in der die Einfluss einer unidirektionalen Spin-Orbit-Wechselwirkung (USOC) von Fermionen ein Leiter-artigen optischen Gittern bei Halb-Füllung untersucht wird. Insbesondere zeigen wir für den stark-wechselwirkenden Limes, wie der zur USOC gehörende Dzyaloshinskii-Moriya Term zur Entstehung einer Néel-Phase zwischen einer Rung-Singlett- und einer ferromagnetischen Phase führt.

Contents

A mis padres.

Introduction

"The interest of research workers has frequently been focused on the phenomenon of regularly shaped crystals suddenly forming from a liquid"

– Werner Heisenberg, *Nobel lecture 1933.*

Overview

After achieving Bose Einstein condensation (BEC) [3–5] and taking fermionic gases into quantum degeneracy [6, 7], research in ultracold atoms points towards strongly correlated phenomena. The collective and strongly interacting nature of the latter offer a natural protection against temperature fluctuations and it may underlay some of the high-temperature quantum phenomena such as cuprate and iron based superconductors. Realization of high-Tc superconductivity with atoms in optical lattices is difficult because the typical dilute conditions of ultracold atoms lead to very small critical temperatures that can only be compensated by large scattering lengths. Instead, the focus is in proofs of principle for proposed mechanisms, such as d-wave pairing [8]. Moreover, as a simulation environment it is expected to provide new insights into physics that remains challenging even for numerical calculations, such as the sign problem in high dimensions [9]. One of the first signatures of strongly correlated behavior in ultracold atoms is the Mott insulator, a mechanism initially proposed to explain the poor conduction of some transition-metal oxides with partially filled bands, a counterintuitive phenomena from the Fermi-Landau theory of metals [10]. The Mott insulator may undergo a quantum phase transition ($T = 0$) to a superfluid phase driven by the competition between kinetic energy and particle-particle interactions. Superfluids generated by strongly interacting fermions in one dimension are described by the Tomonaga-Luttinger liquid, an effective fluid description of many body fermions beyond the Fermi-Landau liquid paradigm [11]. Superfluid to Mott transitions of ultracold atoms in optical lattices have been studied [12, 13] and realized for bosons and fermions [14, 15]. Another interesting phenomena associated to Luttinger liquids is charge fractionalization and the possibility of spin-charge

separation. Their realization in ultracold atoms remains a challenge [16–18], evidence in quantum wires have already been reported [19–22].

The interest in low dimensional physics is two-fold as it offers physics beyond the Fermi liquid model and allows the use of powerful analytical tools to understand it. The high controllability of cold atoms in optical lattices is specially suitable to study quantum phase transitions and non-adiabatic evolution, and allows the reduction of spatial dimensions. Of particular interest are hyperfine-spin systems where some degree of control on their scattering lengths can be achieved. This is promising for proofs of principle in spintronics [23] and offers an opportunity to realize many of the phases predicted for high spin systems [24–26]. An example is the $SU(N)$-Hubbard model, whose low energy properties at $1/N$ filling can be mapped into the $SU(N)$-Heisenberg model. The latter is analytically tractable in the large-N limit. Unlike condensed matter systems where usual carriers are electrons (spin-1/2), the hyperfine levels of ultracold atoms open the possibility of higher spin models, some examples being spin-2 in ^{87}Rb and spin-3 in ^{52}Cr [27–30]. For the case of fermionic gases with high spin and attractive interactions theory predicts clustering phases that resemble barionic phases in quantum chromodynamics (QCD) [31, 32]. The experimental realisation remains a challenge due to many body loses and chemical instabilities. Creating quantum magnetism based on effective exchange interactions, despite the difficulty of accessing the perturbative t^2/U regime –intrinsically small– is becoming feasible for bosons and fermions [33, 34]. A promising alternative are polar molecules where dipole-exchange interaction is much greater than in cold atoms [35–37]. They also exhibit unwanted chemical instabilities, an obstacle for quantum degeneracy but promising for chemistry. The advantages of high spin are not reduced to the large-N limit nor $SU(N)$ symmetry, already atoms with hyperfine spin $F = 1$ and with $F = 3/2$ exhibits new physics associated to spin-changing collisions. The latter exhibits BCS superfluidity, quartetting phases[1], non-abelian vortices [39, 40] and, when symmetry is slightly broken, Néel and Haldane insulator phases [41]. Characterisation of ground states can be addressed analytically from techniques such as density matrix renormalization group (DMRG) or with low energy analysis such as bosonization. Observation of 4-component coherent spin dynamics in ultracold ^{40}K alkali-metal [1] brings new interest to this system; the quadratic Zeeman coupling (QZC) can be used to control the scattering length of spin-changing interactions.

In this thesis we explore the ground states of the one dimensional ^{40}K at half filling, in the strong coupling regime. In particular, we provide a phase diagram of QZC and average interaction; the latter controllable by lattice depth. Notable is the identification

[1]The system retains high symmetry $SO(5)$ even after $SU(4)$ symmetry is broken; this allows bypassing the numerical sign-problem [38] and partially supports mean-field approaches.

of the Haldane insulator, a phase with non local order parameter. The result is specially relevant for experimentalists as it is found slightly below a Band insulator, a classic phase easy to stabilise.

The dawn of quantum statistics

The study of thermodynamic equilibrium has been one of the most fruitful topics in physics. The Maxwell-Boltzmann distribution encompasses the set of empirical laws that led to the combustion engine, as it relates the microscopic and macroscopic properties of gases at combustion temperatures. Another gas, this time of photons, was behind a second revolution. In 1900 Max Planck for the first time reported that light captured indiscriminately by an effective black body emitted energy by discrete amounts. His empirical law of radiation seemed difficult to fit into the frame of Maxwell-Boltzmann theory. By 1924 Satyendra Nath Bose conjectured that a new distribution for light was necessary to fit the data; its fundamental assumption was that an unbound population of light (photons) could share the same microscopic state of energy. Einstein quickly understood the relevance of the result and further conjectured the possibility of 'matter', massive bodies such as atoms, to behave according to Bose distribution at sufficiently low temperatures. It took almost 70 years to prove experimentally that indeed some atoms could undergo a transition into what is now known as a Bose-Einstein condensate (BEC) [3–5]. Again back in 1925, Enrico Fermi gave an alternative statistics based on the quantum degeneracy of electrons in atomic orbits. Based on different algebraic properties –as it became clear by Heisenberg's formalism– the two theories described two seemingly different particles: bosons and fermions. In 1928 Paul Dirac formulates a relativistic equation for the free electron introducing a new quantised degree of freedom, the spin, an internal magnetic moment of pure quantum nature whose units are half-integers and classifies bosons (integer spin) and fermions (half-integer spin) according to parity.

The reason why it took so long to achieve experimentally the quantum degeneracy of both types of gases is because the maximal temperatures for which quantum interference is observed was well below the technological capabilities of the first half of the twentieth century. Present experiments use a combination of strategies to cool the gas at different stages. Laser cooling plays a key role, this is a set of techniques that use atom-photon coupling to lower the average kinetic energy of the gas. Two of its most representative techniques are the Doppler and Sisyphus cooling. Doppler cooling is one of the most versatile techniques, it reaches temperatures of the order of hundreds of microkelvin; the lower temperature that can reach is associated to the point where the cooling rate

is equal or lower than the heating rate associated to the induced excitations. The last step is to use evaporative cooling, a process by which atoms with kinetic energy above average are let to scape from the trap by introducing a trapping potential slightly above the thermal energy. As this happens in a slowly controlled way it keeps the gas in its thermal ground state at all times and the average kinetic energy slowly shifts to smaller values. In principle, this would lead to zero temperature but at low enough densities quantum degeneracy is compromised. This technique relies on interaction to redistribute the kinetic energy; for fermions interaction is limited by Pauli's exclusion principle, in this case evaporative cooling can be enhanced by inter-specie interactions, usually a mixture with some chemically neutral bosonic gas in a procedure called sympathetic cooling.

Chapter 1

Ultracold atoms

The modeling of ultracold gases undergo many approximations. The specific sequence depends on the physical regime. Parameters such as temperature, number of particles, range of interactions, etc. have to be estimated starting from logarithmic precision. Are we to include higher order perturbation processes? This depends not only on the scale of the perturbation parameter, but also on the kind of physics we want to address. As we shall see in the next chapter there are processes that go beyond finite order corrections.

One of the first estimations is associated to the onset of quantum behaviour. Pure quantum objects such as a single particle and electromagnetic radiation have well defined wavelength through which quantum probability propagates along space-time. In a thermal gas this wavelength is only well defined within a finite range, inversely proportional to the temperature of the gas[1], this is the thermal de Broglie wavelength. When the average inter-particle distance is of the order of the de Broglie wavelength the gas makes use of quantum interference to minimise its energy; in the case of bosons, many finite wavefunctions "add up" to behave as only one with a de Broglie wavelength well defined along the whole confining potential. In the case of fermions they form the so called Fermi sea, which in the isotropic limit looks like a sphere of finite radius and homogenous probability density in the momentum space. If the inter-particle distance is not too small as for interactions to become important, it is sufficient to describe the system in terms of a quantum distribution. The distribution can be bosonic or fermionic depending on the constituency of the gas (atoms, electrons, light, etc.).

The relation between the energy of a particle and its associated de Broglie wavelength is $E = \frac{p^2}{2m} = \frac{1}{2m}\left(\frac{h}{\lambda}\right)^2$ for a massive particle, and $E = \frac{hc}{\lambda}$ for light. The estimate of the de Broglie wavelength via thermal energy is $\lambda^2 = \frac{h^2}{2\pi m k_B T}$ for a massive particle, and

[1] Temperature is a partial trace on non-tractable interactions

$\lambda = \frac{ch}{2\pi^{1/3}kT}$ for light. Hence, the onset of quantum behaviour estimated by macroscopic parameters is $\left(\frac{V}{N}\right)^{1/3} \leq \lambda$. Therefore the strategy to achieve quantum degeneracy is either to increase the density or to lower the temperature. Increasing the density brings about body losses and that's why lowering the temperature by laser cooling is so important.

Quantum magnetism demands even lower temperatures as it relies on perturbative corrections in the strong coupling regime (Sect.1.4). In highly symmetric Hamiltonians the two terms arise simultaneously in the form of Heisenberg interactions at a second order perturbation of hopping with respect to onsite interaction. When the $SU(N)$ symmetry of the Heisenberg interaction is not present the Ising interaction remains at second order while exchange process requires higher order perturbation, this is observed in the strong coupling regime of the 4-components of ^{40}K (Chapter 4). Quantum magnetism remains a challenge in ultracold atoms; at such low energies lowering of thermal fluctuations focus in reducing entropy [42]. A cooling strategy is to transfer entropy between different sectors, e.g. spatially inhomogeneous phases or different physical channels such as charge and spin channels [43–45]. For quantum magnetism this means lowering entropy in some of the magnetic channels[46]. In systems such as spin-3/2 fermions one can use a channel that couples into the QZC to extract entropy from magnetic channels. This is done by inducing a band insulating phase that results in zero entropy in a given channel. Then, by adiabatically lowering the QZC, entropy from other channels is transferred to the low entropy channel.

1.1 Local density approximation

In a realistic setting the ultracold gases are subjected to an overall confining potential. At the center the gas is closer to the homogeneous spatial density distribution expected for a gas without confinement. If the harmonic trap is large enough, most physical properties of the gas can be predicted using the local density approximation: if the inter-particle distance is above the range of interactions, but below the de Broglie wavelength, the system is expected to obey a quantum distribution function $f(\mathbf{k},\ \mu(x))$, where the spatial dependence of the chemical potential is the density inhomogeneity induced by the trapping potential. For strong (repulsive) interactions, at least in the case of condensed bosons where translational symmetry is not broken, the system may be described by a special case of the Gross-Pitaevskii Equation (GPE) [47]. We recall that there is no GPE for fermions as its derivation relies heavily in the assumption that a few quantum states are occupied by a macroscopic number of particles, something forbidden in fermions by the Pauli exclusion principle.

In general, the approximation takes place when the scale of relevant variations of the kinetic energy differs considerably with that of the potential energy (external potential and particle-particle interactions). Under such conditions we can solve the system separately: in one Schrödinger equation are the terms expected to renormalize the kinetic energy and in the other those expected to renormalize the potential. In a box geometry, the approximation is expected to fail close to the boundaries.

1.2 Scattering length

In general, the scattering between particles depends on the inner structure of particles[2], their velocity, angles of incidence, etc. If the velocity is small compared to the strength of interaction the particles will not penetrate into the inner potential, the one encoding the inner structure of the particle. In the low energy limit the scattering shows the greatest symmetry, that of a spherical potential[3]. In the context of cold atoms we say that we restrict our model to the s-orbital. Although the latter is a universal property –valid for any potential–, ultracold alkali atoms are specially suited for this description, it will remain valid for greater values of the kinetic energy. The reason is because their outermost electrons belong to the s-orbital, assuring that the greatest contribution to the interaction potential posses already orbital symmetry. In particular, alkali earth atoms will retain higher symmetry because besides their orbital symmetry they show magnetic symmetry due to the double occupation of its outer shell. The latter condition is weakened in alkali metals where the outer shell is not magnetically symmetric, there is single occupation of the outer shell and is magnetically compensated by interacting with the nuclear spin –hyperfine coupling–. But alkali metals still retain high symmetry as is the case for example of the $SO(5)$ symmetry in exact spin-3/2 systems. The orbital stability is associated to the transition between s and p orbitals. More difficult is to guarantee magnetic stability, which requires avoiding transitions between their two characteristic hyperfine multiplets [49]; in this respect, optical dipole traps plays a key role, complementing the cooling and storing strategies based on magnetic dipole moment in an inhomogeneous field [50].

[2]For example, the spin state for electrons or the electronic configuration for atoms.

[3]We refer to a hard-sphere with delta Dirac potential because the rate between potential and kinetic energy near the scattering event goes to infinity in the low velocity limit. See for example [48].

Measurement

To estimate experimentally the scattering length one usually measures the scattering cross section σ. This is proportional to the square of the scattering amplitude[4], which can be derived from the solution of the Schrödinger equation with the boundary conditions associated to a free particle in the presence of a contact potential $U(r) = a_s\delta(r - r_0)$. As the momentum of free particles is carried by the phase of its plane wave, the effect of scattering is a phase shift of π between the incident and refracted plane waves from the location of the scattering: $\psi(r) \propto (e^{ik(r-r_0)} + e^{-ik(r-r_0)+i\pi})$, where in the low-$k$ limit $r_0 \approx a_s$. This is how we obtain, for the s-wave elastic scattering, the relation $\sigma \approx 4\pi a_s^2$. Some important remarks regarding the use of this type of pseudo-potentials in the context of ultracold atomic gases can be found in [51].

Control

The advantage of optical dipole traps go beyond the release of internal magnetic degrees of freedom, it allows the creation of multi-well potentials that resemble crystal order[5]. Its quintessential phenomena is the Superfluid to Mott Insulator transition, first reported in [14]. The unequal renormalization between the tunneling and the collisional strength by changes in lattice depth –via Wannier states– is a suitable mechanism to induce the phase transition [13]

$$t_{\langle i,j\rangle} = \int d^3x\; w^*(\mathbf{x}-\mathbf{x}_i)\left[-\frac{\hbar^2}{2m}\nabla^2 + V(\mathbf{x})\right] w(\mathbf{x}-\mathbf{x}_j), \tag{1.1a}$$

$$U = \frac{4\pi a_s\hbar^2}{m}\int d^3x\; |w(\mathbf{x})|^4. \tag{1.1b}$$

The amplitude of the Wannier states grows with the intensity of the optical lattice (see App.C.1). The change in amplitude has no effect in $\int dx\; |w(\mathbf{x})|^2$ because is fixed by normalisation but becomes relevant for $\int dx\; |w(\mathbf{x})|^4$. The system resembles a Hubbard like Hamiltonian which is known to have a quantum phase transition for critical values of U/t.

An alternative approach is to directly control the scattering length in a scheme called Feshbach resonance. This approach relies on the perturbative correction of the scattering length by either magnetic or optical transitions; not all the incident states remain in the

[4] In the simplest ansatz of scattering it theory corresponds to the amplitude f, where $\psi(r) = e^{ikz} + f(\theta)e^{ikr}/r$. Wherein the s-orbital approximation $f(\theta) = f$. In the Bohr Approximation f reveals as the Fourier transform of the potential in real space, in the limit $k \to 0$.

[5] It actually allows more exotic potentials to the point that artificial gauge potentials has become an important topic within the field of cold (neutral) atoms [52].

same magnetic channel specially as the transition energy vanishes. Far from resonance we have a perturbative correction associated to the natural transition energy E_0 of the system [53]

$$\tilde{a} = a + \frac{a\Gamma_0}{-E_0 + i(\gamma/2)} \tag{1.2}$$

where a is the scattering length (dropped s-index), γ is the decay rate of excitation and Γ_0 is the resonance strength. Renormalization focuses on induced resonance because the control of Γ_0 is highly limited. Nearly resonant magnetic (B) and optical (I, ν) external fields leads to

$$\begin{aligned} \tilde{a}(B) &= a - \frac{a\Gamma_0}{(\mu - \mu_c)(B - B_c)}, \\ \tilde{a}(\nu, I) &= a - \frac{a\Gamma(I)}{h[\nu - \nu_c - \delta\nu(I) + i(\gamma/2)]}, \end{aligned} \tag{1.3}$$

where $E_0 \equiv (\mu - \mu_c)B_c = h\nu_c$ is the contextual interpretation of the transition energy between unbound and bound states. The control over lattice depth has the advantage of

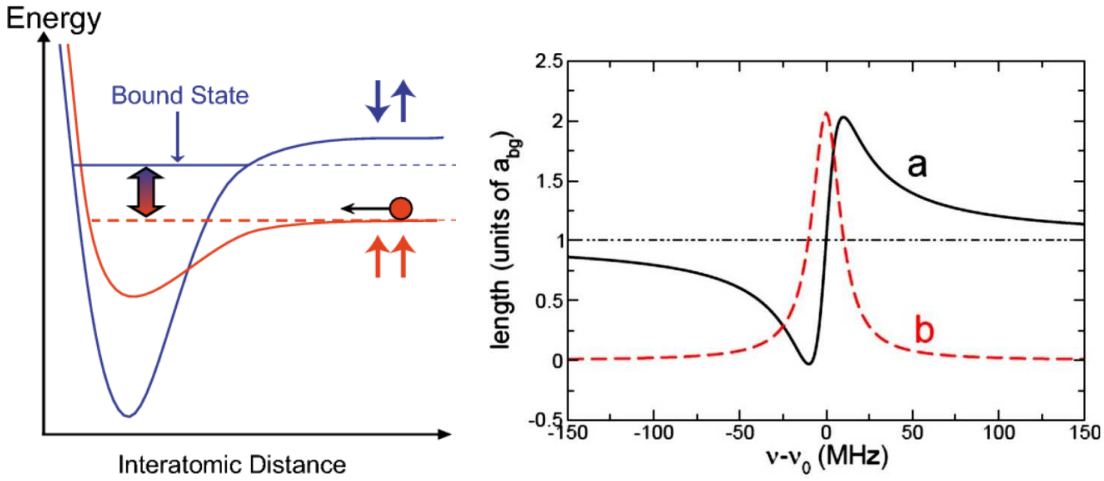

FIGURE 1.1: Transitions between bound and unbound states induced by Feshbach resonance controls effective scattering length [53, 54].

being easier to implement and allowing a large range of U/t values. One of its drawbacks is the difficulty to control each of the spin channels separately[6]. The advantage of Feshbach resonance is that it offers a more clear —not exactly easy– path towards differentiated control of the scattering length [55]. Some of its drawbacks are that the width of the resonance is usually narrow, offering limited access to intermediate regimes of interaction. This technique is broadly used in bosonic gases: for quantum phase

[6]The renormalization is different in every channel as much as the Wannier functions depend on the hyperfine states. A differentiated control, in this scheme, seems challenging. Knowing how the differentiated renormalization changes with the intensity may allow us to understand transitions between massive phases driven by the optical lattice intensity.

transitions, evaporative cooling and approaching the unitarity limit ($a \to \infty$), etc. This technique is also important for fermions, where the high energy of the Fermi surface ($k_F \sim (\#_{atoms})^{1/d}$) makes the rate U/t very small. It has been used to drive the first MI to SF transition in fermionic gases [15] and to explore the BEC-BCS crossover [56]. Control over lattice depth, together with QZC control of spin changing collisions [57], has been used recently to study coherent spin dynamics [1].

1.3 Good quantum numbers

For an interacting gas the first perturbative correction to the hyperfine hamiltonian is carried by the scattering of two atoms. The conservation of angular momentum suggests *total* hyperfine spin is a good quantum number to describe the interaction. This picture is modified by an increasing magnetic field, which induces a crossover in the leading multiplets from hyperfine to electronic spin. This is a consequence of the quadratic Zeeman coupling with the hyperfine hamiltonian and the large mismatch between the nuclear and electronic angular momenta: $\mu/\mu_e \sim \mu_N/\mu_B = m_e/m_p \ll 1$.

Interaction

The low energy scattering operator of two particles, integrating out spatial degrees of freedom, is defined as

$$\mathbf{I} = \sum_{\mathbf{m}',\mathbf{m}} a_{\mathbf{m}',\mathbf{m}} |\mathbf{m}'\rangle\langle\mathbf{m}|, \qquad \mathbf{m} = (m_1, m_2), \tag{1.4}$$

where $m_{1,2}$ is the corresponding single particle hyperfine spin projection, assume to be associated to the same hyperfine spin number in the absence of a strong magnetic field. Conservation of total angular momenta guarantees a reformulation via Clebsch-Jordan coefficients

$$\mathbf{I} = \sum_{F} a_F |F, M\rangle\langle F, M|. \tag{1.5}$$

Not all total spin channels are relevant: The probability of scattering is non-vanishing for symmetric wavefunctions in space, hence only (anti)symmetric wavefunctions in spin are relevant for bosons (fermions) *i.e.* $S_T + 2S$ even (odd). The usual procedure is to estimate experimentally the coefficients $a_{\mathbf{m}',\mathbf{m}}$'s and then find the a_F's by solving the implicit linear equation [53]. The s-wave scattering cross section retains its general low energy form but subdivided into magnetic channels. The scattering length at every channel can be modified by selective induced resonance as shown in Eq.(1.3).

Coupling to an external magnetic field

The relevant Hamiltonian describing the effect of an external magnetic field $\vec{B} = B\hat{z}$ on s-orbital hyperfine levels is[7]

$$\mathcal{H} = A\ \vec{I}.\vec{J} - \mu_e\ \vec{S}.\vec{B} \tag{1.6}$$

In general these two terms don't commute, hence there is no common diagonal basis. In the limits $B/A \to 0, \infty$ the system has well defined hyperfine and electronic spin, respectively. The crossover is driven by quadratic and higher order corrections. Lets consider the first limit: A good basis is given by $|f, m_f\rangle$, where m_f is the spin projection over the quantization axis[8]. The spectrum is characterized by two multiplets $F = (I \pm 1/2)$. In particular, the two terms of the Hamiltonian in Eq.(1.6) commute in the subspace $\mathcal{E}(m_F = \pm(I + 1/2))$, associated to the upper multiplet[9]. These levels are protected from higher order corrections; one of them will meet the levels of the lower multiplet for sufficiently high magnetic fields (Paschen-Back regime). As for the remaining levels what the QZC does is to amplify the splitting between the two hyperfine multiplets.

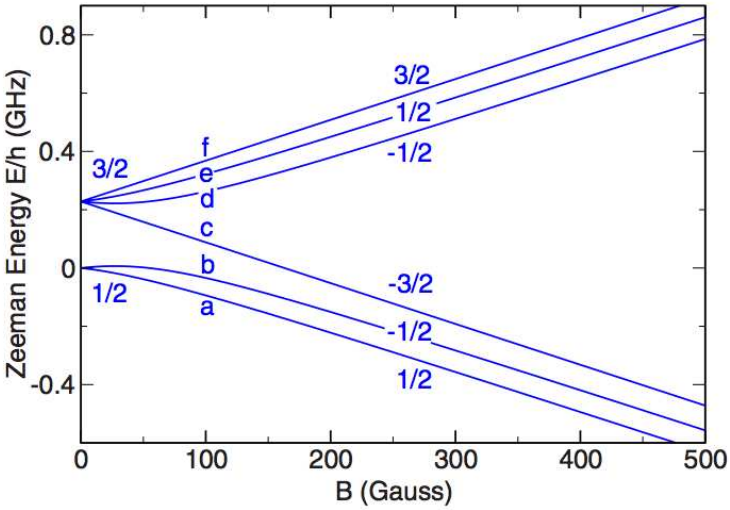

FIGURE 1.2: Atomic energy levels of the ^6Li atoms ($S = 1/2$, $I = 1$). In the Zeeman regime ($B \approx 0$) the two multiplets correspond to projections $f = 1/2, 3/2$. In the Paschen-Bach regime ($B \gtrsim 100$) the sublevels m_f recombine into new multiplets [53].

[7] Not to confuse the nuclear spin vector $\vec{I}$ withs the scattering operator $\mathbf{I}$ from Eq.(1.5).

[8] Not to confuse the hyperfine spin f with the total spin F of scattering from Eq.(1.5).

[9] These are the highest weight vectors of the representation, they are associated to full polarization. The linear Zeeman effect is invariant from orientation of the quantization axis ($\hat{z} \to -\hat{z}$), hence the splitting is restricted to a $\mathbb{Z}_2$ broken symmetry, i.e. $E \to E \pm \Delta E(B)$.

1.4 Effective exchange interaction

The Hubbard model is one of the most useful Hamiltonians to describe systems with interaction in optical lattices and condensed matter systems. It is simple enough and already provides non-trivial predictions such as the Mott insulator, where interaction instead of complete band filling is responsible for suppression of conductivity. The Hamiltonian has two limits for which perturbation theory can be applied. In the *strong coupling* limit ($U/t \to \infty$) a spin-$\frac{N-1}{2}$ at $1/N$-filling creates an effective Heisenberg (anti)ferromagnet for bosons (fermions); away of $1/N$-filling it leads the so-called t–J model[10]. Fermions allow the direct realization of antiferromagnetism (bosons allow this indirectly by suitable shaking of the lattice), when combined with the versatility of the optical lattice it opens the possibility of studying magnetic frustration and the effect of perturbations of their underlying geometry –such as deformations on the triangular lattice. In the *weak coupling* limit $U/t \to 0$ the Fermi-Landau theory in successfully predicts, in three dimensions, a renormalization of the free Hamiltonian. Weak coupling conditions are often found in three dimensions because of the high number of local configurations, dominated by nearly zero overall interaction. In two dimensions the number of local configurations decrease by an order of magnitude, collective excitations become more important. In one dimension, excitations due to interactions require non-perturbative methods (Ch.2).

For $U/t \to \infty$ the system is dominated by a Mott insulator but as the value of interaction decrease it predicts a quantum phase transition to a superfluid phase. Here is a brief introduction to the strong coupling mediated exchange (Kramers-Anderson). Consider its simplest realization: fermions with spin-1/2, the Hubbard Hamiltonian is given by

$$\begin{aligned} \mathcal{H}_0 &= -t \sum_{\langle \mathbf{r}_i, \mathbf{r}_j \rangle, \sigma=\uparrow,\downarrow} \left(c_\sigma^\dagger(\mathbf{r}_i) c_\sigma(\mathbf{r}_j) + h.c. \right), \\ \mathcal{H}_1 &= U \sum_{\langle \mathbf{r}_i \rangle} n_\uparrow(\mathbf{r}_i) n_\downarrow(\mathbf{r}_i), \end{aligned} \tag{1.7}$$

where $c_\sigma^\dagger$, c_σ are second quantization operators with local density $n_\sigma = c_\sigma^\dagger c_\sigma$. Since only spin and charge are considered relevant degrees of freedom, the exclusion principle discards the onsite interaction of fermions with same spin projection. In the strong coupling limit the zero order is provided by $\mathcal{H}_1$. Large attraction could lead to a BCS-BEC transition; here we focus on the large repulsion limit, where a magnetic ground

[10] The quantum magnetism that arise from this combination of tunnelling and onsite interaction is sometimes referred as superexchange. I prefer to call it effective exchange and refer to the latter as the renormalization of exchange interaction via intermediate exchange.

state is expected. The Jordan map $\vec{S} = \frac{\hbar}{2} c_\sigma^\dagger \vec{\tau} c_{\sigma'}$ reveals local $SU(2)$ symmetry[11]

$$\mathcal{H}_1 = -\frac{2U}{3} \sum_{\mathbf{r}_i} \left(\vec{S}(\mathbf{r}_i) \right)^2 + const \tag{1.8}$$

The brake of the *local* symmetry by $\mathcal{H}_0$ is not evident until we evaluate its effect in the second order of perturbation –at half-filling first order perturbation is unstable for large onsite repulsion–. A *global* $SU(2)$ symmetry survives the perturbation and is the signature of spin-charge separation.

Next is the derivation of the second order perturbative hopping, which can be described for general spin-$1/N$ at $1/N$-filling. Start from the Schrödinger equation of Hamiltonian $\mathcal{H}_0 + \mathcal{H}_1$ from Eq.(1.7).

$$(\mathcal{H}_0 + \mathcal{H}_1)\ |\psi\rangle = E\ |\psi\rangle. \tag{1.9}$$

The aim is to find an effective Hamiltonian for the projected space of one particle per site. If such projection operator is $\mathcal{P}$, then $\mathcal{H}_{eff}:\ \mathcal{H}_{eff}\mathcal{P}|\psi\rangle = \mathcal{P}|\psi\rangle$. To find it you can project Eq.(1.9) to the space of one particle per site and its complement

$$(\mathcal{H}_0 + \mathcal{H}_1)(\mathcal{P} + \mathcal{P}^\perp)|\psi\rangle = E\ |\psi\rangle. \tag{1.10}$$

Using properties of the projection operators in relation with the hamiltonian terms[12]

$$\mathcal{P}\mathcal{H}_0\mathcal{P}^\perp|\psi\rangle = E\ \mathcal{P}|\psi\rangle, \tag{1.11a}$$

$$\mathcal{P}^\perp(\mathcal{H}_0 + \mathcal{H}_1)\mathcal{P}^\perp + \mathcal{P}^\perp\mathcal{H}_0\mathcal{P}\ |\psi\rangle = E\ \mathcal{P}^\perp|\psi\rangle. \tag{1.11b}$$

Under the perturbative condition $U/t \to \infty$, notice that $\mathcal{P}^\perp(\mathcal{H}_0 + \mathcal{H}_1)\mathcal{P}^\perp \approx |U|$. From Eq.(1.11b) we get

$$\mathbf{1} \approx -\frac{\mathcal{P}^\perp\mathcal{H}_0\mathcal{P}}{|U|}. \tag{1.12}$$

Applying this relation in Eq.(1.11a)

$$\mathcal{P}\mathcal{H}_0\mathcal{P}^\perp \left(-\frac{\mathcal{P}^\perp\mathcal{H}_0\mathcal{P}}{|U|} \right) |\psi\rangle = E\ \mathcal{P}|\psi\rangle. \tag{1.13}$$

Again using properties of the projectors the effective Hamiltonian takes the simple form

$$\mathcal{H}_{eff} = -\mathcal{P}\frac{\mathcal{H}_0^2}{|U|}\mathcal{P} = -\frac{2t^2}{|U|} \sum_{\langle i,j \rangle} \left(\mathbf{1}_{i,j} \pm P_{i,j} \right). \tag{1.14}$$

[11] The components τ_i corresponding to he Pauli matrices. The Fierz identity for $SU(2)$ is used. For more details, see for example [58].

[12] Such as $\mathcal{P}\mathcal{H}_{0,1}\mathcal{P} = \mathcal{P}\mathcal{H}_1\mathcal{P}^\perp = \mathcal{P}^\perp\mathcal{H}_1\mathcal{P} = 0$.

Where + is for fermions and − for bosons. Notice that the first stable correction can be expressed in terms of the identity and the permutation $P_{i,j}$ of nearest neighbors. These operators naturally preserve $1/N$-filling. Moreover they suggest an intimate relation between high order perturbation theory and the braiding group, an insight that provides a way to generalize exchange[13]. A more physical insight is given by the spin-chain representation; the mapping from Eq.(1.14) can be realized as a composition of two maps: from a permutation model to a total spin model and from the latter to a spin-chain

$$\begin{aligned} P_{i,j} &= \sum_{S^T=0}^{2S} (-1)^{S^T+2S} \tilde{\mathcal{P}}_{i,j}(S^T), \\ \tilde{\mathcal{P}}_{i,j}(S^T) &= \alpha_{S^T} \prod_{S' \neq S^T} [\vec{S}(\mathbf{r}_i).\vec{S}(\mathbf{r}_j) - S'(S'+1)/2 + S(S+1)]. \end{aligned} \tag{1.15}$$

where $\tilde{\mathcal{P}}_{i,j}(S^T)$ is the projector into the subspace of total spin S^T and α_{S^T} is a normalization factor which depends on total spin. For the case of spin-1/2 ($S^T = 1, 0$) Eq.(1.14) becomes

$$\mathcal{H}_{eff} = \frac{2t^2}{|U|} \sum_{\langle \mathbf{r}_i, \mathbf{r}_j \rangle} \vec{S}(\mathbf{r}_i).\vec{S}(\mathbf{r}_j). \tag{1.16}$$

Notice that for spin-1/2 (fermions) the Hamiltonian favors singlet ordering. In spin-chains the strength of the latter interaction is represented by J; as we depart from half-filling first order hopping becomes relevant forming the so called t–J model.

[13] The t–J model, relevant away of half filling, would provide a 'blowing' to the 'stiff' model found at half filling; first order hopping playing the role of the (trivial) geometric structure. See for example [59, 60].

Chapter 2

The bosonization technique

"Faced with information overload, we have no alternative but pattern recognition."

– Marshall McLuhan and IBM technicians

The evolution of the concept of bosonization is an interesting example of how theories are developed. In 1933 Felix Bloch proposed the use of low vibrational modes in order... *die Bremsung rasch bewegter elektrischer Teilchen bei ihrem Durchgang durch Materie zu berechnen*[1] [61]. Where few-particle correlators are expected to dominate excitations the results coincide with those of the perturbative method. In other words, if interactions can be averaged such that physics –response or correlation functions– remains close to the full description. In low effective dimensions the number of neighboring particles –relevant for contact interaction– decrease to the extent that fundamental effects are often lost by the averaging –*mean field*– procedure. This is the case for fermions or hard-core bosons. For the direct perturbative method this is the worst case scenario; a macroscopic number of particles is expected to be correlated, demanding calculation of very high orders of the perturbative expansion. For collective excitations is ideal; ubiquitous collisions provide the necessary communication between particles to coordinate simple vibrational modes. But the connection between the harmonic like oscillators and the hard-core particles in Bloch's development was still missing. This is where Tomonaga comes on the scene [11]; he was able to foresee the relation between Bloch's intuitive approach and Jordan's development of Schwinger terms to provide a one dimensional bosonic description of fermionic current algebras modified by the presence of the Dirac sea [62, 63]. The context of the formalism was now identified and what followed would mainly compromise matters of refinement. It would be crowned by Daniel Mattis and Elliot Lieb in 1965 as a correction to the prior work of Luttinger in the subject [64].

[1] *...to study the slow down of fast moving electric particles as they go across [metallic] matter.*

Later work by particle physicist Coleman and Mandelstam [65, 66] would settled the interpretation of the one dimensional fermion as a soliton excitation of bosons.

It is also worth mentioning the contributions of F. D. M. Haldane to bosonization in condensed matter physics [67, 68]. He showed how versatile is this technique providing effective theories not only for fermions, but also for bosons and spin chain models. Moreover, his formulation of bosonization as vibrational modes of the Fermi surface provides conceptual clearance and a framework to address the limitations and possible extensions of the bosonization formalism [72].

Briefly, the distinction between statistical particles becomes blurred in one dimension because their algebraic properties are almost indistinguishable of interaction; there's no smooth exchange process in one dimension. A full account of this involves the bijective map between interactions and generalized statistics [60, 69–71].

2.1 The relativistic fermion

It is known from the Fermi liquid theory that mean-field interacting electrons can give rise to massless fermionic quasiparticles. Special relativity predicts a similar effect for free electrons approaching the velocity of light. The possibility of treating interactions beyond mean-field becomes clear in Dirac's formalism for relativistic fermions. In the context of collective excitations the velocity of light c is to be replaced by the "sound" velocity v, the Dirac sea is an extrapolation of the linear dispersion around the Fermi surface and is consistently introduced by a cut off procedure[2].

The action for the spinless Dirac fermion describes left and right moving particles

$$\Psi = \begin{pmatrix} \psi_L \\ \psi_R \end{pmatrix}, \quad \bar{\Psi} = \begin{pmatrix} \psi_R^\dagger, & \psi_L^\dagger \end{pmatrix}. \tag{2.1}$$

Together with massive terms ($\Delta = M_1 + iM_2$), the action is[3]

$$\mathcal{S}_F(\bar{\Psi}, \Psi) = \int dz d\bar{z}\ \bar{\Psi}(z, \bar{z}) \begin{pmatrix} \Delta & 2\partial \\ 2\bar{\partial} & \Delta^* \end{pmatrix} \Psi(z, \bar{z}), \tag{2.2}$$

[2] A similar cut off procedure underlies the validity of contact interaction as mentioned in Ch.1.

[3] The massless terms are generated by Pauli matrices σ_1 and σ_2 while massive terms by $\sigma_0 = id$ and σ_3. This is not an *a posteriori* observation: the spin is the necessary copy of the spinless action to guarantee invariance under relativistic change of coordinates.

where $(dz, d\bar{z}) = (d\tau + idx/v, d\tau - idx/v)$ and $(\partial, \bar{\partial})$ are the respective duals. Let the partition function be

$$\mathcal{Z} = \int D[\Psi, \bar{\Psi}]\ exp\left[-\mathcal{S}_F(\bar{\Psi}, \Psi)\right]. \tag{2.3}$$

In the limit $|\Delta| \to 0$, this is a Gaussian integral for fermions and is to be calculated with Grassmann variables[4]; the differential is to account for time-ordering. Let any correlation function be defined as

$$\langle \mathcal{F}[\bar{\Psi}, \Psi] \rangle = \int D[\bar{\Psi}\Psi]\ e^{-\mathcal{S}_F(\bar{\Psi}, \Psi)} \mathcal{F}[\bar{\Psi}, \Psi] \tag{2.4}$$

In the context of physics this is often interpreted as the average induced by quantum fluctuations to an observation, or the quantum correlation between two different excitations from a common ground state. Mathematically could be interpreted using suitable auxiliary fields in the action as the hessian components of the partition function. Consider the following Gaussian identity of independent Grassmann variables $\bar{\xi}$ and ξ $(j = 1, 2, ..., N)$ for any invertible complex matrix A

$$\int\int \prod_{j=1}^{N} d\bar{\xi}_j \xi_j\ exp\left[-\sum_{i,j}^{N} \bar{\xi}_i A_{i,j} \xi_j + \sum_{j}^{N} \left(\bar{\xi}_j \chi_j + \bar{\chi}_j \xi_j\right)\right] = Det(A) exp\left[\sum_{i,j} \bar{\chi}_i (A^{-1})_{i,j} \chi_j\right]. \tag{2.5}$$

The auxiliary terms χ_j and $\bar{\chi}_j$ allows to redefine the correlator $\langle \bar{\xi}_i \bar{\xi}_j \rangle$ as

$$\langle \bar{\xi}_i \xi_j \rangle = \frac{\partial^2 ln \mathcal{Z}}{\partial \chi_i \partial \chi_j} = (A^{-1})_{i,j}. \tag{2.6}$$

Knowing $A_{i,j}$, derivation of $(A^{-1})_{i,j}$ comes as resolution of the identity[5]

$$A_{i,j}\ (A^{-1})_{i,j} = \frac{1}{\pi} \begin{pmatrix} \partial\ (\bar{z} - \bar{w})^{-1} & 0 \\ 0 & \bar{\partial}\ (z - w)^{-1} \end{pmatrix} \tag{2.7}$$

In our case $A_{i,j}$ is the bilinear form in Eq.(2.2) while $(A^{-1})_{i,j}$ is to be interpreted as

$$(A^{-1}) \equiv \begin{pmatrix} \langle \psi_L(z, \bar{z}) \psi_R^\dagger(w, \bar{w}) \rangle & \langle \psi_L(z, \bar{z}) \psi_L^\dagger(w, \bar{w}) \rangle \\ \langle \psi_R(z, \bar{z}) \psi_R^\dagger(w, \bar{w}) \rangle & \langle \psi_R(z, \bar{z}) \psi_L^\dagger(w, \bar{w}) \rangle \end{pmatrix} \tag{2.8}$$

[4] Fock's space eigenvalues of fermionic particle's creation and annihilation operators.

[5] See for example [73]. Conformal invariance plays an important role and is present in the limit of vanishing mass.

In the limit $|\Delta| \to 0$ the non-vanishing correlators are[6]

$$\langle \psi_R(z,\bar{z})\psi_R^\dagger(w,\bar{w})\rangle = \frac{1}{2\pi(\bar{z}-\bar{w})}, \tag{2.9a}$$

$$\langle \psi_L(z,\bar{z})\psi_L^\dagger(w,\bar{w})\rangle = \frac{1}{2\pi(z-w)}, \tag{2.9b}$$

which are to be interpreted as the operator product expansion (OPE): $(z,\bar{z}) \to (w,\bar{w})$ of the normal ordered[7] currents $J_R(\bar{w})$ and $J_L(w)$, respectively. They give rise to the algebra

$$[J_{R,L}(x), J_{R,L}(y)] = \pm\frac{i}{2\pi}\delta(x-y), \tag{2.10}$$

where we have used the identity $\pi\delta(x) = \bar{\partial}(1/z) = \partial(1/\bar{z})$. In momentum space[8]

$$[J_{R,L}(q), J_{R,L}(-q')] = \pm\frac{Lq}{2\pi}\delta_{q,q'}. \tag{2.11}$$

This is the algebra of bosons, which is often very convenient; for example, partition functions (path integrals) can be calculated in complex variable instead of grassmannians. The equation of motion for massless free bosons (light) is that of a propagating wave: $\partial_\tau \Phi_{R(L)} = \pm iu\partial_x \Phi_{R(L)}$, where u is the velocity of propagation. In the Heisenberg picture this implies the Hamiltonian:

$$\mathcal{H}_B = (u/2)\int dx\ \left[(\partial_x\Theta(x))^2 + (\partial_x\Phi(x))^2\right], \tag{2.12}$$

where $iu\partial_x\Theta \equiv \partial_\tau\Phi$ and $[\partial_x\Theta(x), \Phi(y)] = -i\delta(x-y)$. There's also a chiral left/right moving representation: $\Phi = \Phi_R + \Phi_L$, $\Theta = \Phi_R - \Phi_L$, obeying

$$[\Phi_R, \Phi_L] = i/4 \quad \text{and} \quad [\Phi_{R(L)}(x), \Phi_{R(L)}(y)] = \pm(i/4)sign(x-y) \tag{2.13}$$

to guarantee the anticommutation relations for the vertex representation of fermions. The algebra isomorphism between bosonic operators and the fermionic currents in Eq.(2.10) suggests there is a canonical transformation between free bosons and massless fermions. To prove this is necessary to show that the massless action can be written in terms of currents. Indeed, they are self-interacting terms. Applying derivatives in both sides of Eq.(2.10) one gets[9]

$$\langle \psi_R\partial\psi_R(z)\rangle \approx \langle 2\pi J_R J_R(z)\rangle \ \text{ and } \ \langle \psi_L\bar{\partial}\psi_L(\bar{z})\rangle \approx \langle 2\pi J_L J_L(\bar{z})\rangle \tag{2.14}$$

[6] I won't put my hand on fire to defend the consistency of proportionality factors in this derivation.

[7] Equivalent to the cut off procedure. Resumed in the *point splitting* formula: $J_R(\bar{z}) \equiv lim_{\varepsilon\to 0}[\psi_R^\dagger(\bar{z}+\varepsilon)\psi_R(\bar{z}) - \langle\psi_R^\dagger(\bar{z}+\varepsilon)\psi_R(\bar{z})\rangle]$. Idem for $J_L(z)$.

[8] Notice that the OPE condition in real space $z \to w$ becomes $q \to 0$ in momentum space.

[9] Henceforth, wherever I omit space and/or time on left action operator, it should be understood as equal point correlator, i.e. $\Phi_r\Phi_{\bar{r}}(x) \equiv \Phi_r(x)\Phi_{\bar{r}}(x)$ up to a fundamental regularization (point splitting).

in the leading terms of the OPE. The important insight is that non perturbative interactions in the fermionic basis can give rise to conformally invariant excitations, allowing a simple calculation of correlators. In the bosonic basis (or in 'fermionic' currents) these excitations including those associated to interacting fermions look rather simple: a rescaling of space-time.

2.2 Collective excitations in one dimension

The latter formalism is developed for a relativistic fermion. In our single particle picture this behaviour is to be found at very high energies where general relativity predicts that all massive objects are to become massless as they approach the velocity of light. Matters of budget, technology or plain curiosity may inspire the question whether there is a low energy realization. The answer is yes, and is to be found in the collective behavior of fermions and hard core bosons in one dimension, e.g. electrons in quantum wires and neutral atoms in optical lattices. The energy of a free lattice fermion is given by $\varepsilon(k) \sim -cos(k)$. The Fermi surface k_F is defined as the set of states with maximal ground state energy, i.e. $n(k > k_F) = 0$ at $T = 0$; the filling of electrons in a lattice being defined as $\nu = ak_F/\pi$, where a is the lattice constant *i.e.* the distance between nearest lattice sites. In this context, a single particle can be understood as an excitation in a background of holes (dilute limit: $k_F \approx 0$); a single hole, as an excitation in a background of particles (saturation limit: $k_F \approx \pi$). Equivalently, since the effective mass is associated to the curvature of dispersion, one may think in terms of particles with positive and negative mass. In between, at half filling, something interesting happens: fermions can give rise to a massless excitation.

A direct consequence of one dimension is the possibility of a Fermi surface with discrete degeneracy[10] which allows, near half filling, the separability of density and current fluctuations into massless excitations (gapless) that replicate the algebra in Eq.(2.10). This can be inferred from the separability of the retarded density-density Green's function in frequency momentum (Lindhardt formula) in one dimension [74]. Assuming all relevant processes take place near the Fermi surface one can approximate the lattice fermion operator as ($N = L/a$)

$$\begin{aligned} \psi(x) &\approx (1/\sqrt{L}) \sum_{-k_F-\Lambda/2}^{-k_F+\Lambda/2} e^{ikx}\psi(k) + (1/\sqrt{L}) \sum_{k_F-\Lambda/2}^{k_F+\Lambda/2} e^{ikx}\psi(k) + \alpha \\ &\equiv e^{ik_Fx}\psi_R(x) + e^{-ik_Fx}\psi_L(x) + \alpha, \end{aligned} \tag{2.15}$$

[10] Continuum degeneracy is restored in a quantum gapped phase.

where L is the lattice size, $\Lambda \to a/L$ is the ultraviolet cutoff and the term $\alpha \sim \sqrt{\langle\rho(x)\rangle}$ are components away of the Fermi surface. Consider the lattice density and current, related by the continuity equation $\partial_x J + \partial_t \rho = 0$

$$\rho(x_i) = \psi^\dagger\psi(x_i) \quad \text{and} \quad J(x_i, x_{i+1}) = -iat(\psi^\dagger(x_i)\psi(x_{i+1}) - H.c.), \tag{2.16}$$

where t is the hopping between lattice size, which in the continuum limit $at \to u$. Notice that $\psi(x_i) \to \sqrt{a}\psi(x)$, $\rho(x_i) \to a\rho(x)$ and $J(x_i, x_{i+1}) \to aJ(x)$. Upon expansion near the Fermi surface they give rise to massless and staggered terms

$$\rho(x) \approx J_R(x) + J_L(x) + (e^{-i2k_F x_i}\psi_R^\dagger\psi_L(x_i) + H.c.), \tag{2.17a}$$

$$J(x)/u \approx -J_R(x) + J_L(x) - (e^{-i2k_F x_i}\psi_R^\dagger(x_i)\psi_L(x_{i+1}) + H.c.), \tag{2.17b}$$

where$k_F x_{i+1} = k_F x_i + \pi/2$. When excitations are gapped by interaction density waves dominate the action and quantum fluctuations are reduced to massive terms, this is a Mott insulator. When compared with the massive terms of Dirac's action one may notice that a finite k_F is the imprint of collective particles, this is the many body mechanism through which mass is created and annihilated[11].

If we are interested to distinguish short from long range excitations, bare correlators such as $\langle\rho(x)\rangle$ and $\langle J(x)\rangle$ are insufficient. A quantum gapped phase is characterized by the oscillatory behavior of quantum fluctuations; the separability of left and right moving currents is replaced by the separability of local states describing an alternation of either static (Néel order) or dynamic (Dimer order) states[12]. Upon this insight one may define the following order parameters

$$\mathcal{N} \equiv 1/(N-1)\sum_{i=1}^{N}(-1)^i\psi^\dagger(x_i)\psi(x_i), \tag{2.18a}$$

$$\mathcal{D} \equiv 1/(N-1)\sum_{i=1}^{N}(-1)^i\psi^\dagger(x_i)\psi(x_{i+1}). \tag{2.18b}$$

The bosonization of the massive fermion is introduced in the next section following a more historical approach.

[11] The miracle of losing weight without investing energy has always a catch: when energy is ubiquitous you have to pay a price to remain cool.

[12] The Dimer is associated to alternation of strong and weak coupling.

2.3 Bosonization term by term

It is worth to distinguish three approaches to bosonization: the one followed by Mattis and Lieb [64] and Luther and Peschel [75], a continuation of the work by Luttinger and Tomonaga, is based on an educated guess on the quantum equation of motion, providing an effective representation for the Hamiltonian. Next is the approach of Coleman [65] showing that all relevant correlators of the sine-Gordon model, a well known interacting model for bosons, match all relevant correlators of the free massive fermion with a straightforward mapping. Finally Mandelstam's approach [66], proving that a soliton excitation in bosons obeys fermionic anticommutation relations. The three approaches provide valuable insight on theory and theorizing. Here I restrict to Coleman's article to bring about the most important bosonization relations; his starting point is the sine-Gordon interaction, which resembles in condensed matter physics the potential of a crystal; it makes clear that the explicit mapping of fermions into vertex bosonic operators, despite being beautiful and useful, is not necessary.

Consider the Lagrangian of the quantum sine-Gordon and massive Thirring model

$$\mathcal{L}_B = \frac{1}{2}\partial_\mu\Phi\partial^\mu\Phi + \frac{\alpha_0}{\beta^2}cos\beta\Phi, \tag{2.19a}$$

$$\mathcal{L}_F = \frac{1}{2}\bar{\Psi}\gamma_\mu\partial^\mu\Psi - \frac{g}{2}j^\mu j_\mu - m'\bar{\Psi}\Psi, \tag{2.19b}$$

where in Pauli matrices: $j^0 = \bar{\Psi}\sigma_1\Psi$ and $j^1 = \bar{\Psi}\sigma_2\Psi$, and γ_μ are the two dimensional gamma matrices: $\gamma_0 = \sigma_1$ and $\gamma_1 = -i\sigma_2$. These are self-interacting models whose specific form is related to integrability conditions[13]. The Lagrangian density $\mathcal{L}_F$, up to the interaction g, is a relabeling from Eq.(2.2) with the constraint $\Delta = Re(\Delta)$. All relevant correlations can be expressed as perturbative expansions of

$$T\langle 0|\prod_{i=1}^{n} N_m e^{+i\beta\Phi(x_i)} N_m e^{-i\beta\Phi(y_i)}|0\rangle = \frac{\prod_{i>j}[(x_i-x_j)^2(y_i-y_j)^2c^2m^4]^{\beta^2/(4\pi)}}{\prod_{i,j}[cm^2(x_i-x_j)^2]^{\beta^2/(4\pi)}}, \tag{2.20a}$$

$$\langle 0|T\prod_{i=1}^{n}(\psi_R^\dagger\psi_L)(x_i)(\psi_L^\dagger\psi_R)(y_i)|0\rangle = \left(\frac{1}{2}\right)^{2n}\frac{\prod_{i>j}[(x_i-x_j)^2(y_i-y_j)^2M^4]^{1/(1+g/\pi)}}{\prod_{i,j}[M^2(x_i-x_j)^2]^{1/(1+g/\pi)}}. \tag{2.20b}$$

The cutoffs, implicit on the left by normal order, are controlled by the auxiliary terms cm and M. I try to be faithful to the expressions used by Coleman; in App.A you may find a more modern approach to similar correlators. Notice in Eq.(2.20a) the correlator

[13] Classical integrable models, such as the original sine-Gordon, have a long history; their interest to quantum physics can be appreciated in the quantization program based on the inverse scattering method.

respects the translational invariance of the free bosonic action[14]: $\Phi(x) \to \Phi(x) + \lambda$, and in Eq.(2.20b) reordering of operators yields a product of the massless currents depicted in Eq.(2.9). The equivalence between the two correlators is fulfilled term by term with

$$e^{i\beta\Phi} \equiv Z\psi_R^\dagger \psi_L, \tag{2.21}$$

$$\frac{1}{1+g/\pi} \equiv \frac{\beta^2}{4\pi}, \qquad M^2 \equiv cm^2. \tag{2.22}$$

where Z is a regularization parameter. The first term is the bosonic realization of the massive fermion; it has the form of an exponential in the field operator $\Phi(x)$. Together with the commutators[15]

$$\left[\partial_\nu \Phi(x), N_m e^{\pm i\beta\Phi(y)}\right] = \pm\beta\ D_\nu(x-y) N_m e^{\pm i\beta\Phi(y)}, \tag{2.23a}$$

$$[j^\mu(x), \sigma_\mp(y)] = \mp 2\left(1+\frac{g}{\pi}\right)^{-1} \epsilon^{\mu\nu} D_\nu(x-y)\sigma_\mp(y), \tag{2.23b}$$

where $\sigma_+ = (\sigma_-)^\dagger = \psi_R^\dagger \psi_L$, renders the massless currents for interacting fermions

$$j^\mu \equiv -\frac{\beta}{2\pi}\epsilon^{\mu\nu}\partial_\nu \Phi, \tag{2.24}$$

where $\epsilon^{\mu,\nu}$ is an anti-symmetric tensor. The free fermion corresponds to a well defined bosonic interaction: $\beta(g)^2 = 4\pi$. Scaling laws support massless excitations up to finite values of the interaction, in particular down to $\beta^2 > 8\pi$. In this regime the signature of interaction is encoded in the Luttinger parameter K, depicted in Eq.(3.6); it can be measured in optical lattices through the compressibility: $\kappa = d\rho/d\mu \propto K$, where μ is the lattice depth [76, 77].

At $\beta^2 = 8\pi$ the system undergoes a quantum phase transition (Berezinsky-Kostherlitz-Thouless); the model behaves like a free massless fermion. In the strong coupling regime, $\beta^2 < 8\pi$, the sine-Gordon spectrum is gapped; the fermion acquires an effective mass and the compressibility is drastically suppressed, evidence that the system is closer to a solid state[16]. As β^2 approaches 4π (g approaches zero) the fermion recovers its original mass m'. The general framework is known as the Tomonaga-Luttinger model [68].

For the sake of completeness this section is closed with the vertex representation of

[14] This criteria leads to a generalization of the relevant products of vertex operators: $\sum_{i=1}^{n} \beta_i = 0$. This formula allows the treatment of more than one sine-Gordon term, and its continuum limit renders conformal dimensions behaving like quantum fields. Notice the subindex is not to be confused with the discretization of space-time.

[15] D_ν is the gradient of the massless free scalar commutator, proportional to delta of Dirac.

[16] For electrons in a crystal this corresponds to an interaction induced insulator, where valence electrons replicate the order of the underlying crystal.

a fermion (annihilation operator)

$$\psi_{R(L)}(x) = \left(\frac{1}{\sqrt{2\pi\varepsilon}}\right) : exp\{(i/2)(\pm\Phi(x)\beta + \Theta(x)4\pi/\beta)\} :, \tag{2.25}$$

whose interpretation was brilliantly developed by Mandelstam [66] as the soliton excitation of bosons. Where $\Theta(x) = (1/u)\int_{-\infty}^{x}\partial_t\Phi(x,t)$ and ε is the usual regularization parameter. In the ground state of free bosons a right (left) moving soliton excitation $\psi_{R(L)}$ is associated to the spatial boundary conditions $\langle\psi_R^\dagger\Phi(\pm\infty)\psi_R\rangle = \pm 1/(2\beta)$ (invert right hand signs for L); this implies commutators $[\Phi(y), \psi_{R(L)}(x<y)] = \pm\beta^{-1}\psi_{R(L)}(x)$ and zero for $x > y$. In this context, tractable deviations of β^2 from 4π fall into phase-shift scattering theory ($8\pi > \beta^2 > 4\pi$) and soliton-antisoliton pairs also known as *breathers* ($\beta^2 < 4\pi$) [74]. The massless currents can be derived from Eq.(2.25) as the product of fermions with positive and negative mass moving in the same direction[17]

$$\begin{aligned} :J_{R(L)}(x): &= Lim_{\varepsilon\to 0}\ \psi_{R(L)}^\dagger(x+\varepsilon)\psi_{R(L)}(x) - \langle\psi_{R(L)}^\dagger\psi_{R(L)}(x)\rangle \\ &= \left(\frac{i}{2\pi\varepsilon}\right)(1 - i\varepsilon\beta\partial_x\Phi_{R(L)}(x) + O(\varepsilon^2)) - \langle\psi_{R(L)}^\dagger\psi_{R(L)}(x)\rangle \end{aligned} \tag{2.26}$$

where we use the Baker-Campbell-Haussdorf (BCH) formula in account of Eqs.(2.13). The meaning of the regularization parameter becomes clear:

$$\left(\frac{i}{2\pi\varepsilon}\right) \equiv \langle\psi_{R(L)}^\dagger(x)\psi_{R(L)}(x)\rangle. \tag{2.27}$$

The latter is an introduction to bosonization via the most simple model, the spinless fermion; generalizations can be found in the vast literature; worth mentioning is the extension to affine Kac Moody algebras, the so called Wess-Zumino-Novikov-Witten model (WZNW), describing in a unified frame finite (e.g. $SU(N)$) and infinite (e.g. $SU(k)$) dimensional lie algebras [74]. A review of foundational articles can be found in [78]. Some perspectives of bosonization in the realm of condensed matter physics concerns the effects of nonlinearity in the dispersion [79] and out of equilibrium phenomena [80].

A final remark: The three approaches to bosonization [64–66] share a common feature: the fundamental role played by commutation relations. This suggest an intimate relation between algebra homomorphisms and physical equivalence. The bosonization technique makes it clear in one spatial dimension, but this seems to be a more generic feature: Heisenberg's equation of motion, regardless of the spatial dimension, characterize the evolution of the physical fields through the adjoint action of the Hamiltonian, which is an expansion in commutators. This notion was formalized by the "Russian

[17] For the complex extension recall that $J_L = J_L(z)$ and $J_R = J_R(\bar{z})$, where $z = \tau + ix$.

School" in [70]. In this perspective one uses the homomorphism between the algebra of momentum-energy tensors for free massless bosons and fermions and develops the Luttinger terms as a deformation of the algebra, and massive terms as its "regularization" (finite size effects), see for example [73]. The idea of understanding all relevant quantum correlators as functions over an algebra –or explicitly on the adjoint representation– is powerful and natural: the core of quantumness is a finite commutation relation proportional to Planck's constant, from which all fundamental certainties and uncertainties are to be derived.

2.4 Density waves

The variational nature of the action manifests through the high symmetry of the ground states. In the limit to the continuum, excitations stabilize –via scaling laws– around the only two non-dynamic parameters of the action: the inter-site distance a and the lattice size L. This gives rise to distinctive long and short range excitations: *Luttinger liquids* and *density waves*, respectively. Bosonization of Eq.(2.17) yields

$$\rho(x) = \frac{1}{\sqrt{\pi}}\partial_x\Phi(x) + \frac{1}{\pi a}\, sin(\sqrt{4\pi}\Phi(x) - 2k_F x), \tag{2.28a}$$

$$J(x)/u = -\frac{1}{\sqrt{\pi}}\partial_x\Theta(x) - \frac{1}{\pi a}\, sin(\sqrt{4\pi}\Phi(x) - 2k_F x). \tag{2.28b}$$

where we use Eqs.(2.13) and $\Phi(x_{i+1}) \approx \Phi(x_i) + O(a)$. The oscillatory term $e^{i2k_F x}$ tends to suppress density waves upon integration, unless suitable interactions and fillings cancels it. This is the case for Néel and dimerization terms in Eqs.(2.18)

$$\mathcal{N} \sim 1/(N-1)\sum_{i=1}^{N} sin(\sqrt{4\pi}\Phi(x_i)), \tag{2.29a}$$

$$\mathcal{D} \sim 1/(N-1)\sum_{i=1}^{N} cos(\sqrt{4\pi}\Phi(x_i)). \tag{2.29b}$$

Density waves are usually characterized by a well defined periodicity $a = \pi/(2k_F)$. This is not always the case for a multicomponent system; periodicity will depend on the degree of freedom (i.e. channel) you probe. Consider a balanced population of spin-1/2 at half filling ($k_{F,\uparrow} = k_{F,\downarrow} = \pi/2$): In the channels $\Phi_\uparrow$ and $\Phi_\downarrow$ density waves introduce a period $a_{\uparrow(\downarrow)} = \pi/(2k_{F,\uparrow(\downarrow)}) = 1$. It is often convenient to change the basis of the bosonic fields. The basis $\Phi_{c,s} = (\Phi_\uparrow \pm \Phi_\downarrow)/\sqrt{2}$ makes explicit the existence of a massless spin

excitations. From the interaction $\rho_\uparrow\rho_\downarrow(x)$ one obtains the relevant term

$$\begin{aligned} cos(\sqrt{8\pi}\Phi_c(x)) &= cos(\sqrt{4\pi}(\Phi_\uparrow(x)+\Phi_\downarrow(x))), \\ &= cos(\sqrt{4\pi}(\Phi_\uparrow(x))cos(\sqrt{4\pi}(\Phi_\downarrow(x)) \\ &- sin(\sqrt{4\pi}(\Phi_\uparrow(x))sin(\sqrt{4\pi}(\Phi_\downarrow(x)). \end{aligned} \tag{2.30}$$

The charge channel, whose filling is $k_{F,c} = k_{F,\uparrow} + k_{F,\downarrow}$ has a periodicity $a_c = a_{\uparrow(\downarrow)}/2$. The quantum symmetry characterizing the magnetic Néel phase could be is summarized in the equation

$$\langle\Phi_\uparrow(x)\rangle_{\text{Néel}} = -\langle\Phi_\downarrow(x+a)\rangle_{\text{Néel}}. \tag{2.31}$$

In the magnetic Néel phase, the quantum symmetry of Φ_c is broken due to the presence of an external lattice potential, which enables –via chemical potential– the polarization of *particle* states, otherwise *hole* states would always fill the void and restore the quantum symmetry. To minimize the action, the term in Eq.(2.30) should be negative, hence the fields will adjust such that

$$\begin{aligned} \langle cos(\sqrt{4\pi}\Phi_\uparrow(x))cos(\sqrt{4\pi}\Phi_\downarrow(x))\rangle &< 0 \quad \text{and} \\ \langle sin(\sqrt{4\pi}\Phi_\uparrow(x))sin(\sqrt{4\pi}\Phi_\downarrow(x))\rangle &> 0. \end{aligned} \tag{2.32}$$

which is Eq.(2.31).

Chapter 3

The spinor fermi gas

3.1 High spin Alkali metals

Alkali atoms exhibit two hyperfine multiplets whose energy difference –many orders of magnitude the frequency of typical traps– allows spin dependent scattering restricted to the lower multiplet [49]. The Hamiltonian for s-wave scattering and conserved total angular momenta reads

$$\mathcal{H} = -t \sum_{i,\alpha} \left[\psi^{\dagger}_{\alpha,i} \psi_{\alpha,i+1} + H.c. \right] + \sum_{i,J} g_J \sum_{M=-J}^{J} P^{\dagger}_{J,M;i} P_{J,M;i} \tag{3.1}$$

where α is the single particle spin state while the pair creation operator $P^{\dagger}_{J,M;i} = \sum_{\alpha\beta} \langle JM|F,F;\alpha,\beta\rangle \psi^{\dagger}_{\alpha,i} \psi^{\dagger}_{\beta,i}$ is labeled by the total spin J and its sub-levels M. In the case of fermionic atoms, some scattering channels are forbidden by the Pauli principle.

Transitions with broken discrete symmetry $\mathbb{Z}_N$ are predicted for the case $U_{J>0} = U_2 \neq U_0$ [81]. In this case the latter Hamiltonian can be written as

$$\mathcal{H} = -t \sum_{i,\alpha} \left[\psi^{\dagger}_{\alpha,i} \psi_{\alpha,i+1} + H.c. \right] + \frac{U}{2} \sum_i n_i^2 + V \sum_i \pi_i^{\dagger} \pi_i,$$

where $n_i = \sum_\alpha \psi^{\dagger}_{\alpha,i} \psi_{\alpha,i}$, $U = 2g_2$, $V = g_0 - g_2$ and $\pi^{\dagger} = \sqrt{2N} P^{\dagger}_{0,0;i} = \psi^{\dagger}_{\alpha,i} \mathcal{J}_{\alpha\beta} \psi^{\dagger}_{\beta,i}$. The fine tuning $V = 0$ leads to the $SU(2N)$ Hubbard model, characterized by the Mott to superfluid transition. When $V \neq 0$ interesting physics occurs in the spin channels where infrared properties at $1/(2N)$ filling shows competition between Mott phases[1]. From

[1] They arise from the coset between the center of $SU(2N)$, which is $\mathbb{Z}_{2N}$, and the center of the remaining symmetry at $V \neq 0$.

RG flow we identify three phases: (I) Spin-density wave (SDW) for U and V positive; (II) $SU(2N)$-singlet superconductor for $U<0$ and $V>NU/2$, and (III) $SU(2)$-singlet superconductor (BCS pairs) for $U<0$ and $V<NU/2$. Each of the superfluids has also a crossover into a charge density wave (CDW). At the infrared limit phase (II) takes the form of the $SU(2N)$ Gross-Neveu (GN) model which is an integrable massive field theory. Its dominant order parameters are the atomic density $n_{2k_F}=L_\alpha^\dagger R_\alpha$ and the extended singlet superconductor $\Pi_0^{2N\dagger}=\epsilon^{\alpha_1\ldots\beta_N}R_{\alpha_1}^\dagger\ldots R_{\alpha_N}^\dagger L_{\beta_1}^\dagger\ldots L_{\beta_N}^\dagger$. From the power law behavior of their correlators

$$\langle n_{2k_F}^\dagger(x)n_{2k_F}(x)\rangle\sim x^{-K_c/N}\quad\text{and}\quad\langle\Pi_0^{2N\dagger}(x)\Pi_0^{2N}(x)\rangle\sim x^{-N/K_c},\tag{3.2}$$

where K_c is the Luttinger parameter of the charge channel; we see that $K_c<N$ is associated to an atomic CDW, while $K_c>N$ corresponds to quasi long range order (QLRO) of the $SU(2N)$-singlet superconductor. As for phase (III) we can adapt the former results by noticing that the latter is dual $\mathcal{D}$ to the former[2]. One finds that $K_c>1/N$ corresponds to a QLRO BCS, while $K_c<1/N$ is associated to a *molecular* CDW (N-particles clustering). The transition between phases (II) and (III) takes place within their superfluid regions; the self-dual criticality is described by an effective $\mathbb{Z}_N$ Ising model. Power law decay is universal only for $N=2,3$.

The experimental stabilization of a clustering phase with $N>2$ is challenging due to the large losses generated by three (or higher order) body recombinations –outgoing particles may gain sufficient energy to escape from the trapping potential. It becomes relevant above a threshold in two-body interactions [82]. Near Feshbach resonance these processes are non-vanishing even for identical particles, despite Pauli blocking. In one dimension the threshold increases by one order in the collision energy ($g^2\to g^3$). In a Fermi degenerate gas recombination is expected to be suppressed by Pauli blocking if it requires more than the Fermi energy for its realization. Hence, most realistic proposals for spinor gases are either near half filling for the attractive regime, dominated by pairing order; or at $1/N$ filling with repulsive interactions, dominated by superfluidity and bond-cluster order.

3.2 Exact spin-3/2

In the case of spin-1/2, the last two terms in Eq.(3.2) are proportional; thus preserving the $SU(2)$ symmetry for all values of U and V. Only for spin-3/2, where $N=2$, we start

[2] $\mathcal{D}R(L)\mathcal{D}^{-1}=\tilde{R}(\tilde{L})$ with $\tilde{R}_\alpha=\mathcal{J}_{\alpha\beta}R_\beta^\dagger$ and $\tilde{L}_\alpha=L_\alpha$. This leads to the correspondence ($\mathcal{N}\leftrightarrow\mathcal{J}$, $\mathbb{Z}_N\leftrightarrow\tilde{\mathbb{Z}}_N$, $K_c\leftrightarrow 1/K_c$).

to see broken $SU(2N)$ symmetry and the unraveling of two competing Mott phases[3].

For spin-3/2 the relevant scattering channels are $J = 0, 2$. The Hamiltonian of Eq.(3.1) becomes

$$\mathcal{H} = -t \sum_{i,\alpha} \left[\psi^\dagger_{\alpha,i} \psi_{\alpha,i+1} + H.c. \right] + g_0 \sum_i P^\dagger_{0,0;i} P_{0,0;i} + g_2 \sum_i P^\dagger_{2,m;i} P_{2,m;i} \tag{3.3}$$

Low energy theory

The infrared properties of the system are encoded in the linear expansion of the second quantized operators: $\psi_\alpha(x) \approx \psi_{R,\alpha}\ e^{ik_F x} + \psi_{L,\alpha}\ e^{-ik_F x}$. The mapping into current algebras follows from the underlying $SO(5)$ symmetry [83]. Part of this chapter can be found in [84] where spin-3/2 cold atomic systems are reviewed from a theoretic point of view. Away from half filling all relevant terms are in the *particle-hole* channel[4]

$$\mathcal{H}_0 = v_F \left[\frac{\pi}{4} J_R J_R + \frac{\pi}{5} (J^a_R J^a_R + J^{ab}_R J^{ab}_R) + (R \to L) \right], \tag{3.4a}$$

$$\mathcal{H}_{int} = \frac{g_c}{4} J_R J_L + g_v J^a_R J^a_L + g_t J^{ab}_R J^{ab}_L, \tag{3.4b}$$

$$\mathcal{H}_{int'} = \frac{g'_c}{8} J_R J_R + \frac{g'_v}{2} J^a_R J^a_R + \frac{g'_t}{2} J^{ab}_R J^{ab}_R + (R \to L), \tag{3.4c}$$

where $J_{R(L)}(x) = \psi^\dagger_{R(L)} \psi_{R(L)}(x)$, $J^a_{R(L)}(x) = \psi^\dagger_{R(L)} \Gamma^a_{\alpha\beta} \psi_{R(L)}(x)$ $(1 \le a \le 5)$, and $J^a_{R(L)}(x) = \psi^\dagger_{R(L)} \Gamma^{ab}_{\alpha\beta} \psi_{R(L)}(x)$ $(1 \le a, b \le 5)$, where Γ^a are the Dirac Gamma Matrices and $\Gamma^{ab} = -(i/2)[\Gamma^a, \Gamma^b]$. Aside from the identity, Γ^a and Γ^{ab} constitute the spinor representation of $SO(5)$ –see for example Ch. XXI in [85]–. Terms in $\mathcal{H}_{int'}$ will renormalize $\mathcal{H}_0$ creating the Tomonaga-Luttinger term. The new interactions are

$$g'_c = g_c = \frac{g_0 + 5g_2}{2}, \quad g_v = g'_v = \frac{g_0 - 3g_2}{2}, \quad g_t = g'_t = -\frac{g_0 + g_2}{2}. \tag{3.5}$$

Using the bosonization of spin-3/2 fermions

$$\psi_{\alpha;\ R,L}(x) = \frac{\eta_\alpha}{\sqrt{2\pi a}}\ e^{i\sqrt{\pi}(\pm\Phi_\alpha(x) + \Theta_\alpha(x))}, \qquad (\alpha = \pm\frac{3}{2}, \pm\frac{1}{2}),$$

[3] For $N = 2$, the symmetry when $V \neq 0$ is $SO(5)$, its center is $\mathbb{Z}_2$. The Mott-to-Mott transition should be characterized by a broken $\mathbb{Z}_4/\mathbb{Z}_2 = \mathbb{Z}_2$ symmetry.

[4] The symmetry implies that the Hamiltonian can be written as a bilinear in the generators of the corresponding algebra. We use the simplified notation $\mathcal{H} \sim \sum_s a_s J^s J^s$, letting implicit integration along space.

and the basis ($\Phi_\alpha \to \Phi_\nu$)

$$\Phi_{c,v} = \frac{1}{2}(\Phi_{3/2} \pm \Phi_{1/2} \pm \Phi_{-1/2} + \Phi_{-3/2}),$$
$$\Phi_{t1,t2} = \frac{1}{2}(\Phi_{3/2} \mp \Phi_{1/2} \pm \Phi_{-1/2} - \Phi_{-3/2}),$$

we get the quadratic Hamiltonian

$$\mathcal{H}_0 = \frac{v_\nu}{2} \sum_\nu \left\{ K_\nu (\partial_x \Theta_\nu)^2 + \frac{1}{K_\nu} (\partial_x \Phi_\nu)^2 \right\}, \tag{3.6}$$

where the microscopic value of the Luttinger parameters K_ν and the sound velocities v_ν is[5]

$$K_\nu = \sqrt{\frac{2\pi + g'_\nu - g_\nu}{2\pi + g'_\nu + g_\nu}}, \qquad v_\nu = \sqrt{(v_F + \frac{g'_\nu}{2\pi})^2 - (\frac{g_\nu}{2\pi})^2},$$

together with sine-Gordon terms in the spin sector

$$\begin{aligned} \mathcal{H}_{int}(x) &= \frac{-1}{2(\pi a)^2} \left\{ cos\sqrt{4\pi}\Phi_{t1} + cos\sqrt{4\pi}\Phi_{t2} \right\} \left\{ (g_t + g_v)\ cos\sqrt{4\pi}\Phi_v \right. \\ &+ \left. (g_t - g_v)\ cos\sqrt{4\pi}\Theta_v \right\} - \frac{g_t}{(2\pi a)^2}\ cos\sqrt{4\pi}\Phi_{t1} cos\sqrt{4\pi}\Phi_{t2}. \end{aligned} \tag{3.7}$$

We discard Umklapp terms for the moment and focus on the quarter filling behavior. There is a transition driven by the competition between the conjugated variables Φ_v and Θ_v within the strong coupling limit of g_t. The fermionic realization of the corresponding sine-Gordon terms[6]

$$\begin{aligned} \frac{1}{2}(\psi^\dagger_{3/2}\psi^\dagger_{-3/2} - \psi^\dagger_{1/2}\psi^\dagger_{-1/2}) &\propto e^{i\sqrt{\pi}\Theta_c} cos\sqrt{\pi}\Theta_v, \quad \text{and} \\ \frac{1}{2}(\psi^\dagger_{3/2}\psi^\dagger_{-3/2}\psi^\dagger_{1/2}\psi^\dagger_{-1/2}) &\propto e^{i\sqrt{4\pi}\Theta_c} cos\sqrt{4\pi}\Phi_v \end{aligned}$$

suggest they are a transition between singlet pairs and quartets, respectively[7]. We can use a mean field approach to further simplify the model. The t-sector fields are pinned by the very last term. They can be treated as mean fields in the v-sector

$$\mathcal{H}_{int} = \frac{-1}{2(\pi a)^2} \left(g\ cos\sqrt{4\pi}\Phi_v + g_\gamma\ cos\sqrt{4\pi}\Theta_v \right), \tag{3.8a}$$

$$g, g_\gamma = (g_t \pm g_v) \left(\langle cos\sqrt{4\pi}\Phi_{t1}\rangle + \langle cos\sqrt{4\pi}\Phi_{t2}\rangle \right). \tag{3.8b}$$

[5] Although their macroscopic value is determined by scaling, the latter relations provide some insight into the Luther-Emery liquid found along the critical line.

[6] In these relations, the Klein factors, which are not made explicit, play a crucial role.

[7] In the generic approach they correspond to $\Pi_0^{2\times 2\dagger}$ and $\mathcal{D}^*\Pi_0^{2\times 2\dagger}$, respectively.

The system exhibits an Ising transition for $g = g_\gamma$, this is clear from its decomposition into majoranas [86]

$$\begin{aligned}\xi^1_R + i\xi^2_R &= \frac{1}{\pi} : exp\left(i\sqrt{4\pi}\Phi_{v,R}\right) : \\ \xi^1_L + i\xi^2_L &= \frac{1}{\pi} : exp\left(-i\sqrt{4\pi}\Phi_{v,L}\right) :\end{aligned}$$

Together with the chirality component in Eq.(3.6)

$$\begin{aligned}\mathcal{H}^{(v)}_0 + \mathcal{H}_{int} &= \sum_{a=1,2}\left[\frac{v_F}{2i}\left(\xi^a_R\partial_x\xi^a_R - \xi^a_L\partial_x\xi^a_L\right) + im_a\ \xi^a_R\xi^a_L\right] \\ &\quad -\frac{g_4}{2}\left[(\xi^1_R\xi^2_R)^2 + (\xi^1_L\xi^2_L)^2\right] - g_2\ \xi^1_R\xi^2_R\xi^1_L\xi^2_L. \qquad (3.9)\end{aligned}$$

where $m_{1,2} = 2\pi(g \mp g_\gamma)$ and $g_{2,4}$ are the Tomonaga-Luttinger terms in consistency with Eq.(3.6)

$$v_v K_v = v_F\left(1 + \frac{g_4}{2\pi v_F} - \frac{g_2}{2\pi v_F}\right), \qquad (3.10a)$$

$$\frac{v_v}{K_v} = v_F\left(1 + \frac{g_4}{2\pi v_F} + \frac{g_2}{2\pi v_F}\right). \qquad (3.10b)$$

The signature of the $\mathbb{Z}_2$ Ising transition is associated to the Majorana ξ_1 becoming massless as $g_\gamma \to g$. Notice that the critical value of the Luttinger parameter K_ν is 1; this assures the exact self-duality of the quadratic terms in the bosonic Hamiltonian. The presence of an external magnetic field will weaken the self-duality in the transition by taking the Luttinger parameter away from one. In such case, the new microscopic expression of the Luttinger parameter –of qualitative interest– is to be found by identifying the Tomonaga-Luttinger terms in the canonic basis of free massive Majoranas with external magnetic field which is non-trivial because the latter interacts with g_γ–terms.

Quadratic Zeeman coupling (QZC)

The magnetic channels couple linearly to an external magnetic field, while chirality couples quadratically. Only the latter is relevant since it has spin changing collisions, which breaks perfect commensurability. The coupling is given by

$$\begin{aligned}\mathcal{H}_{QZC}(x) &= -q\sum_\alpha \alpha^2\psi^\dagger_\alpha\psi_\alpha(x) \\ &= -q\frac{1}{\sqrt{\pi}}\sum_\alpha \alpha^2\partial_x\Phi_\alpha(x) \\ &= -q\frac{5}{2\sqrt{\pi}}\partial_x\Phi_c(x) - q\frac{2}{\sqrt{\pi}}\partial_x\Phi_v(x). \qquad (3.11)\end{aligned}$$

The term proportional to $\partial_x\phi_c$ is irrelevant since in experiments the number of particles remains fixed. The relation $\partial_x\phi_v(x) \sim \sum_\alpha C_{|\alpha|}\ \psi^\dagger_\alpha\psi_\alpha(x)$, where $C_{|3/2|} = -C_{|1/2|} = 1$, associates the v-sector to "color" balance or imbalance, in contrast with magnetization. The mean value along the lattice is referred to as the *chirality* τ. In the Majorana basis

$$\frac{1}{\sqrt{\pi}}\partial_x\Phi_v \propto\ -i(\xi^1_R\xi^2_R + \xi^1_L\xi^2_L), \tag{3.12}$$

which is a coupling of two Majorana fermions; one remains massive while the other becomes massless at criticality. To prove the existence of such critical line in the presence of the QZC we use the Luther Emery approach, App.B.2.

Umklapp terms

At half filling ($k_F = \pi/2$) some of the oscillatory modes ignored in Eq.(3.4) become relevant; terms like $e^{i(k^\alpha_F+k^\beta_F+k^\gamma_F+k^\delta_F)x}\psi^\dagger_{R,\alpha}\psi^\dagger_{R,\beta}\psi_{L,\gamma}\psi_{L,\delta}(x)$ will now depend only on slowly varying fields. These are the so called Umklapp terms, which for high-spin fermions show non-trivial spin-charge interactions affecting the magnetic order of the system. Their bosonization follows from their description in terms of current algebras. This takes place in the *particle-particle* channel. The *Fierz identity* suggest the new currents[8]

$$\eta^\dagger(x) = \frac{1}{2}\psi^\dagger_\alpha R_{\alpha,\beta}\psi^\dagger_\beta(x), \tag{3.13a}$$

$$\chi^\dagger_a(x) = \frac{1}{2i}\psi^\dagger_\alpha(\Gamma^a R)_{\alpha,\beta}\psi^\dagger_\beta(x). \tag{3.13b}$$

Using the relation with the pairing operators of Eq.(3.3)

$$P^\dagger_{0,0} = -\frac{1}{\sqrt{2}}\eta^\dagger, \quad P^\dagger_{2,\pm2} = \frac{\mp\chi^\dagger_1 + i\chi^\dagger_5}{2}, \quad P^\dagger_{2,\pm2} = \frac{-\chi^\dagger_3 \pm i\chi^\dagger_2}{2}, \quad P^\dagger_{2,\pm2} = -\frac{1}{\sqrt{2}}\chi^\dagger_4; \tag{3.14}$$

we get the Hamiltonian,

$$\mathcal{H}^{um}_{int} = \frac{\lambda_s}{2}\eta^\dagger_R\eta_L + \frac{\lambda_v}{2}\chi^{a\dagger}_R\chi^a_L + H.c. \tag{3.15}$$

[8]For the $SO(5)$ algebra:

$$(\Gamma^a R)_{\Lambda\beta}(R\Gamma^a)_{\gamma\delta} = \frac{5}{4}\delta_{\Lambda\gamma}\delta_{\beta\delta} - \frac{3}{4}\Gamma^a_{\Lambda\gamma}\Gamma^a_{\beta\delta} - \frac{1}{4}\Gamma^{ab}_{\Lambda\gamma}\Gamma^{ab}_{\beta\delta},$$

$$R_{\Lambda\beta}R_{\gamma\delta} = \frac{1}{4}\delta_{\Lambda\gamma}\delta_{\beta\delta} + \frac{1}{4}\Gamma^a_{\Lambda\gamma}\Gamma^a_{\beta\delta} - \frac{1}{4}\Gamma^{ab}_{\Lambda\gamma}\Gamma^{ab}_{\beta\delta}.$$

where $\lambda_v = 2g_2$ and $\lambda_s = 2g_0$. Bosonization yields

$$\mathcal{H}^{um}_{int}(x) = \frac{-1}{2(\pi a)^2} \quad cos\sqrt{4\pi}\Phi_c \quad \Big\{(\lambda_v + \lambda_s)\ cos\sqrt{4\pi}\Phi_v + (\lambda_v - \lambda_s)\ cos\sqrt{4\pi}\Theta_v + \ 2\lambda_v\ (cos\sqrt{4\pi}\Phi_{t1} + cos\sqrt{4\pi}\Phi_{t2})\Big\} \tag{3.16}$$

A mean field of the charge channel as in Eq.(3.8) for $t_{1,2}$, leads to a Hamiltonian similar to Eq.(3.17). The new phases correspond to half filling, quartets are replaced by a dimer phase.

3.3 Phase Diagram

Both, spin-spin interactions and umklapp interactions exhibit a self-dual criticality in the chirality channel. Upon mean field in other (pinned) channels refermionization yields (App.B)

$$\mathcal{H}_{lattice} = \sum_j [(-t + g(-1)^j)\ c^\dagger_j c_{j+1} + g_\gamma c^\dagger_j c^\dagger_{j+1} - 2q\ c^\dagger_j c_j] + H.c. \tag{3.17}$$

In the context of spin-spin interactions: $g_\gamma \sim g_t - g_v$ and $g \sim g_t + g_v$, while in the context of umklapp terms: $g_\gamma \sim \lambda_v - \lambda_s$ and $g \sim \lambda_v + \lambda_s$. The spectrum of low energy excitations is[9]

$$\omega_\pm(k) = \sqrt{g^2 + g_\gamma^2 + 4q^2 + k^2 \pm 2\sqrt{g^2 g_\gamma^2 + 4q^2(g^2 + k^2)}},$$

where we set the hopping t as the energy unit. Only the band $\omega_-(k)$ becomes critical and it does when $q_c = \sqrt{g^2 - g_\gamma^2}/2$. The critical dispersion is linear for all finite values of the anisotropy ($g_\gamma \neq 0$) and is proportional to g/g_γ; its actual value depends on the renormalization group. Without the need to know the exact value of the velocity we can already know some important information, for instance the fact that as g_γ goes from g to zero, the transition behaves as a deformed $\mathbb{Z}_2$ Ising transition until becoming a Commensurate-Incommensurate (C-IC) transition exactly at $g_\gamma = 0$ where the dispersion becomes quadratic and proportional to $1/(2g)$. The C-IC transition is characterized by a chirality $\tau \propto \sqrt{2q - g}$. In Fig.3.1 chirality and susceptibility are depicted for different values of g_γ, based on the regularization from Eq.(3.17). Further details in B.1. The phase diagram of Eq.(3.17) is depicted in Fig.3.3. It shows two critical lines: a transition of C-IC type at $q_c(g_\gamma = 0)$ and of Ising type at $q_c(g_\gamma > 0)$. At $q_c = 0$ the dispersion is gapless with maximal sound velocity. At the crossing of the two critical lines the sound

[9] We go to the half filling of the lattice Hamiltonian, not to confuse with the filling of the original Hamiltonian.

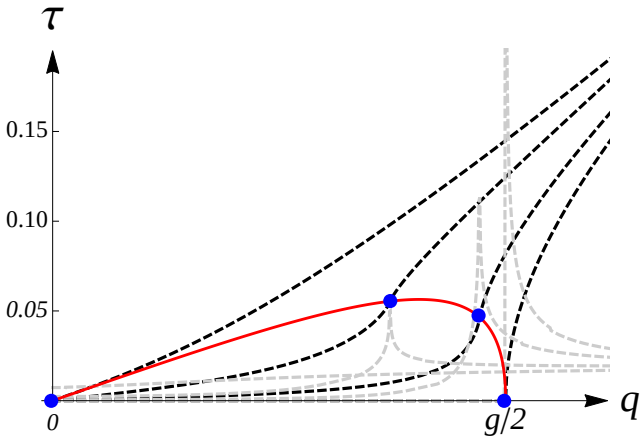

FIGURE 3.1: Chirality (black dashed curve) and susceptibility $\partial\tau/\partial q$ (grey dashed curve) versus QZC. Evaluated for different values of spin changing collisions $0 \leq g_\gamma \leq g$ and fixed dimer interaction g. Calculation based on low energy theory, only valid near criticality (red line). Commensurability is magnetically unstable for $g_\gamma > 0$. The system goes from a C-IC phase transition at $q_c(g_\gamma = 0)$ to Ising transition otherwise. Studied in the context of spin chains [87].

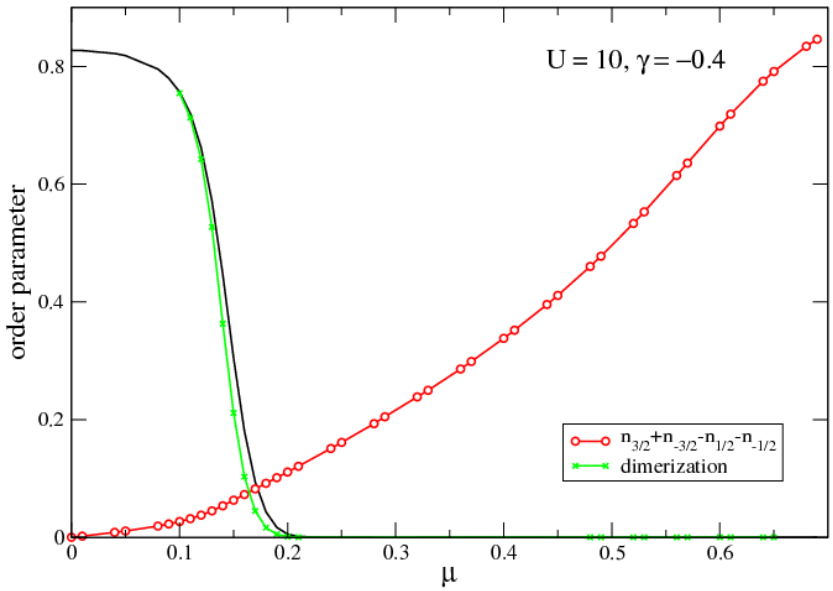

FIGURE 3.2: Chirality (red line) and Dimer order (green and black line for a different lattice size) versus QZC ($q \equiv \mu$) for $g_\gamma/g \approx \gamma/U = -0.04$. The value of U is the average interaction which is close to the interaction strength g dominating the Dimer phase, while anisotropy γ is the same as g_γ. Calculation based on DMRG at lattice size $L = 36$ –work done by Sebastian Greschner in the context of [88]–.

velocity is zero. For high enough QZC the system becomes a band insulator, where all atoms are either in $|S_{eff}| = 3/2$ or $1/2$.

Mapping the total spin scattering in Eq.(3.3) to the single spin basis according to Eq.(1.5)

we get[10]

$$U_{1/2,3/2} = U_{-1/2,3/2} = U_{1/2,-3/2} = U_{-3/2,-1/2} = g_2, \tag{3.18a}$$

$$U_{-3/2,3/2} = U_{-1/2,1/2} = (g_0 + g_2)/2, \tag{3.18b}$$

$$U_\gamma = (g_2 - g_0)/2. \tag{3.18c}$$

Numerics in Fig.3.3 shows that the singlet phase at $q = 0$ is such that $g_2 > g_0$. In the strong coupling limit, the system favors the interactions with minimal energy, the latter inequality implies $U_{-3/2,3/2}$ and $U_{-1/2,1/2}$. The associated pairs form two possible 'singlets', eigenvalues of the U_γ-term. When $U_\gamma > 0$ the system favors negative eigenvalues, i.e. $\psi^\dagger_{3/2}\psi^\dagger_{-3/2} - \psi^\dagger_{1/2}\psi^\dagger_{-1/2}$. At $g_2 \gtrsim g_0$ the system goes from singlet to dimer, and the latter remains even for $g_2 \lesssim g_0$, this despite $(g_0 + g_2)/2 > g_2$. The reason is because magnetic interactions in the exact spin-3/2 Hamiltonian are symmetric; the actual criteria to favor the magnetic phase is $(g_0 + g_2)/2 > 2g_2$.

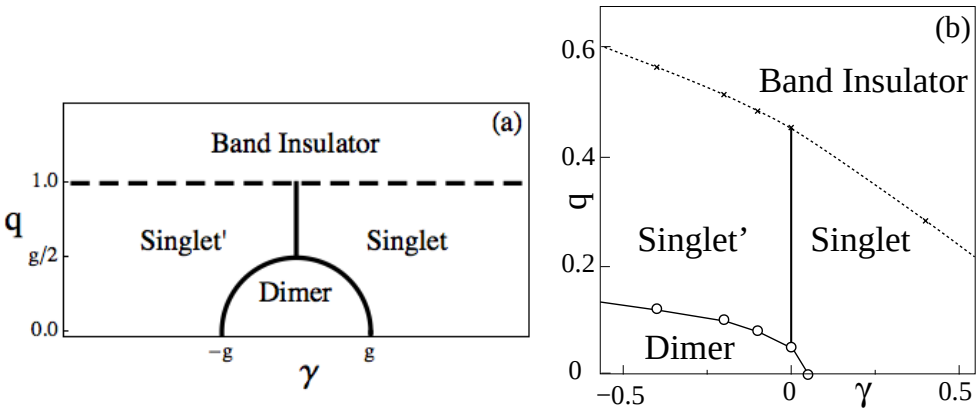

FIGURE 3.3: Phase diagram at half filling of the chirality channel in the spin-3/2 Hamiltonian for different QZC and spin changing collisions ($g_\gamma \equiv \gamma$). Results based on mean field theory (a) and DMRG (b). There is an Ising transition from dimer to singlet pairing. There are two possible singlet pairing phases, separated by a commensurate-incommensurate transition at $g_\gamma = 0$. For high enough QZC there is a crossover into a band insulator.

RG Analysis

The RG equations at quarter filling are given by (App.A)

$$\dot{g}_v = \frac{4}{2\pi} g_v g_t, \quad \dot{g}_t = \frac{1}{2\pi}(3g_t^2 + g_v^2), \quad \dot{g}_c = 0,$$

where $d\dot{g} = dg/d(L/a)$. Umklapp processes are absent, the charge coupling remains microscopic. There are three main phases: a Luttinger liquid in the repulsive region

[10]The interaction $U_{\alpha,\beta}$ is associated to interaction $n_\alpha n_\beta$, and U_γ to $\psi^\dagger_{3/2}\psi^\dagger_{-3/2}\psi_{1/2}\psi_{-1/2} + H.c.$

$g_0 > g_2 > 0$; a quartetting phase in the attractive region $g_{0,2} > 0$, and singlet pairing in the mixed regions $g_2 > 0$ and $g_0 < 0$. The last two phases have a crossover to their respective bond order [84, 89]. In the presence of a strong external magnetic field the separability of right and left currents is no longer satisfied. An alternative to bosonization to study the phase diagram at 1/4-filling is reported in [26]. The results, based on DMRG and strong coupling analysis, predict that at low QZC the system is either in a spin liquid, for $g < 0$, or a dimer phase $g > 0$. Increasing QZC drives the system to an effective isotropic Heisenberg antiferromagnet (iHA); towards the spin liquid (Dimer), the transition is of C-IC (BKT) type. Behind the effective spin-1/2 chain there is a band insulator in the chirality channel, suppressing all populations of with spin-1/2.

At half-filling, umklapp terms become relevant and affects magnetic ordering. Combining interactions from Eq.(3.4) and Eq.(3.15) we get

$$\frac{dg_c}{dln(L/a)} = \frac{1}{2\pi}(\lambda_s^2 + 5\lambda_v^2), \qquad \frac{dg_v}{dln(L/a)} = \frac{1}{2\pi}(4g_v g_t + 2\lambda_s\lambda_v),$$
$$\frac{dg_t}{dln(L/a)} = \frac{1}{2\pi}(3g_t^3 + g_v^2 + 2\lambda_v^2), \qquad \frac{d\lambda_s}{dln(L/a)} = \frac{1}{2\pi}(g_c\lambda_s + 5g_v\lambda_v),$$
$$\frac{d\lambda_v}{dln(L/a)} = \frac{1}{2\pi}(g_c\lambda_v + g_v\lambda_s + 4g_t\lambda_v).$$

In Fig.3.4 we can the see numerical solution for microscopic values $g_0, g2 > 0$. Notice that the symmetric $SU(4)$ line, determined by $g_\gamma \sim \lambda_v - \lambda_s = 0$, lies within the Dimer phase in consistent with Fig.3.3 at $q = 0$; increasing the positive value of anisotropy ($\lambda_v > \lambda_s$) takes the system closer to the Singlet phase, but negative anisotropy will retain the Dimer phase.

Special Cases: strong anisotropy

In this section are shown the effective bosonic hamiltonians near criticality for strong ($g_\gamma \approx g,\ q \approx 0$) and weak ($g_\gamma \approx 0,\ 2q \approx g$) spin changing interaction. This is developed in [90] within the context of spin chains.

As shown in Eqs.(3.9) and (3.12) the external field couples the two Majoranas with a strength q. When g_γ is close enough to g, near the critical line ($q \approx q_c = \sqrt{g^2 - g_\gamma^2}/2$) the interaction between Majoranas can be treated perturbatively. Furthermore, as we are interested in the low energy physics, we can average out the degrees of freedom of the Majorana which remains massive

$$S_{eff} \approx S_1 - \frac{1}{2}\langle S_q^2\rangle_2, \tag{3.19}$$

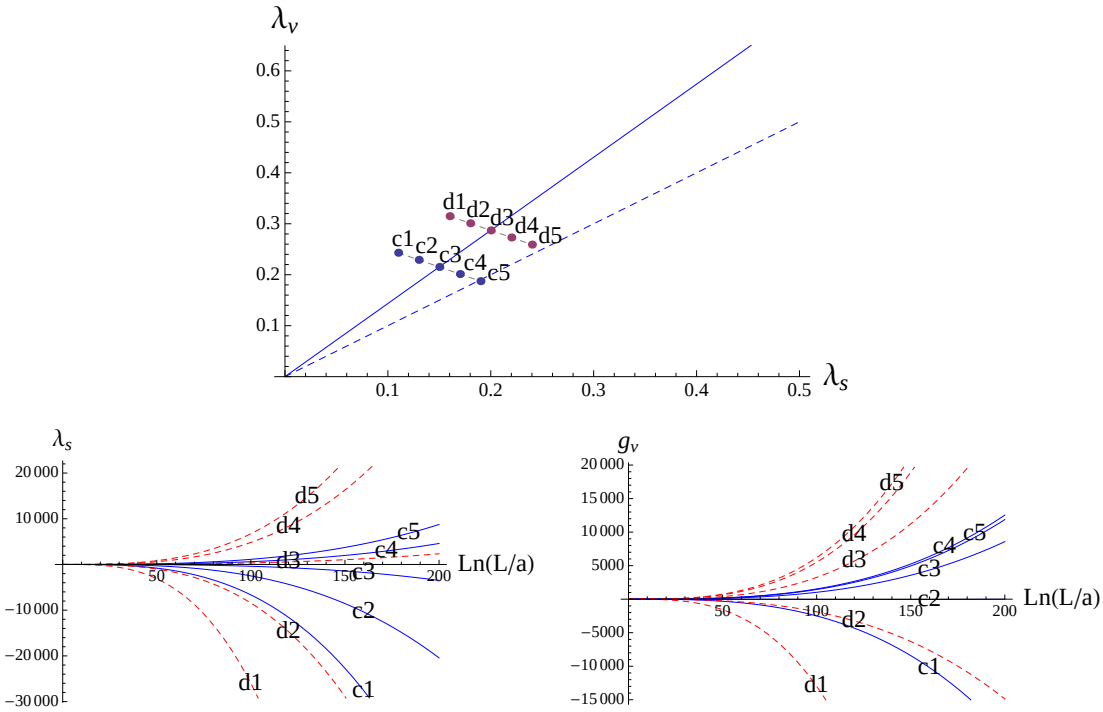

FIGURE 3.4: Scaling at half filling ($g_c, g_t, g_v > 0$). *Above*: the solid line estimates a Dimer ($\lambda_s \to +\infty$) to Singlet ($\lambda_s \to -\infty$) phase transition. The dashed line corresponds to $SU(4)$ symmetry. *Below*: Scaling of λ_s (left) and g_v (right) while crossing the phase transition at two different points, these are the only terms changing sign.

where

$$\begin{aligned} S_1 &= \int dx d\tau \; [\xi^1_R \partial_- \xi^1_R + \xi^1_L \partial_+ \xi^1_L - i m_1 \; \xi^1_R \xi^1_L], \\ S_q &= i(2q) \int dx d\tau \; [\xi^1_R \xi^2_R + \xi^1_L \xi^2_L], \\ \partial_\pm &= \frac{\partial_\tau \pm i v_v \partial_x}{2}, \end{aligned}$$

where $m_{1,2} = 2\pi(g \mp g_\gamma)$. Since the second Majorana remains massive, one can integrate out terms $\langle \xi^2_R \xi^2_L \rangle_2$ in the partition function to get

$$\mathcal{L}_{eff} = \xi^1_R \partial_- \xi^1_R + \xi^1_L \partial_+ \xi^1_L - i \left[m_1 - \frac{(2q)^2}{m_2} \right] \xi^1_R \xi^1_L,$$

which corresponds to a renormalization of the mass of the first Majorana. The phase transition at $q_c = 0$ is of the Ising type; it remains as such for small but finite values of q_c, since the same Majorana is becoming massless.

Weak anisotropy

By solving the Hamiltonian in Eq.(3.17) for $g_\gamma = 0$, adding the g_γ-interaction in the latter eigenbasis, integrating out high-energies and (re)bosonizing slightly above the critical filling ($k_F = \sqrt{((2q)^2 - g^2)/v^2}$), we arrive at the following effective Hamiltonian

$$\mathcal{H}_{g_\gamma} = -\frac{g_\gamma}{\pi}\sqrt{1 - \frac{g^2}{(2q)^2}}\int dx\ cos(\beta\tilde{\Theta}_v). \tag{3.20}$$

This interaction, valid for $2q > g$, explains the instability of the Luttinger Liquid associated to the C-IC transition. The values of β depend on the q-field and the interaction terms absorbed by the Luttinger parameter in the v-channel. We should not expect β to be closed to $\sqrt{4\pi}$ as in Eq.(3.8); the field $\tilde{\Theta}_v$ is not to be confused with Θ_v, they bosonize different fermions. A possible extension of the latter interaction Hamiltonian, still for small values of g_γ, is to consider the renormalization $g \to \sqrt{g^2 - g_\gamma^2}$, such that $2q$ is allowed to take values slightly below g. Indeed, the effective dimerization left in the commensurate phase, near the C-IC transition, could be made irrelevant by the presence of a sine-Gordon term with conjugated variables, such as the one in Eq.(3.20).

The fact that the sine-Gordon terms for strong and weak anisotropy seem to be related by a rotation of the quantized bosonic field is not fortuitous as one would expect a symmetry preserving field characterizing the whole critical line. This issue is partially solved by the canonic transformation of the Hamiltonian in Eq.(3.17), but in such approach keeping track of the Luttinger parameter is not so clear. An alternative is provided by non-abelian bosonization, where symmetry preserving fields are build from the start. We leave this for future work as it is beyond the level of experimental precision of our main results.

Chapter 4

Spinor gas of ^{40}K

Spin-changing collisions in ultracold alkali atoms offer the opportunity to study coherent spin-oscillations as it provides a scattering process by which particles change their hyperfine spin. In the case of spin-3/2 it corresponds to coherent oscillations between spin 3/2 and 1/2. These oscillations are similar to the quantum harmonic oscillator; in equilibrium, the oscillations are associated to zero point energy. The signal is stronger when the system is driven out of equilibrium, where greater oscillation amplitudes are expected. This comes at the cost of driving the system out of the linear regime where simple analytical models can describe the oscillations. As time goes on the system will relax to the ground state amplitude and frequency, up to thermal fluctuations. In [1] the four components ground state of an ultracold alkali gas ^{40}K is studied. Two ways of controlling scattering lengths were used: intensity modulation of the optical lattice and quadratic Zeeman coupling (QZC), as suggested in [57]

4.1 Experiment

The alkali metal ^{40}K has nuclear spin $I = 4$. The magnetic ground state, associated to its lower multiplet has 10 spinor components, it is a 9/2-manifold. It exhibits multiple spin-changing collisional channels, however, in an optical lattice this number is considerably reduced because many of them lead, on second order, to highly unstable configurations when combined with tunnelling processes. The dynamic signal in [1] confirms this behaviour showing that after quench from high to low magnetic fields only one channel is relevant. The coherent oscillations are between the populations $n_{9/2} + n_{1/2}$ and $n_{7/2} - n_{3/2}$.

4.2 4-component Hamiltonian

We identify the relevant spin changing channel of ^{40}K in [1] as the "chirality" channel in the spin-3/2 model, this suggests the choice of basis

$$n_v \equiv (n_{9/2} + n_{1/2} - n_{7/2} - n_{3/2})/2, \tag{4.1a}$$
$$n_c \equiv (n_{9/2} + n_{1/2} + n_{7/2} + n_{3/2})/2. \tag{4.1b}$$

Regarding the "polarization" channels $t_{1,2}$, all we know is that they should be orthogonal to the latter. We take the choice

$$n_{t_1} \equiv (n_{9/2} - n_{1/2} - n_{7/2} + n_{3/2})/2, \tag{4.2a}$$
$$n_{t_2} \equiv (n_{9/2} - n_{1/2} + n_{7/2} - n_{3/2})/2. \tag{4.2b}$$

An effective 4-component Hamiltonian for ^{40}K can be reconstructed

$$\begin{aligned}\mathcal{H}_{int,K}(j) &= \sum_{\alpha<\beta}\left[U_{\alpha,\beta}n_{\alpha,j}n_{\beta,j} + q\ \alpha^2 n_{\alpha,j}\right] \\ &+ U_\gamma\left[\psi^\dagger_{\frac{9}{2},j}\psi^\dagger_{\frac{1}{2},j}\psi_{\frac{7}{2},j}\psi_{\frac{3}{2},j} + H.c.\right],\end{aligned} \tag{4.3}$$

where $\alpha, \beta = \{9/2, 7/2, 3/2, 1/2\}$; $U_{\alpha,\beta}$ and the spin changing amplitude U_γ are linear combinations of the s-wave total spin scattering lengths: $\{a^K_n\}_{n=2,4,6,8}$, see App.C.2. The average scattering length $U = \frac{1}{6}\sum_\alpha U_{\alpha,\beta}$ is renormalized by modulating the intensity of the optical lattice. Interactions are given by

$$U_{7/2,9/2} \propto a^K_8, \tag{4.4a}$$
$$U_{3/2,9/2} \propto \left(\frac{7}{10}\ a^K_6 + \frac{3}{10}\ a^K_8\right), \tag{4.4b}$$
$$U_{1/2,9/2} \propto \left(\frac{3}{5}\ a^K_6 + \frac{2}{5}\ a^K_8\right), \tag{4.4c}$$
$$U_{3/2,7/2} \propto \left(\frac{2}{5}\ a^K_6 + \frac{3}{5}\ a^K_8\right), \tag{4.4d}$$
$$U_{1/2,7/2} \propto \left(\frac{50}{143}\ a^K_4 + \frac{3}{2\times 55}\ a^K_6 + \frac{81}{2\times 65}\ a^K_8\right), \tag{4.4e}$$
$$U_{1/2,3/2} \propto \left(\frac{25}{2\times 33}\ a^K_2 + \frac{75}{2\times 143}\ a^K_4 + \frac{7}{33}\ a^K_6 + \frac{21}{143}\ a^K_8\right), \tag{4.4f}$$
$$U_\gamma \propto \sqrt{\frac{3}{50}}\ (a^K_8 - a^K_6), \tag{4.4g}$$

where the common proportionality constant is $\frac{4\pi\hbar^2}{m}$. Recalling that Eq.(4.3) is an effective Hamiltonian but not yet restricted to the infrared (IR) limit, in [88] we used

Density-Matrix Renormalization Group (DMRG) to explore the phase diagram in a region of experimental relevance. In Fig.4.1 is depicted a three-critical region in the strong coupling regime. In App.C.1 is shown the corresponding values of interaction in terms recoil energy. Features such as Dimer, Singlet and Band Insulator phases can be ex-

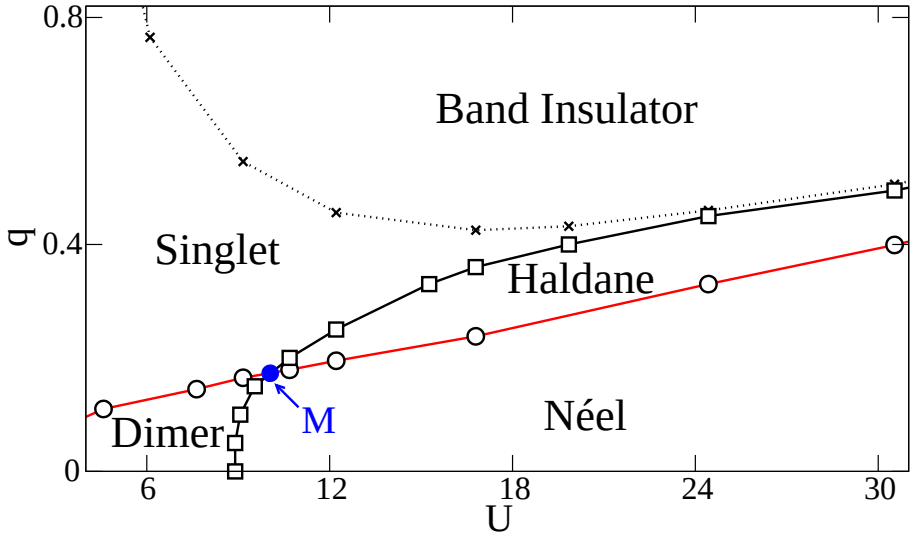

FIGURE 4.1: Phase diagram of 4-component mixture of ^{40}K atoms at half filling in the strong coupling regime. QZC versus average interaction U. Calculated using DMRG [88] –all DMRG calculations in [88] where done by Sebastian Greschner–. At point M an Ising criticality (red) intersects a gaussian criticality (solid black). The Singlet has a crossover (dashed line) into the Band Insulator for high enough QZC.

plained in the low energy theory of the spin-3/2 Hamiltonian, discussed in Ch.3. The magnetic Néel phase requires deviation from the exact spin-3/2 model.

4.3 Low energy theory

Upon bosonization the spin-spin interaction is

$$\begin{aligned}\mathcal{H}_{int,K}(x) &= \frac{1}{2(\pi a)^2}\left\{\left[U_{t1,v}\ cos\sqrt{4\pi}\Phi_{t_1} + U_{t2,v}\ cos\sqrt{4\pi}\Phi_{t_2}\right] cos\sqrt{4\pi}\Phi_v\right. \\ &+ U_\gamma\ \left[cos\sqrt{4\pi}\Phi_{t_1} + cos\sqrt{4\pi}\Phi_{t_2}\right]\ cos\sqrt{4\pi}\Theta_v \\ &+ \left. U_{t1,t2}\ cos\sqrt{4\pi}\Phi_{t_1} cos\sqrt{4\pi}\Phi_{t_2}\right\}, \end{aligned} \tag{4.5}$$

where

$$U_{t1,v} = U_{7/2,9/2} + U_{1/2,3/2}, \quad U_{t2,v} = U_{3/2,9/2} + U_{1/2,7/2}, \quad U_{t1,t2} = U_{1/2,9/2} + U_{3/2,7/2}.$$

At half filling, the interaction is dominated by the umklapp interaction

$$\begin{aligned}\mathcal{H}^{um}_{int,K}(x) &= \frac{1}{2(\pi a)^2}\Big\{cos\sqrt{4\pi}\Phi_c\ \Big[U^{um}_v\ cos\sqrt{4\pi}\Phi_v + U_\gamma\ cos\sqrt{4\pi}\Theta_v \\ &+ U^{um}_{t1}\ cos\sqrt{4\pi}\Phi_{t1} + U^{um}_{t2}\ cos\sqrt{4\pi}\Phi_{t2}\Big]\Big\}. \end{aligned} \tag{4.6}$$

where

$$U^{um}_v = U_{1/2,9/2} + U_{3/2,7/2}, \quad U^{um}_{t1} = U_{3/2,9/2} + U_{1/2,7/2}, \quad U^{um}_{t2} = U_{7/2,9/2} + U_{1/2,3/2}.$$

Compare with Eqs.(3.7) and (3.16). The mismatch $U^{um}_{t1} \neq U^{um}_{t2}$ introduce an asymmetry between Φ_{t1} and Φ_{t2} that makes possible the stabilization of a magnetic Néel. It takes place in the RG region $\langle cos\sqrt{4\pi}\Phi_v\rangle > \langle cos\sqrt{4\pi}\Theta_v\rangle$ at the strong coupling limit, Sect. 4.4. Following definitions in Eq.(2.29), its order parameter is given by

$$\mathcal{N} = (1/4)\sum_\alpha sign(\alpha)\ \mathcal{N}_\alpha, \tag{4.7}$$

where $\alpha = \{+3/2, +1/2, -1/2, -3/2\}$. The latter is maximized at $\langle\Phi_{3/2}\rangle = \langle\Phi_{1/2}\rangle = -\langle\Phi_{-1/2}\rangle = -\langle\Phi_{-3/2}\rangle = \sqrt{\pi}/4$ or, equivalently, $\langle\Phi_c\rangle = \langle\Phi_v\rangle = \langle\Phi_{t1}\rangle = \langle\Phi_{t2}\rangle - \sqrt{\pi}/2 = 0$. As the average interaction U decrease, the mismatch between Φ_{t1} and Φ_{t2} becomes irrelevant and the pinning of $\langle\Phi_{t2}\rangle$ goes to zero through a gaussian transition; the new phase maximize the Dimer order

$$\mathcal{D} = (1/4)\sum_\alpha \mathcal{D}_\alpha. \tag{4.8}$$

Increasing the QZC in the Néel phase change –via Ising transtition– the dominant order in the chirality channel from $\langle cos\sqrt{4\pi}\Phi_v\rangle$ to $\langle cos\sqrt{4\pi}\Theta_v\rangle$. The relevant interaction becomes

$$\mathcal{H}_{Haldane} = \frac{-1}{2(\pi a)^2}\langle cos\sqrt{4\pi}\Phi_c\rangle\ (U^{um}_\gamma\ cos\sqrt{4\pi}\Theta_v + U^{um}_{t2}\ cos\sqrt{4\pi}\Phi_{t2}) \tag{4.9}$$

which for relevant $\langle cos\sqrt{4\pi}\Phi_{t2}\rangle$ exhibits maximal string order, Eq.(4.16c). As the average interaction U decreases it undergoes a gaussian transition into a singlet phase where the Néel diluted excitations, characteristic of the Haldane phase, totally vanish. The singlet ground state is determined in Sec.3.3 in the context of exact spin-3/2 and adapted to the components of ^{40}K through the mapping in Eq.(4.1). To discard the possibility of the Haldane phase being a finites size effect, in Fig.4.3 we report the finite size analysis for the Ising transition from Néel to Haldane phase.

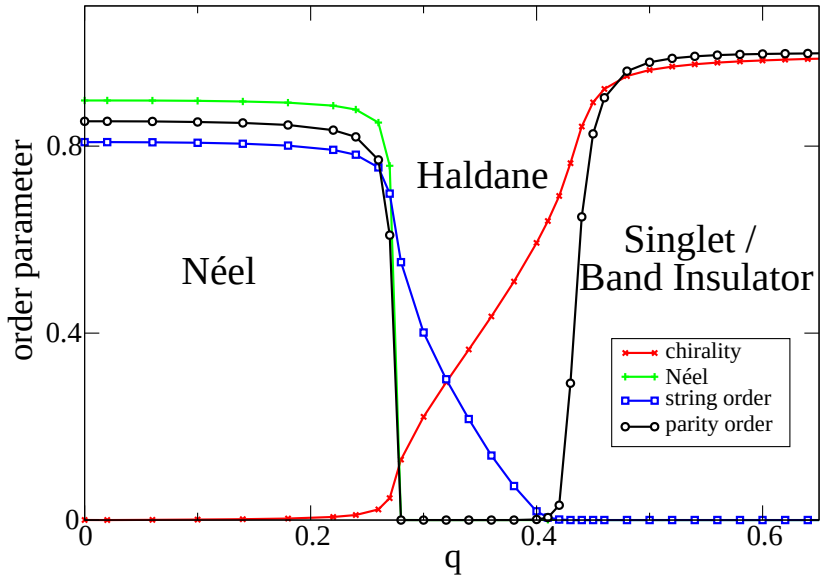

FIGURE 4.2: Order parameters along the vertical cross section $U = 20$ in the phase diagram of Fig.4.1.

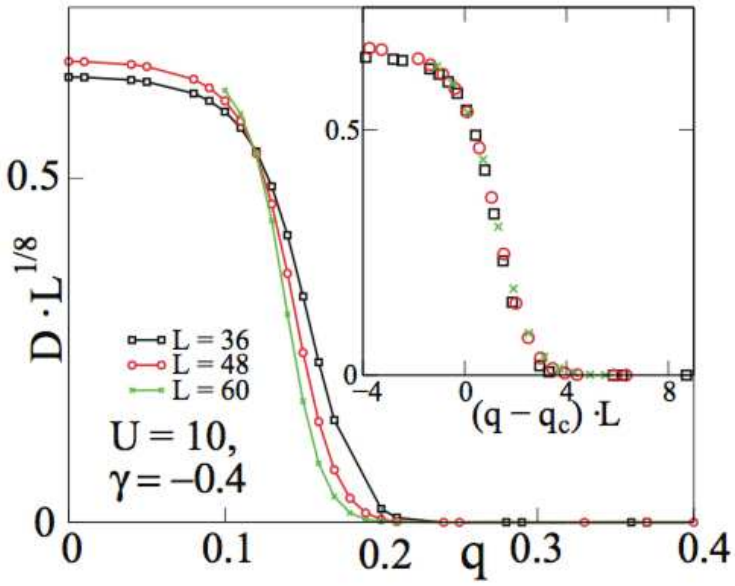

FIGURE 4.3: Scaling of the Dimer parameter against QZC in the vicinity of the Dimer-to-Singlet phase. The inset shows data collapse confirming the Ising criticality.

4.4 Strong coupling analysis

To determine which channel is responsible for the Néel order we study the limit $t/U \to 0$, where the smaller onsite interaction should be favored. Three candidates are depicted in Fig.4.4, one for every spin channel. Even for low QZC the v-Néel state is unstable due to small but non vanishing spin-changing collisions. Using the scattering lengths in

[1] (units of Bohr radius): $a_2^K = 147.83,\ a_4^K = 161.11,\ a_6^K = 166.00,\ a_8^K = 168.53$ one finds that

$$(U_{7/2,9/2} + U_{1/2,3/2}) < (U_{3/2,9/2} + U_{1/2,7/2}) < (U_{1/2,9/2} + U_{3/2,7/2}), \tag{4.10}$$

with a difference proportional to the overall average interaction U in Fig.4.1. The minimal energy is associated to pairs $\psi^\dagger_{7/2}\psi^\dagger_{9/2}$ and $\psi^\dagger_{1/2}\psi^\dagger_{3/2}$. At half filling (for every pair) and zero hopping the degeneracy is $N!/(N/2)!^2$. One can introduce an effective spin-1/2 chain by restricting to the low energy states

$$|\uparrow\rangle_j = \psi^\dagger_{j,7/2}\psi^\dagger_{j,9/2}|0\rangle, \quad |\downarrow\rangle_j = \psi^\dagger_{j,1/2}\psi^\dagger_{j,3/2}|0\rangle, \tag{4.11}$$

where $\psi_{7/2}\psi_{9/2}|0\rangle = \psi_{1/2}\psi_{3/2}|0\rangle = 0$; with spin operators

$$\tilde{S}^z_j = \frac{1}{4}(n_{j,9/2} + n_{j,7/2} - n_{j,1/2} - n_{j,3/2}) = \frac{1}{2}n_{j,t2}, \tag{4.12}$$

$$\tilde{S}^+_j = \psi^\dagger_{9/2}\psi^\dagger_{7/2}\psi_{1/2}\psi_{3/2}. \tag{4.13}$$

The Néel order is predicted by the perturbative effect of tunneling; in the strong coupling

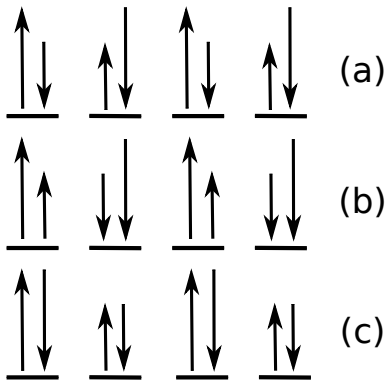

FIGURE 4.4: Three classical Néel states as possible configurations for ^{40}K at half filling: (a) t_1-Néel, (b) t_2-Néel and (c) v-Néel. The latter is highly unstable due to the presence of spin changing collisions.

limit the Hamiltonian in Eq.(4.3) becomes

$$\mathcal{H}_{eff} = J^z_i \sum_i \tilde{S}^z_i \tilde{S}^z_{i+1} + J^{xy}_i (\tilde{S}^+_i \tilde{S}^-_{i+1} + H.c), \tag{4.14}$$

where $J^z_i \sim t^2/U$ and $J^{xy}_i \sim t^4/U^3$. Contrast this with the strong coupling result for exact spin-1/2 in Eq.(1.16) or with the symmetries of the exact spin-3/2. The latter has an $SO(5)$ symmetry in its Dimer phase, reduced to $SU(2) \times SU(2)$ in the presence of QZC. The four components projected from the 9/2−manyfold of ^{40}K, in general, only retain $U(1) \times U(1)$ symmetry from the filling constrain $N_{9/2} - N_{7/2} = N_{3/2} - N_{1/2} = 0$. This is a fundamental difference between ^{40}K and alkali metals with exact hyperfine

spin-3/2 such as ^{4}Be, ^{132}Cs and ^{201}Hg. To explain the transition to a Haldane phase

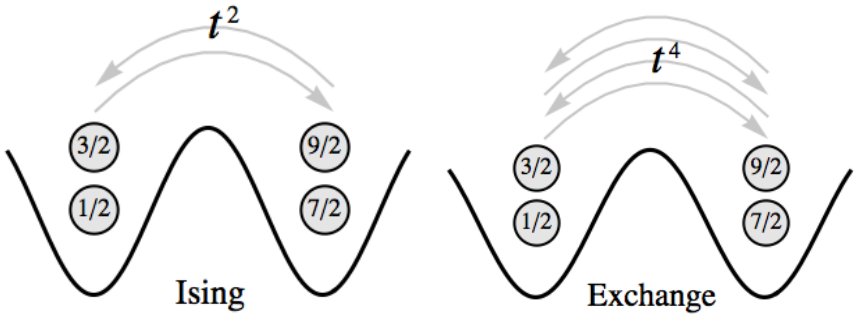

FIGURE 4.5: Formation of Néel phase at half filling: first two leading orders in the strong coupling regime of 4-component alkali metal ^{40}K. The Ising interaction stabilize Néel order; it is realized by hopping forward and backward of one atomic specie; in contrast, the exchange process requires hopping of each of the four atoms.

when increasing the QZC, the spin chain in Eq.(4.14) must be extended to spin-1 by taking into account the singlets generated by spin changing collisions (Sec.3.3), i.e.

$$|\tilde{S}^z = \pm 1/2\rangle \quad \longrightarrow \quad |S^z = \pm 1\rangle, \tag{4.15a}$$

$$|S^z = 0\rangle \quad = \quad \psi^\dagger_{9/2}\psi^\dagger_{1/2} - \psi^\dagger_{7/2}\psi^\dagger_{3/2}. \tag{4.15b}$$

Since the transition to Haldane phase takes place near a band insulator induced by the QZC, we should expect an imbalance between $\psi^\dagger_{9/2}\psi^\dagger_{1/2}$ and $\psi^\dagger_{7/2}\psi^\dagger_{3/2}$. In this effective basis, the Néel, parity, and string order parameters are

$$\mathcal{N} \quad = \quad \lim_{n\gg 1}(-1)^n\langle S^z_j S^z_{j+n}\rangle, \tag{4.16a}$$

$$\mathcal{O}_P \quad = \quad \langle exp[i\pi \sum_j S^z_j]\rangle, \tag{4.16b}$$

$$\mathcal{O}_S \quad = \quad \langle S^z_j exp[i\pi \sum_j S^z_j] S^z_{j+n}\rangle. \tag{4.16c}$$

Their values are reported in Fig.4.2 for a cross section of the phase diagram in Fig.4.1 starting from the Néel phase ($U = 20$) and changing QZC from zero to saturation values. As ilustrated in Fig.4.6, string order captures non-local Néel order while absence of parity order confirms these are not diluted excitations on top of the band insulator background [91].

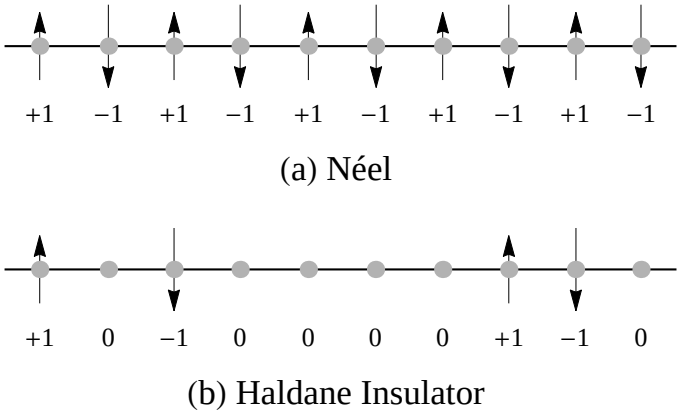

FIGURE 4.6: In the Haldane insulator local singlets dilute magnetic sates preserving global Néel order.

Chapter 5

Spin-orbit coupling in optical lattices

Along the developments in quantum Hall physics and topological insulators is the interest to realize synthetic electromagnetism in optical lattices where many parameters can become dynamic and fined tuned. Spin-orbit coupling (SOC) plays a key role in the formation of the spin Hall effect [92]; in 2D it is realized by a linear combination of Rashba $\alpha(\sigma_x k_y - \sigma_y k_x)$ and Dresselhaus $\beta(\sigma_x k_y + \sigma_y k_x)$ terms. In ultracold neutral atoms there is no natural coupling between the spin and the position of the atom. There have been proposed optical and magnetic schemes to induce SOC in ultracold atoms [93, 94]; in particular, unidirectional spin-orbit coupling (USOC): $\alpha = \beta$, has been realized in both spinor Bose [95] and Fermi gases [96, 97] allowing the observation of the spin Hall effect [98] among other interesting phenomena.

In [2] we report the study of USOC and isotropic SOC for a two component Fermi gas loaded in an optical lattice in the Mott-insulator regime. Some of the results are based on DMRG numeric calculations, in particular the calculation of the non-Abelian vector potential. In the present chapter we emphasize such cases where analytic techniques are at hand, in particular the strong rung-coupling approach and, for weakly coupled chains, bosonization. Consider the Fermi-Hubbard model

$$\mathcal{H}_{FH} = -\sum_{(i,i'),\sigma,\sigma'} t_{i,i'} \sigma^0_{\sigma,\sigma'} a^\dagger_{i,\sigma} a_{i',\sigma'} + \frac{U}{2} \sum_i n_i(n_i - 1). \tag{5.1}$$

The SOC is introduced by the Peierls substitution $t_{i,i'} \to t_{i,i'} exp(i\frac{\mathbf{A}(\mathbf{r}_{i'}-\mathbf{r}_i)}{\hbar})$. One gets

$$\begin{aligned}\mathcal{H} &= J_{\parallel}\sum_{\sigma,j}\{cos(2k_0^x a)\mathbf{S}_{\alpha,j}\mathbf{S}_{\alpha,j+1} + 2sin(k_0^x a)S^z_{\alpha,j}S^z_{\alpha,j+1} \\ &- sin(2k_0^x a)[\mathbf{S}_{\alpha,j}\times\mathbf{S}_{\alpha,j+1}]^z\} \\ &+ J_{\perp}\sum_{j}\{cos(2k_0^y a)\mathbf{S}_{1,j}\mathbf{S}_{2,j} + 2sin(k_0^y a)S^z_{1,j}S^z_{2,j} \\ &+ 2sin(2k_0^y a)[\mathbf{S}_{1,j}\times\mathbf{S}_{2,j}]^z\} + \delta\sum_{\alpha,j}S^z_{\alpha,j} - h\sum_{\alpha,j}S^x_{\alpha,j}, \end{aligned} \tag{5.2}$$

where $J_{\parallel} = 4t_x^2/U,\ J_{\perp} = 4t_y^2/U$ and

$$\mathbf{S}_{\alpha,j} = (a^{\dagger}_{\alpha,j,\uparrow}, a^{\dagger}_{\alpha,j,\downarrow})\frac{\vec{\sigma}}{2}\begin{pmatrix} a_{\alpha,j,\uparrow} \\ a_{\alpha,j,\downarrow}\end{pmatrix}. \tag{5.3}$$

The latter Hamiltonian replicates the USOC Hamiltonian

$$H_{USOC} = \frac{1}{2m}(\mathbf{p}\sigma^0 - \mathbf{A})^2 + \frac{\delta}{2}\sigma^z - \frac{h}{2}\sigma^x, \tag{5.4}$$

where $\sigma^{x,y,z}$ are the Pauli matrices, σ^0 is the identity matrix, and $\mathbf{A} = -\hbar\mathbf{k}_0\sigma^z$, with $\mathbf{k}_0 = (k_0^x, k_0^y, 0)$ is the counter-propagating Raman laser on the xy plane provided in Eq.(5.2) by the Dzyaloshinski-Moriya (DM) terms ($\sim [\mathbf{S}_{\alpha,j}\times\mathbf{S}_{\alpha',j'}]^z$) and the anisotropy along $\mathbf{e}_z$.

5.1 Decoupled chains ($J_{\perp} = 0$)

A. Respulsive interactions

The Hamiltonian for decoupled chains is given by

$$\begin{aligned}H_{1D} &= J_{\parallel}\sum_i [S^z_j S^z_{j+1} + cos(2k_0^x a)\ (S^x_j S^x_{j+1} + S^y_j S^y_{j+1}) \\ &+ sin(2k_0^x a)\ (S^x_j S^y_{j+1} + S^y_j S^x_{j+1})] - h\sum_j S^x_j. \end{aligned} \tag{5.5}$$

Noting that the basis

$$\bar{S}^x_{\alpha,j} = cos(2k_0^x aj)S^x_{\alpha,j} - sin(2k_0^x aj)S^y_{\alpha,j}, \tag{5.6a}$$

$$\bar{S}^y_{\alpha,j} = cos(2k_0^x aj)S^y_{\alpha,j} + sin(2k_0^x aj)S^x_{\alpha,j}, \tag{5.6b}$$

$$\bar{S}^z_{\alpha,j} = S^z_{\alpha,j}, \tag{5.6c}$$

is such that

$$\begin{aligned} cos(2k_0^x a)(S_j^x S_{j+1}^x + S_j^y S_{j+1}^y) &= cos^2(2k_0^x a)(\bar{S}_j^x \bar{S}_{j+1}^x + \bar{S}_j^y \bar{S}_{j+1}^y) \\ &+ cos(2k_0^x a) sin(2k_0^x a)(\bar{S}_j^x \bar{S}_{j+1}^y - \bar{S}_j^y \bar{S}_{j+1}^x), \\ sin(2k_0^x a)(S_j^x S_{j+1}^y - S_j^y S_{j+1}^x) &= sin(2k_0^x a) cos(2k_0^x a)(\bar{S}_j^x \bar{S}_{j+1}^y - \bar{S}_j^y \bar{S}_{j+1}^x) \\ &- sin^2(2k_0^x a)(\bar{S}_j^x \bar{S}_{j+1}^x + \bar{S}_j^y \bar{S}_{j+1}^y), \end{aligned}$$

we rewrite Eq.(5.5) as

$$\bar{H}_{1D} = J_{\parallel} \sum_i \bar{\mathbf{S}}_j \bar{\mathbf{S}}_{j+1} - \sum_j \mathbf{h}_j(\mathbf{k}_0) \bar{\mathbf{S}}_j. \tag{5.7}$$

where $\mathbf{h}_j(\mathbf{k}_0) = h(cos(2k_0^x a), sin(2k_0^x a), 0)$. From low energy analysis is easy to see that the case $k_0^x a = \pi/2$ favors Néel order; after the Jordan-Wigner transformation (with gauge)

$$\bar{S}_r^+ \rightarrow (-1)^r c_r^\dagger \; exp\left(i\pi \sum_{j=-\infty}^{r-1} c_j^\dagger c_j + 1/2 \right), \tag{5.8a}$$

$$\bar{S}_r^z = c_r^\dagger c_r - 1/2. \tag{5.8b}$$

one gets the fermionic Hamiltonian

$$\mathcal{H}_{1D} = -t \sum_r [c_{r+1}^\dagger c_r + H.c.] + V \sum_r (c_{r+1}^\dagger c_{r+1} - 1/2)(c_r^\dagger c_r - 1/2) \tag{5.9}$$

where $2t = V = J_{\parallel}$. After bosonization at half filling ($k_F = \pi/2$)

$$\mathcal{H}_{1D} = \int dx \left[uK(\partial_x \Theta(x))^2 + \frac{u}{K}(\partial_x \Phi(x))^2 - \frac{2aJ_{\parallel}}{(2\pi\alpha)^2} cos(4\Phi(x)) \right], \tag{5.10a}$$

$$uK = v_F = J_{\parallel} a \; sin(k_F a), \tag{5.10b}$$

$$u/K = v_F \left(1 + \frac{2J_{\parallel} a}{\pi v_F} [1 - cos(2k_F a)] \right). \tag{5.10c}$$

For the $SU(2)$-symmetric Hamiltonian ($J_{xy} = J_z$): $K = 1/2$; the umklapp term is marginal and the system is a Luttinger liquid (LL). Note that in the quantization axis $\mathbf{e}_x$, the operator S^x yields

$$\bar{S}^x(x) = -\frac{1}{\pi} \partial_x \Phi(x) + \frac{(-1)^x}{\pi\alpha} cos(2\Phi(x)). \tag{5.11}$$

In the case $k_0^x a = 0$ the relevant part of the external magnetic field is the linear potential $\partial_x \Phi(x)$, the system undergoes a commensurate-incommensurate (C-IC) transition at $h_c = 2J_{\parallel}$ to a fully polarized chain along $\mathbf{e}_x$. For $k_0^x a = \pi/2$ a staggered magnetic field

is generated: $\mathbf{h}_j = (-1)^j h\mathbf{e}_x$ that stabilize Néel order as it couples to the staggered part of $\bar{S}^x(x)$. A gap $\Delta E \sim h^{2/3}$ opens in the excitation spectrum [99]. In the original Hamiltonian, Eq.(5.5), the Néel configuration corresponds to a ferromagnetic state (F). Departure from $k_0^x a = \pi/2$ introduces oscillatory terms in the density wave that revive the Luttinger liquid phase for finite magnetic fields. The phase diagram for arbitrary values of USOC is depicted in Fig.5.1.

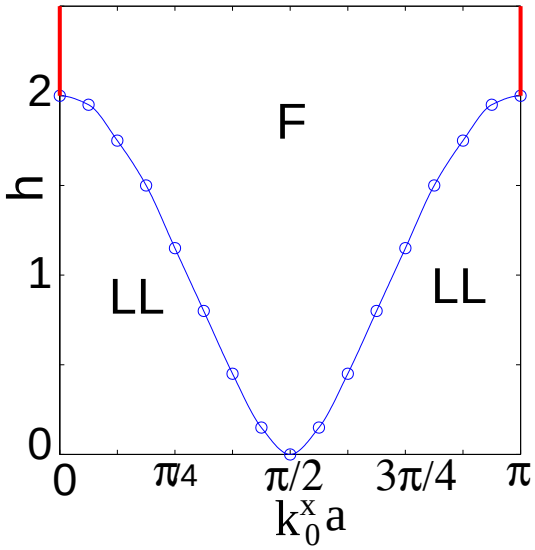

FIGURE 5.1: Phase diagram of a 1D spin-1/2 chain with USOC and transverse magnetic field using DMRG for 96 sites –all DMRG calculations in [2] where done by Gaoyong Sun–. The magnetic field is in units of $J_{\parallel}$. LL, Luttinger Liquid phase; F, ferromagnetic state.

B. Attractive interactions

We consider two component Fermions at half filling near maximal USOC, $k_0^x a \simeq \pi/2$. The system is dual to the repulsive ionic-Hubbard model [100–102]; It is characterized by a superconducting phase that for increasing magnetic field first undergoes a Kosterlitz-Thouless transition into a dimerized (D) and eventually an Ising transtion into F order.

5.2 USOC along ladder rungs ($k_0^x = 0$)

For the case $k_0^y a = 0$, increasing the external magnetic field brings a commensurate-incommensurate (C-IC) transition from rung-singlet (RS) into a Luttinger Liquid (LL)

and eventually a fully polarized F order. To study $k_0^y a = \pi/2$ consider again the basis

$$\bar{S}^x_{\alpha,j} = cos(2k_0^y a\alpha)S^x_{\alpha,j} - sin(2k_0^y a\alpha)S^y_{\alpha,j}, \tag{5.12a}$$
$$\bar{S}^y_{\alpha,j} = cos(2k_0^y a\alpha)S^y_{\alpha,j} + sin(2k_0^y a\alpha)S^x_{\alpha,j}, \tag{5.12b}$$
$$\bar{S}^z_{\alpha,j} = S^z_{\alpha,j}, \tag{5.12c}$$

the Hamiltonian in Eq.(5.2) becomes

$$\bar{\mathcal{H}} = J_\parallel \sum_{\alpha=(1,2),j} \bar{\mathbf{S}}_{\alpha,j}\bar{\mathbf{S}}_{\alpha,j+1} + J_\perp \sum_{\alpha=j} \bar{\mathbf{S}}_{1,j}\bar{\mathbf{S}}_{2,j} - h \sum_{\alpha=(1,2),j} (-1)^\alpha \bar{S}^x_{\alpha,j}. \tag{5.13}$$

In the strong-rung-coupling limit ($J_\perp \gg J_\parallel$), the ground state becomes a rung-product state of the form

$$|\bar{RS}\rangle = \prod_j (|\bar{\uparrow}_{1,j}\rangle \otimes |\bar{\downarrow}_{2,j}\rangle - \beta|\bar{\downarrow}_{1,j}\rangle \otimes |\bar{\uparrow}_{2,j}\rangle)/\sqrt{1+\beta^2}, \tag{5.14}$$

where $\{\bar{\uparrow}, \bar{\downarrow}\}$ refer to the eigenstates of $\bar{S}^x$. For increasing magnetic field h the ground state goes from singlet ($\beta = 1$) to F order ($\beta = 0$).
The intermediate regime ($h \sim J_\perp$) can be addressed through an effective spin-1/2 model where the rung singlet and the positive eigenstate of S^x correspond to pseudo-spin states down and up, respectively [103, 104]. Starting from Eq.(5.13) one obtains the effective Hamiltonian (see D)

$$H_\tau = J_\parallel \sum_j \left(\frac{1}{2}\tau^x_j\tau^x_{j+1} + \tau^y_j\tau^y_{j+1} + \tau^z_j\tau^z_{j+1}\right) - h_x \sum_j \tau^x_j + h_y \sum_j \tau^y_j. \tag{5.15}$$

where $h_x = h - J_\perp cos2k_0^y a - J_\perp(1 - cos2k_0^y a)/4 - J_\parallel/2$ and $h_y = -J_\perp sin2k_0^y a/\sqrt{2}$. The model exhibits three ground-state phases: two F phases –actual RS phase of the ladder– are separated by a Néel phase via an Ising transition. The DM term plays a key role in the formation of the Néel phase as it breaks the $U(1)$ symmetry along the yz plane.

On the other hand, bosonization provides an exact effective description for the weakly coupled chains, $J_\perp \ll J_\parallel$. Setting

$$S^x_{\alpha,j} \to \frac{\partial_x\Phi_\alpha}{\sqrt{2\pi}} + (-1)^j sin\sqrt{2\pi}\Phi_\alpha, \tag{5.16}$$
$$S^y_{\alpha,j} \to (-1)^j sin\sqrt{2\pi}\Theta_\alpha, \tag{5.17}$$
$$S^z_{\alpha,j} \to (-1)^j cos\sqrt{2\pi}\Theta_\alpha, \tag{5.18}$$

where $\alpha = 1, 2$; upon further transformation of the bosonic basis: $\Theta_\pm = (\Theta_1 \pm \Theta_2)/\sqrt{2}$ and $\Phi_\pm = (\Phi_1 \pm \Phi_2)/\sqrt{2}$, one obtains the low energy Hamiltonian

$$\begin{aligned}\mathcal{H}_B = \quad & \sum_{\nu=\pm} \frac{v_\nu}{2}[(\partial_x\Phi_\nu)^2 + (\partial_x\Theta_\nu)^2] - h\partial_x\Phi_+/\sqrt{\pi} \\ & +\tilde{J}_\perp(2cos\sqrt{4\pi}\Theta_- - cos\sqrt{4\pi}\Phi_+ + cos\sqrt{4\pi}\Phi_-) \\ & +\tilde{d}_\perp(cos\sqrt{\pi}\Phi_+ sin\sqrt{\pi}\Theta_+ sin\sqrt{\pi}\Phi_- cos\sqrt{\pi}\Theta_- \\ & -sin\sqrt{\pi}\Phi_+ cos\sqrt{\pi}\Theta_+ cos\sqrt{\pi}\Phi_- sin\sqrt{\pi}\Theta_-) \\ & +d_\perp(cos\sqrt{4\pi}\Theta_- + cos\sqrt{4\pi}\Theta_+), \end{aligned} \tag{5.19}$$

where

$$v_\pm = \frac{J_\parallel a\pi}{2}\left(1 \pm \frac{J_\perp cos(2k_0^y a)}{J_\parallel \pi^2}\right) \tag{5.20}$$

and $\tilde{J}_\perp = J_\perp cos(2k_0^y a)$. For $k_0^y a \ll 1$ ($d_\perp, \tilde{d}_\perp \ll \tilde{J}_\perp$) the antisymmetric sector remains gapped with $\langle\Theta_-\rangle = \sqrt{\pi}/2$, while the symmetric sector is dominated by the magnetic field. In general, the symmetric sector is quadratic in the leading terms and can be solved by a Bogoliubov transformation via Jordan-Wigner mapping. Increasing magnetic field takes the system from RS to Néel state (with order parameter $n = (-1)^{j+\alpha}\langle S^z_{\alpha,j}\rangle$) and eventually to the F phase. Figure 5.2 shows the pattern characterizing the Néel state.

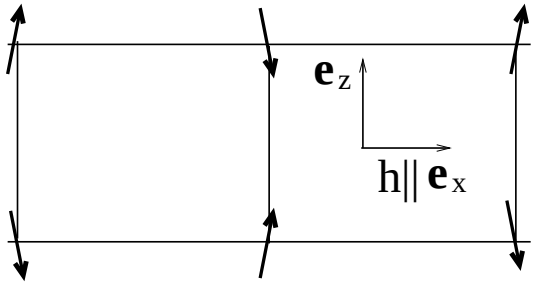

FIGURE 5.2: Néel-state configuration for USOC along rungs. The inter-leg correlations are also antiferromagnetic: $\langle S^z_{1,i} S^z_{2,j}\rangle \sim (-1)^{i-j+1}$.

5.3 Conclusion

A two-leg ladderlike lattice at half filling is a minimal system to study the non-Abelian character of the vector potential. In particular. It is shown that for USOC along the ladder rungs the Néel-state phase is located within the RS-F phase; this is experimentally significant since the RS is adiabatically connected to an F phase in the parameter space

of h and the SOC. For USOC along the ladder legs, in contrast, such adiabatic connection is lost –the Néel phase separates the RS and F states.

Appendix A

Renormalization Group

Consider the bosonic Hamiltonian

$$\begin{aligned}\mathcal{H} &= \mathcal{H}_0 + \mathcal{H}_{int},\\ \mathcal{H}_0 &= \frac{1}{2\pi}\int dx\left[uK(\partial_x\theta)^2 + \frac{u}{K}(\partial_x\phi)\right],\end{aligned}$$

where $\mathcal{H}_{int}$ are sine-Gordon terms (short range interactions). To compute correlators we take the action into imaginary time. By Legendre transformation

$$S = \int_0^\beta d\tau \int dx\{-\frac{i}{\pi}\partial_x\theta\partial_\tau\phi + \mathcal{H}\}.$$

As $\partial_x\theta$ is the conjugate of ϕ, i.e. $[\phi(x), \partial_x\theta(x')] = i\hbar\delta(x-x')$, the equations of motion yield $uK\partial_x\theta = i\partial_\tau\phi$. Hence

$$S = \int_0^\beta d\tau \int dx\{\frac{(\partial_\tau\phi)^2}{2\pi uK} + \frac{u}{K}(\partial_x\phi)^2 + \mathcal{H}_{int})\}.$$

Using Wilson-like renormalization method

$$\begin{aligned}\frac{Z}{Z_0} = \frac{1}{Z_0}\int \mathcal{D}\phi\; e^{-(S_0^< + S_0^>)}e^{-S_{int}[\phi]} &= \frac{1}{Z_0^<}\int \mathcal{D}\phi\; e^{-S_0^<}\left\langle e^{-S_{int}[\phi]}\right\rangle_>\\ &= \frac{1}{Z_0^<}\int \mathcal{D}\phi\; e^{-S_0^<}e^{-S_{int}[\phi^<]} = \frac{Z^<}{Z_0^<}.\end{aligned}$$

To get $S_{int}[\phi^<]$ we treat interactions perturbatively

$$\left\langle e^{-S_{int}[\phi]}\right\rangle_> \approx (1 - \langle S_{int}[\phi]\rangle_> + \frac{1}{2}\langle S_{int}[\phi]^2\rangle_>),$$

Then we exponentiate again to get an approximation for $S_{int}[\phi^<]$.

A.1 RG of Spin-3/2

A.1.1 Quarter filling

For the first order corrections we notice that $S_{int}[\phi]$ has terms like[1]

$$\begin{aligned} cos\sqrt{4\pi}(\phi_t^< + \phi_t^>)cos\sqrt{4\pi}(\phi_v^< + \phi_v^>) &= (cos\sqrt{4\pi}\phi_t^<\ cos\sqrt{4\pi}\phi_t^> - sin\sqrt{4\pi}\phi_t^<\ sin\sqrt{4\pi}\phi_t^>) \\ &\quad (cos\sqrt{4\pi}\phi_v^<\ cos\sqrt{4\pi}\phi_v^> - sin\sqrt{4\pi}\phi_v^<\ sin\sqrt{4\pi}\phi_v^>). \end{aligned}$$

Since we have a free-particles ground state we can treat all fields separately. And since we are not integrating along all the modes, but only high frequencies, the resulting correlators are not expected to be always zero as it would be expected from the translation invariance of the total action. Keeping in mind that,

$$\langle cos\sqrt{4\pi}\phi^> \rangle_> = \frac{1}{2}\ (e^{-2\pi\langle(\phi^>)^2\rangle_>} + e^{-2\pi\langle(\phi^>)^2\rangle_>}) = e^{-2\pi\langle(\phi^>)^2\rangle_>}, \quad \langle sin\sqrt{4\pi}\phi^> \rangle_> = 0.$$

The correlator $\langle(\phi^>)^2\rangle_>$ is easy to compute for free particles by going into k-space. It yields

$$\langle(\phi^>)^2\rangle_> = \frac{K}{2\pi}\ ln\left(\frac{\Lambda}{\Lambda'}\right),$$

where Λ is the renormalization cutoff. We obtain

$$\begin{aligned} \langle cos\sqrt{4\pi}(\phi_t^< + \phi_t^>)cos\sqrt{4\pi}(\phi_v^< + \phi_v^>)\rangle_> &= \langle cos\sqrt{4\pi}\phi_t^> \rangle_> \langle cos\sqrt{4\pi}\phi_v^> \rangle_> cos\sqrt{4\pi}\phi_t^<\ cos\sqrt{4\pi}\phi_v^< \\ &= \left(\frac{\Lambda'}{\Lambda}\right)^{K_t+K_v} cos\sqrt{4\pi}\phi_t^<\ cos\sqrt{4\pi}\phi_v^< \end{aligned}$$

Hence, including the renormalization factor of the integration variables $dx'dt' = (\Lambda/\Lambda')^2 dxdt$, we get[2]

$$g(\Lambda') = \left(\frac{\Lambda}{\Lambda'}\right)^2 \left(\frac{\Lambda'}{\Lambda}\right)^{K_t+K_v} g(\Lambda).$$

Assuming a differential scaling transformation: $\Lambda' = \Lambda + d\Lambda$ and reparametrizing the scaling parameters by a relative scaling length: $(\Lambda/\Lambda') = e^{dl}$ we obtain

$$g(dl) = e^{dl(2-K_t-K_v)} g(0) \quad \Rightarrow \quad \frac{dg}{dl} \approx (2 - K_t - K_v)\ g.$$

[1] Keep in mind the normal ordering and also the Klein factors which are not written explicitly.

[2] Notice this relation is a statement about the stability of the variational solution of the action; it amounts to assuming conformal transformation of interactions under rescaling: $\mathcal{O}_i(l+dl) = \Gamma_i(dl)\ \mathcal{O}_i(l)$.

In the spin-channel the microscopic Luttinger parameters are related to the sine-gordon interactions. Using such relations perturbatively $K_\sigma \approx 1 - g_\sigma/(2\pi)$ we arrive at the scaling equations

$$\dot{g} \approx (g_t + g_v)\frac{g}{2\pi}.$$

where $\dot{g} \equiv dg/dl$. From the complete interactions

$$S_{int} = (g_t + g_v)\ \mathcal{O}_1 + (g_t - g_v)\ \mathcal{O}_2 + 2g_t\ \mathcal{O}_3,$$

where[3]

$$\mathcal{O}_1 = \frac{cos\sqrt{4\pi}\phi_t\ cos\sqrt{4\pi}\phi_v}{(\sqrt{2}\pi a)^2},\quad \mathcal{O}_2 = \frac{cos\sqrt{4\pi}\phi_t\ cos\sqrt{4\pi}\theta_v}{(\sqrt{2}\pi a)^2},\quad \mathcal{O}_3 = \frac{cos\sqrt{4\pi}\phi_{t1}\ cos\sqrt{4\pi}\phi_{t2}}{(\sqrt{2}\pi a)^2}.$$

we arrive to the first order corrections in Eqs.(A.1). As for the second order contributions, coming from $S_{int}[\phi]^2$, these are derived from the operator product expansion

$$\begin{aligned} g_i g_j\ \langle \mathcal{O}_i(z)\mathcal{O}_j(z')\rangle_> &= \pi C_{ij}^k\ \frac{g_i g_j}{(\sqrt{2}\pi a)^2}\left(\frac{\Lambda}{\Lambda'}\right)^4\left(\frac{\Lambda'}{\Lambda}\right)^{K_k}\mathcal{O}_k^<(z), \quad (z \to z'), \\ \Rightarrow\quad \frac{dg_k}{dl} &\approx (...) - \frac{1}{2}\left[\pi C_{ij}^k\ \frac{2g_i g_j}{(\sqrt{2}\pi a)^2}\right], \end{aligned}$$

where C_{ij}^k are the structure constant of the algebra associated to the short range product expansion; if we use the current algebra, for the case of spin-3/2, it corresponds to the generators of $SO(5)$, while in the bosonization language it is associated to the Klein factors. is the Levy-Civita tensor. The rule for contractions is to cancel repeated sine-Gordon terms. For example the contraction[4]

$$\langle cos\sqrt{4\pi}\phi_{t_1} cos\sqrt{4\pi}\phi_v cos\sqrt{4\pi}\phi'_{t_1} cos\sqrt{4\pi}\phi'_{t_2}\rangle_> \propto \langle cos\sqrt{4\pi}\phi'_{t_2} cos\sqrt{4\pi}\phi_v\rangle_>.$$

leads to a contribution of $(g_t+g_v)(2g_t)$ to $(\dot{g}_t+\dot{g}_v)$ as these are the interactions associated to the terms at left and right hand side of the latter equation. In that way we arrive to

[3] Actually $\mathcal{O}_1 = (cos\sqrt{4\pi}\phi_{t1} + cos\sqrt{4\pi}\phi_{t2})\ cos\sqrt{4\pi}\phi_v$, but its RG is the same because $K_{t1} = K_{t2}$. Idem for $\mathcal{O}_2$. We should specify it when necessary.

[4] I didn't derive the sign of ϵ_{ij}^k. It was choose to match Wu's article. It kind of has sense because we are exchanging vertex operators with Klein factors. Since the correlator is not over all modes the algebra is not closed. To assure the latter, in addition to $z \to z'$, we need to restrict to $g \to 0$. We were already in such regime, so is not a problem.

corrections

$$\dot{g}_t + \dot{g}_v \approx \frac{1}{2\pi}\left[\underbrace{(g_t+g_v)^2}_{S_{int}[\phi]} + \underbrace{(g_t+g_v)(2g_t)}_{\frac{1}{2}S_{int}[\phi]^2}\right], \tag{A.1a}$$

$$\dot{g}_t - \dot{g}_v \approx \frac{1}{2\pi}\left[(g_t-g_v)^2 + (g_t-g_v)(2g_t)\right], \tag{A.1b}$$

$$\dot{g}_t \approx \frac{1}{2\pi}\left[(2g_t)^2 + (g_t-g_v)^2 + (g_t+g_v)^2\right]. \tag{A.1c}$$

Which is

$$\dot{g}_v = \frac{4}{2\pi}g_v g_t, \qquad \dot{g}_t = \frac{1}{2\pi}(3g_t^2+g_v^2), \qquad \dot{g}_c = 0. \tag{A.2}$$

Where the last term states the absence of Umklapp terms in the charge channel.

A.1.2 Half filling

At half filling umklapp terms are relevant. In addition to the former interactions we include terms from Eq.(3.16). Contractions such as

$$\langle cos\sqrt{4\pi}\phi_c cos\sqrt{4\pi}\phi_{t_1} cos\sqrt{4\pi}\phi'_c cos\sqrt{4\pi}\phi'_v\rangle_> \propto \langle cos\sqrt{4\pi}\phi'_{t_1} cos\sqrt{4\pi}\phi_v\rangle_>.$$

contribute with $(2\lambda_v)(\lambda_v+\lambda_s)$ to $(\dot{g}_t+\dot{g}_v)$. The scaling of spin-charge interactions yield

$$\dot{\lambda}_v \pm \dot{\lambda}_s \approx \frac{1}{2\pi}\left[\underbrace{(\lambda_v\pm\lambda_s)(g_c\pm g_v)}_{S_{int}[\phi]} + \underbrace{2(2\lambda_v)(g_t\pm g_v)}_{\frac{1}{2}S_{int}[\phi]^2}\right],$$

where first order contributions include the Luttinger parameters of the charge channel $K_c \approx 1 - g_c/(2\pi)$ together with those in the spin-channels. And also pure umklapp terms ($\dot{g}_c \neq 0$) arise from contractions such as

$$\langle cos\sqrt{4\pi}\phi_c cos\sqrt{4\pi}\phi_v cos\sqrt{4\pi}\phi'_c cos\sqrt{4\pi}\phi'_v\rangle_> \propto \langle cos\sqrt{4\pi}\phi'_c cos\sqrt{4\pi}\phi_c\rangle_>.$$

At the end we get

$$\dot{g}_c = \frac{1}{2\pi}(\lambda_s^2+5\lambda_v^2), \qquad \dot{g}_v = \frac{1}{2\pi}(4g_v g_t + 2\lambda_s\lambda_v),$$
$$\dot{g}_t = \frac{1}{2\pi}(3g_t^3+g_v^2+2\lambda_v^2), \qquad \dot{\lambda}_s = \frac{1}{2\pi}(g_c\lambda_s + 5g_v\lambda_v),$$
$$\dot{\lambda}_v = \frac{1}{2\pi}(g_c\lambda_v + g_v\lambda_s + 4g_t\lambda_v).$$

Appendix B

Refermionization

Notice that the sine-Gordon terms in Eq.(3.8) may be written in terms of backscattering and Josephson pairing of spinless fermions, respectively

$$\frac{1}{2\pi\alpha}cos(\sqrt{4\pi}\Phi_v(x)) = c_R^\dagger c_L(x) + H.c., \tag{B.1a}$$

$$\frac{1}{2\pi\alpha}cos(\sqrt{4\pi}\Theta_v(x)) = c_R^\dagger c_L^\dagger(x) + H.c. \tag{B.1b}$$

In the absence of magnetic field critical properties doesn't depend on the Tomonaga-Luttinger terms. For finite quadratic Zeeman the critical Luttinger parameter deviates from one and takes values according to the RG equations. Finite gap effects can be addressed through the Luther-Emery approach [105].

Our starting point is the lattice Hamiltonian from Eq.(3.17). All relevant information related to the original system of spin-3/2 fermions is associated to its low energy excitations at half-filling. It is straightforward to check that the chiral decomposition[1] $c(x) \approx c_R(x)\ e^{ik_F x} + c_L(x)\ e^{-ik_F x}$ applied on the g and g_γ–terms in Eq.(3.17) renders the corresponding sine-Gordon terms in Eq.(B.1).

B.1 Bogoliubov transformation

The Hamiltonian in Eq.(3.17) is quadratic and has local discrete translational symmetry[2]; it can be diagonalized by a Bogoliubov transformation in the momentum space.

[1] The limit into the continuum is $x_n \to na/L$. Where a and L are the lattice constant and total size. That a/L is the regularization parameter becomes clear once we realize the cut-off condition for the lowest mode excitations: $a|k - k_F| \sim a/L \ll 1$.

[2] Even after dimerization, the new translational symmetry remains local.

After the discrete Fourier transformation

$$c_n = \frac{1}{\sqrt{N}} \sum_{|k|<\pi} e^{ikn}\ c_k, \tag{B.2}$$

where $Nk/2\pi$ are integers with arithmetic modulo N. The Hamiltonian in Eq.(3.17) becomes (setting N and t to one)

$$\mathcal{H}_{lattice} = \sum_{|k|<\pi} \Big[cos(k)\ c_k^\dagger c_k - ig\ sin(k)\ c_k^\dagger c_{k+\pi} + ig_\gamma\ sin(k)\ c_k^\dagger c_{-k}^\dagger - 2q\ c_k^\dagger c_k \Big] + H.c. \tag{B.3}$$

Hermiticity and parity invariance implies one can write

$$\mathcal{H}_{lattice} = \sum_{0<k<\pi} \mathcal{A}_k + \mathcal{P}\mathcal{A}_k\mathcal{P}. \tag{B.4}$$

where, $\mathcal{P}c_k = c_{-k}^\dagger$. Let $\mathcal{T}_0$ be the (non-unitary) transformation s.t. $\mathcal{T}_0^\dagger \mathcal{A}_k \mathcal{T}_0 = Diag(\mathcal{A}_k)$. Using the fact that $\mathcal{A}_k\mathcal{P} = \mathcal{P}\mathcal{A}_k = 0$ and $\mathcal{P}\mathcal{T}_0 = \mathcal{T}_0\mathcal{P}$ one can write

$$Diag(\mathcal{H}_{lattice}) = \sum_{0<k<\pi} (\mathbf{1}+\mathcal{P})\mathcal{T}_0^\dagger \mathcal{H}_{lattice}(k)\mathcal{T}_0(\mathbf{1}+\mathcal{P}). \tag{B.5}$$

Setting

$$\mathcal{E} = gen\{c_k, c_{-k}^\dagger, c_{k-\pi}, c_{-k+\pi}^\dagger\}, \tag{B.6}$$

$$\tilde{\mathcal{E}} \oplus \mathcal{P}\tilde{\mathcal{E}} = gen\{u_k, d_k\} \oplus gen\{u_{-k}^\dagger, d_{-k}^\dagger\}; \tag{B.7}$$

then

$$\tilde{\mathcal{E}} \oplus \mathcal{P}\tilde{\mathcal{E}} = \mathcal{T}_0(\mathbf{1}+\mathcal{P})\mathcal{E}, \tag{B.8}$$

which is to say

$$\tilde{\mathcal{E}} = \mathcal{T}_0\mathcal{E} \quad \text{and} \quad \mathcal{P}\tilde{\mathcal{E}} = \mathcal{T}_0\mathcal{P}\mathcal{E}. \tag{B.9}$$

From section B.1, $\mathcal{T}_0$ corresponds to[3]

$$\begin{aligned} u_k &= cos(\omega_2)sin(\theta_2/2)\ c_{-k}^\dagger + sin(\omega_2)sin(\tilde{\theta}_2/2)\ c_{k+\pi} \\ &\quad + i\ sin(\omega_2)cos(\tilde{\theta}_2/2)\ c_{-k+\pi}^\dagger + i\ cos(\omega_2)cos(\theta_2/2)\ c_k, \end{aligned} \tag{B.10a}$$

$$\begin{aligned} d_k &= cos(\omega_1)sin(\tilde{\theta}_1/2)\ c_{-k}^\dagger - sin(\omega_1)sin(\theta_1/2)\ c_{k+\pi} \\ &\quad - i\ sin(\omega_1)cos(\theta_1/2)\ c_{-k+\pi}^\dagger + i\ cos(\omega_1)cos(\tilde{\theta}_1/2)\ c_k. \end{aligned} \tag{B.10b}$$

[3]Notice the angles $\theta_{1,2}$ perform a deformation of Majoranas.

The Hamiltonian becomes

$$\mathcal{H}_{lattice} = \sum_{|k|<\pi/2} \left[\omega_u(k)\ u_k^\dagger u_k + \omega_d(k)\ d_k^\dagger d_k\right] \tag{B.11}$$

with energies above and below the Fermi surface

$$\omega_{u,d}(k) = \pm\sqrt{(g^2+g_\gamma^2)sin(k)^2 + 4q^2 + cos(k)^2 \mp 2\sqrt{g^2 g_\gamma^2 sin(k)^4 + 4q^2(g^2 sin(k)^2 + cos(k)^2)}}. \tag{B.12}$$

Only the upper band becomes gapless at half-filling, and it does with linear dispersion, confirming that the excitations are Majorana quasiparticles.

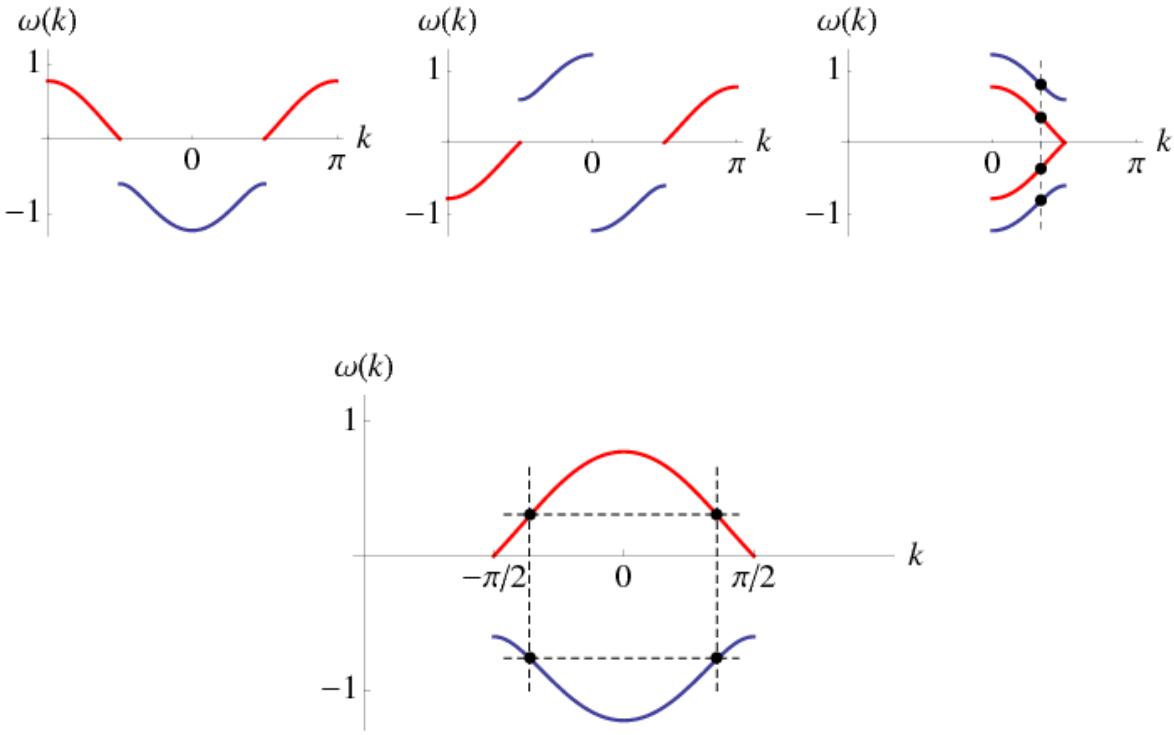

FIGURE B.1: Folding of the spectrum: from 2π-single-band (left-above) to $\pi/2$-four-bands (right-above): the first is useful to understand the deformation of the free particle and the second to understand the final diagonal matrix associated to the Hamiltonian bilinear form. In the center (above and below) is the two band picture, useful to distinguish the Fermi sea (blue) from the excitation band (red).

Bogoliubov coefficients

The Bogoliubov transformation should provide a diagonal representation of Eq.(B.3) that preserves commutation relations[4]. The implicit angles in Eq.(B.10) are

$$\begin{aligned}
tan\left(\theta_1(k,q)/2\right) &= \frac{cos(k)+\omega_d}{g_\gamma sin(k)+\sqrt{g^2 sin(k)^2+\left(\frac{2q}{g_\gamma}\right)^2(cot(k)^2+g^2)}+\left(\frac{2q}{g_\gamma}\right)\frac{(\omega_d+2q)}{sin(k)}},\\
tan\left(\theta_2(k,q)/2\right) &= \frac{cos(k)+\omega_u}{g_\gamma sin(k)-\sqrt{g^2 sin(k)^2+\left(\frac{2q}{g_\gamma}\right)^2(cot(k)^2+g^2)}+\left(\frac{2q}{g_\gamma}\right)\frac{(\omega_u-2q)}{sin(k)}},\\
tan(\omega_1(k,q)) &= tan(\omega_2(k,-q))=\sqrt{\frac{\omega_u sin(\theta_2(k,-q))-\omega_d sin(\theta_1(k,-q))}{\omega_u sin(\theta_2(k,q))-\omega_d sin(\theta_1(k,q))}} \qquad \text{(B.13)}
\end{aligned}$$

and $\tilde{\theta}(k,q)=\theta(k,-q)$. Notice that $tan(\omega_1)=cot(\omega_2)$; we may often use only $\omega\equiv\omega_1$. Together, Eqs.(B.10) and (B.13) are a solution of the two set of equations: i) Similarity

$$\begin{aligned}
-|\omega_d|cos(\omega_1)^2cos(\tilde{\theta}_1)+|\omega_u|cos(\omega_2)^2cos(\theta_2) &= -cos(k)+q,\\
i|\omega_d|cos(\omega_1)^2sin(\tilde{\theta}_1)-i|\omega_u|cos(\omega_2)^2sin(\theta_2) &= -ig_\gamma\ sin(k),\\
-i|\omega_d|sin(2\omega_1)sin\left(\frac{\tilde{\theta}_1+\theta_1}{2}\right)-i|\omega_u|sin(2\omega_2)sin\left(\frac{\tilde{\theta}_2+\theta_2}{2}\right) &= ig\ sin(k);
\end{aligned}$$

and ii) anticommutation relations

$$\begin{aligned}
\{d^\dagger_{-k},d_{-k}\} &= cos(\omega_1)^2sin(\tilde{\theta}_1/2)^2+sin(\omega_1)^2sin(\theta_1/2)^2\\
&+ sin(\omega_1)^2cos(\theta_1/2)^2+cos(\omega_1)^2cos(\tilde{\theta}_1/2)^2=1,\\
\{d^\dagger_{-k},d^\dagger_{k}\} &= icos(\omega_1)^2cos(\tilde{\theta}_1/2)sin(\tilde{\theta}_1/2)-isin(\omega_1)^2cos(\theta_1/2)sin(\theta_1/2)\\
&+ isin(\omega_1)^2cos(\theta_1/2)sin(\theta_1/2)+icos(\omega_1)^2cos(\tilde{\theta}_1/2)sin(\tilde{\theta}_1/2)=0,\\
\{d^\dagger_{-k},u^\dagger_{-k}\} &= cos(\omega_1)cos(\omega_2)cos\left(\frac{\tilde{\theta}_1-\theta_2}{2}\right)-sin(\omega_1)sin(\omega_2)cos\left(\frac{\theta_1-\tilde{\theta}_2}{2}\right)=0,\\
\{d^\dagger_{-k},u^\dagger_{k}\} &= -icos(\omega_1)cos(\omega_2)sin\left(\frac{\tilde{\theta}_1-\theta_2}{2}\right)+isin(\omega_1)sin(\omega_2)sin\left(\frac{\theta_1-\tilde{\theta}_2}{2}\right)=0.
\end{aligned}$$

Using the map

$$z_{1,2}=|\omega_{d,u}|^{1/2}sin(\omega)e^{-i\theta_{1,2}/2},\quad \tilde{z}_{1,2}=|\omega_{d,u}|^{1/2}cos(\omega)e^{-i\tilde{\theta}_{1,2}/2} \qquad \text{(B.14)}$$

[4] A simple method is to use the Pauli matrices as generators of the associated bilinear form. Using their algebra is easy to solve $\mathcal{H}^2$, which provides a block diagonalization $\mathcal{H}$. The remaining blocks are 2×2 matrices distinguishing particles from holes and can be directly diagonalized.

the former equations can be rewritten in compact form. Respectively,

$$|\tilde{z}_{1,2}|^2 + |z_{1,2}|^2 = |\omega_{d,u}|, \tag{B.15a}$$

$$\tilde{z}_1 z_2^* - z_1 \tilde{z}_2^* = 0; \tag{B.15b}$$

and

$$-\tilde{z}_1^2 + z_2^2 = x, \tag{B.16a}$$

$$\tilde{z}_1 z_1 + \tilde{z}_2 z_2 = y, \tag{B.16b}$$

where $x = -cos(k) + q - ig_\gamma\ sin(k)$ and $y = ig\ sin(k)$. Notice that

$$-z_1^2 + \tilde{z}_2^2 = \tilde{x} \quad \text{and} \quad -\tilde{z}_1^2 + z_2^2 = x, \tag{B.17}$$

where $\tilde{x} = x(-q)$, are two decoupled equations intersected by

$$z_1 \tilde{z}_1 + z_2 \tilde{z}_2 = y. \tag{B.18}$$

Similarly, in the new basis $f_i = (z_i + \tilde{z}_i)/2$ and $\tilde{f}_i = (z_i - \tilde{z}_i)/2$, the decoupled equations

$$\tilde{f}_1^2 + f_2^2 = [y + (x + \tilde{x})]/2 \quad \text{and} \quad f_1^2 + \tilde{f}_2^2 = [y - (x + \tilde{x})]/2$$

are intersected by

$$f_1 \tilde{f}_1 + f_2 \tilde{f}_2 = \frac{x - \tilde{x}}{2} = q. \tag{B.19}$$

I will show some straightforward results from Eqs.(B.15) and (B.16). From Eq.(B.15b) we get

$$arg(\tilde{z}_1 z_2^*) = arg(z_1 \tilde{z}_2^*), \tag{B.20a}$$

$$|\tilde{z}_1 z_2^*| = |z_1 \tilde{z}_2^*|. \tag{B.20b}$$

From the first line we get $\theta_1 + \theta_2 = \tilde{\theta}_1 + \tilde{\theta}_2$; the second line proves consistency for trigonometric functions of ω.

$$\begin{aligned} x\tilde{x} &= [(\tilde{z}_1 z_1)^2 + (\tilde{z}_2 z_2)^2] - [(\tilde{z}_1 \tilde{z}_2)^2 + (z_1 z_2)^2], \\ &= [(\tilde{z}_1 z_1 + \tilde{z}_2 z_2)^2 - 2\tilde{z}_1 z_1 \tilde{z}_2 z_2] - [(\tilde{z}_1 \tilde{z}_2 + z_1 z_2)^2 - 2\tilde{z}_1 z_1 \tilde{z}_2 z_2], \\ &= \underbrace{(\tilde{z}_1 z_1 + \tilde{z}_2 z_2)^2}_{y^2} - (\tilde{z}_1 \tilde{z}_2 + z_1 z_2)^2, \end{aligned}$$

Hence

$$\sqrt{\varepsilon_1 \varepsilon_2}\ exp(i\theta_1 + \theta_2) = \sqrt{y^2 - x\tilde{x}}. \tag{B.21}$$

From Eq.(B.15b) we get

$$\varepsilon_1^2 + \varepsilon_2^2 = |\tilde{x}|^2 + |x|^2 + 2|y|^2, \tag{B.22}$$

which is enough to find the spectrum in Eq.(B.12). Finally I derive ω and let the reader derive the remaining angles. From Eq.(B.16a) and Eq.(B.15b)

$$\begin{aligned} |x|^2 - |\bar{x}|^2 &= |\bar{z}_1|^4 + |z_2|^4 - |z_1|^4 - |\bar{z}_2|^4 \\ &= (|\bar{z}_1|^2 + |z_1|^2)(|\bar{z}_1|^2 - |z_1|^2) + (|z_2|^2 + |\bar{z}_2|^2)(|z_2|^2 - |\bar{z}_2|^2) \\ &= -\omega_d^2\ cos(2\omega) + \omega_u^2\ cos(2\omega). \end{aligned} \tag{B.23}$$

Hence

$$\begin{aligned} cos(2\omega) &= \frac{|\bar{x}|^2 - |x|^2}{\omega_d^2 - \omega_u^2} \\ &= \frac{2q\ cos(k)}{\sqrt{g^2 g_\gamma^2 sin(k)^4 + 4q^2(g^2 sin(k)^2 + cos(k)^2)}}. \end{aligned} \tag{B.24}$$

You may check that the latter expression match the one in Eq.(B.13).

Chirality correlator

In the context of the interacting high-spin gas the chirality channel refers to spin degrees of freedom whose "polarization" is not associated to orientation of spin along a given direction. In this sense they resemble the charge degree of freedom, but unlike the latter, is not pinned directly by the optical lattice. The effective spin S_{eff} of individual atoms, when exposed to two body interactions, becomes an isotropic degree of freedom since total spin is the new conserved quantity. The process that change individual spin through interaction, known as spin changing collision, is generated by a term in the Hamiltonian which do not commute with the chirality. For the spin-3/2 Hamiltonian in Eq.(3.3) the chirality is defined as

$$\begin{aligned} N_v(x) &= N_{|3/2|}(x) - N_{|1/2|}(x) \\ &= \psi^\dagger_{-3/2}\psi_{-3/2}(x) + \psi^\dagger_{3/2}\psi_{3/2}(x) - \psi^\dagger_{-1/2}\Psi_{-1/2}(x) - \psi^\dagger_{1/2}\psi_{1/2}(x). \end{aligned} \tag{B.25}$$

In the corresponding low energy theory the chirality is proportional to $\partial_x\Phi_v(x)$ and the spin changing collisions are identified with the sine-Gordon term $cos\sqrt{4\pi}\Theta_v$ from Eq.(3.8). When acting over a ground state pinned by $cos\sqrt{4\pi}\Phi_v$, the spin changing collisions are quantum disorder operators in the context of the quantum Ising spin chain. In the refermionization, Eq.(3.17), the chirality becomes $n_i = c_i^\dagger c_i$, and the spin changing collisions are associated to the g_γ-term. Here the chirality correlator is calculated using

refermionization. The information that this model provides is only valid when closed to criticality, where a mapping into the original fermionic interacting Hamiltonian is possible, in the low energy sector. In equilibrium, the mean chiral spatial density is

$$\langle n_i \rangle = \int_0^{2\pi} dk \ \langle c_k^\dagger c_k \rangle \tag{B.26}$$

where, according to Eq.(B.10), the ground state is s.t. $\langle u_k^\dagger u_k \rangle = 0$ and $\langle d_k^\dagger d_k \rangle = 1$. Calculation yields

$$\langle n_i \rangle = \int_0^{\pi} dk \ (sin^2(\omega) sin^2(\theta_1/2) + cos^2(\omega) cos^2(\tilde{\theta}_2/2)). \tag{B.27}$$

B.2 Residual interactions

After a Bogoliubov transformation of Eq.(3.17) new interaction terms coming from the non-trivial Luttinger parameter may arise. Calculating their dependence near the Fermi surface is fundamental to address the reliability of the quadratic Hamiltonian. This section is complementary to results in [106], where calculation of correlators is developed based on Toeplitz determinants. Our starting point is the low energy chirality sector of the Hamiltonian in Eq.(3.3) exposed to the quadratic Zeeman effect. After averaging commensurate channels (see Eq.(3.8)), bosonization yields a Hamiltonian density

$$\mathcal{H}_v = \int dx \left[\frac{u}{2} \left\{ K(\partial_x \Theta)^2 + \frac{1}{K} (\partial_x \Phi)^2 \right\} - \frac{1}{2(\pi a)^2} \left(g \ cos\sqrt{4\pi}\Phi + g_\gamma \ cos\sqrt{4\pi}\Theta \right) - \frac{2q}{\sqrt{\pi}} \partial_x \Phi \right], \tag{B.28}$$

where v-indexes are dropped and $v_v \equiv u$. In terms of density fluctuations of spinless fermions in momentum space

$$\mathcal{H}_v \ = \ \mathcal{H}_{lattice} + \frac{\pi u sinh(2\vartheta)}{L} \sum_p [2\rho_R(p)\rho_L(-p) - f_1 \ (\rho_R(p)\rho_R(-p) + \rho_L(p)\rho_L(-p))], \tag{B.29}$$

where f_1 is an arbitrary variable, $\mathcal{H}_{lattice}$ is the quadratic Hamiltonian depicted in Eq.(B.3) with (normalized) hopping: $v = u(cosh(2\vartheta) + f_1 \ sinh(2\vartheta))$ where $e^{2\vartheta} = 1/K$. Is easy to check that this parametrization leads to Eq.(B.28); contributions to the Tomonaga-Luttinger liquid are identified as i) scattering of left onto right electrons (g_2) and ii) amplitude for forward scattering (g_4)

$$g_2 \equiv \frac{\pi u sinh(2\vartheta)}{L}, \qquad g_4 \equiv -g_2 \ f_1.$$

They renormalize the free bosonic Hamiltonian. In the case of $\partial_x\Phi_v$ (idem for $\partial_x\theta_v$)

$$v\ (\partial_x\Phi_v)^2 \quad \rightarrow \quad (v+g_4-g_2)\ (\partial_x\Phi_v)^2;$$

indeed, parametrization of v is such that

$$(v+g_4-g_2) = u\ K$$

regardless of the value of f_1. What is left are sine-Gordon terms as depicted in Eq.(B.1a). The next procedure is to use f_1 to cancel some of the latter terms. This is partially achieved and one is left with a quartic term with proportionality factor f that is a function of Bogoliubov coefficients associated to $\mathcal{H}_{lattice}$.

We now determine the relevance of quartic terms after the Bogoliubov transformation of Eq.(B.10). From the charge density fluctuations $\rho_{R(L)}$ we keep only those quasiparticles exhibiting low energy excitations. We want to see how interactions

$$\sum_p [2\rho_R(p)\rho_L(-p) - f_1\ (\rho_R(p)\rho_R(-p) + \rho_L(p)\rho_L(-p))] \tag{B.30}$$

are transformed after a Bogoliubov transformation on $\mathcal{H}_{lattice}$ at the Fermi surface. Keeping only upper band density fluctuations: $\rho^{(u)}_{R(L)}(p) = \sum_{0<|k-\pi/2|<\Lambda} u^\dagger_{\pm(k+p)} u_{\pm k}$, one gets[5]

$$\rho_R(-p) = \sum_{0<(k-\pi/2)<\Lambda} c^\dagger_{R,k+p} c_{R,k} \simeq |\alpha_{k_c}|^2\ \rho^{(u)}_R(-p) + |\alpha_{-k_c}|^2\ \rho^{(u)}_L(-p), \tag{B.31}$$

$$\rho_L(-p) = \sum_{\Lambda<(k+\pi/2)<0} c^\dagger_{L,k+p} c_{L,k} \simeq |\beta_{k_c}|^2\ \rho^{(u)}_R(-p) + |\beta_{-k_c}|^2\ \rho^{(u)}_L(-p), \tag{B.32}$$

[5]Mixing of particles and holes leads to some negative density contributions and extra quadratic terms. Both are, nevertheless, proportional to the coefficient of residual interaction.

where α's and β's are to take values around the Fermi surface, i.e. $k_c = k_F \pm p$. The new interaction becomes

$$\begin{aligned}
&\sum_p \left[2\rho_R(p)\rho_L(-p) - f_1\ (\rho_R(p)\rho_R(-p) + \rho_L(p)\rho_L(-p))\right] \\
= &\sum_p \Big\{\left[2|\alpha_{k_c}|^2|\beta_{k_c}|^2 - f_1\ (|\alpha_{k_c}|^4 + |\beta_{k_c}|^4)\right]\ \rho_R^{(u)}(p)\rho_R^{(u)}(-p) \\
+ &\left[2|\alpha_{-k_c}|^2|\beta_{-k_c}|^2 - f_1\ (|\alpha_{-k_c}|^4 + |\beta_{-k_c}|^4)\right]\ \rho_L^{(u)}(p)\rho_L^{(u)}(-p) \\
+ &\left[2|\alpha_{-k_c}|^2|\beta_{k_c}|^2 - f_1\ (|\alpha_{k_c}|^2|\alpha_{-k_c}|^2 + |\beta_{k_c}|^2|\beta_{-k_c}|^2)\right]\ \rho_R^{(u)}(p)\rho_L^{(u)}(-p) \\
+ &\left[2|\alpha_{k_c}|^2|\beta_{-k_c}|^2 - f_1\ (|\alpha_{k_c}|^2|\alpha_{-k_c}|^2 + |\beta_{k_c}|^2|\beta_{-k_c}|^2)\right]\ \rho_L^{(u)}(p)\rho_R^{(u)}(-p)\Big\}, \\
= &\sum_p \Big\{\left[2|\alpha_{k_c}|^2|\beta_{k_c}|^2 - f_1\ (|\alpha_{k_c}|^4 + |\beta_{k_c}|^4)\right]\ (\rho_R^{(u)}(p)\rho_R^{(u)}(-p) + \rho_L^{(u)}(p)\rho_L^{(u)}(-p)) \\
+ &2\left[(|\alpha_{-k_c}|^2|\beta_{k_c}|^2 + |\alpha_{k_c}|^2|\beta_{-k_c}|^2) - f_1\ (|\alpha_{k_c}|^2|\alpha_{-k_c}|^2 + |\beta_{k_c}|^2|\beta_{-k_c}|^2)\right]\ \rho_R^{(u)}(p)\rho_L^{(u)}(-p)\Big\}.
\end{aligned} \tag{B.33}$$

The choice

$$f_1 = \frac{2|\alpha_{k_c}|^2|\beta_{k_c}|^2}{|\alpha_{k_c}|^4 + |\beta_{k_c}|^4} \tag{B.34}$$

cancels $\rho_r^{(u)}(p)\rho_r^{(u)}(-p)$ $(r = R, L)$ and the remaining interaction is proportional to

$$f(k_c) = 2\left[\left(|\alpha_{-k_c}|^2|\beta_{k_c}|^2 + |\alpha_{k_c}|^2|\beta_{-k_c}|^2\right) - f_1\ \left(|\alpha_{k_c}|^2|\alpha_{-k_c}|^2 + |\beta_{k_c}|^2|\beta_{-k_c}|^2\right)\right]. \tag{B.35}$$

Below is shown the case $g_\gamma = 0$, which corresponds to the well known Mott transition [105]. Dimerization doesn't mix particles and holes and the transformation must preserve orthogonality, hence from Eq.(B.10)

$$g_\gamma = 0: \quad sin(\theta_2(\pm|k|)/2) = cos(\tilde{\theta}_2(\pm|k|)/2) = 0, \tag{B.36a}$$

$$cos(\theta_2(\pm|k|)/2) = \pm sin(\tilde{\theta}_2(\pm|k|)/2) = 1. \tag{B.36b}$$

Upper band excitations transform as

$$u_k = \frac{1}{\sqrt{2}}\ [\ \pm cos(\omega)\ c_{k+\pi} + i\ sin(\omega)\ c_k\ ] \qquad (0 < |k \mp \pi/2| < \Lambda). \tag{B.37}$$

Up to a gauge, and relabeling[6]

$$\tilde{R}_k = cos(\omega_c)\ L_k + i\ sin(\omega_c)\ R_k, \tag{B.38a}$$

$$\tilde{L}_k = cos(\omega_c)\ R_k - i\ sin(\omega_c)\ L_k. \tag{B.38b}$$

[6] E.g. $0 < |k - \pi/2| < \Lambda:\ \ u_k = \tilde{R}_k,\ u_{k+\pi} = \tilde{L}_k$. Notice we use $\omega_c \equiv \omega(k_c)$.

From the inverse transformation, the terms in Eq.(B.32) become

$$|\alpha_{k_c}| = |\beta_{-k_c}| = |sin(\omega_c)|, \tag{B.39a}$$
$$|\beta_{k_c}| = |\alpha_{-k_c}| = |cos(\omega_c)|. \tag{B.39b}$$

From trigonometric identities we get

$$|\alpha_{k_c}|^4 + |\beta_{k_c}|^4 = \left(1 + cos^2(2\omega_c)\right)/2, \tag{B.40a}$$
$$2|\alpha_{k_c}|^2|\beta_{k_c}|^2 = sin^2(2\omega_c)/2. \tag{B.40b}$$

Hence Eq.(B.34) reduces to

$$f_1(k_c) = \frac{1 - cos^2(2\omega_c)}{1 + cos^2(2\omega_c)}. \tag{B.41}$$

Interactions are proportional to

$$f(k_c) = 2\left[|\alpha_{k_c}|^4 + |\beta_{k_c}|^4 - f_1\ 2|\alpha_{k_c}|^2|\beta_{k_c}|^2\right] \tag{B.42}$$
$$= 1 + cos^2(2\omega_c) - f_1\ sin^2(2\omega_c) \tag{B.43}$$

Near half-filing –regardless of chemical potential– quasi-particles have nearly equal probability to be in left or right moving particles[7]; from Eq.(B.38) this implies $sin^2\omega \approx cos^2\omega$, or equivalently $cos^2(2\omega) \ll 1$. Hence

$$f_1(k_c) \lesssim 1, \tag{B.44}$$
$$f(k_c) \approx cos^2(2\omega_c). \tag{B.45}$$

From Eq.(B.24) we may conclude : $f \sim p^2$, where p is the small momentum fluctuation around $k_F = \pi/2$. The latter result implies that the quadratic Hamiltonian in Eq.(B.3) for $g_\gamma = 0$ is equivalent at low energies to the Hamiltonian in Eq.(3.3).

[7]Draw a vertical line in the dimer spectrum at $k = \pi/2$; it always cross the spectrum in a region with quadratic dispersion. Alternatively you can use the parametrization of ω derived in the former section.

Appendix C

Supplementary information

C.1 Recoil energy

In this section is shown numerically that the phase diagram in Fig.4.1 is within the values of lattice depth in [1]. The term U/t is estimated from Eqs.(1.1b) as a function of lattice depth in units of recoil energy. The latter is the imprint momentum of the optical lattice in a single atom; if the $3d$-lattice potential is $V(\mathbf{x}) = \sum_{j=1}^{3} V_j sin^2(kx_j)$ the recoil energy is $E_R = \hbar^2 k^2/2m$, where m is the mass of the atomic specie[1]. We approximate the Wannier states to solutions of an harmonic potential around every lattice site, the characteristic frequencies being

$$\omega_{xy} = \sqrt{4V_{xy}}\ E_R/\hbar, \qquad \omega_z = \sqrt{4V_z}\ E_R/\hbar, \tag{C.1}$$

where V_{xy} and V_z are the corresponding lattice depths in units of recoil energy. For the experiments with a gas of ^{40}K in [1] the restricted dimensions were fixed setting $V_{xy} = 35$; in the remaining dimension, values $|V_z| < 10$ exhibit high-tunneling regime. Fig.C.1 shows that the U/t regime where the three-critical point is found can be obtained with values of lattice depth $|V_z|$ between 4 and 5, in units of recoil energies.

A *Mathematica* working code, illustrative rather than efficient, is depicted in Fig.C.2.

[1] Notice $k = 2\pi/\lambda = \pi/a$ where λ is the laser light wavelength and a is the lattice periodicity.

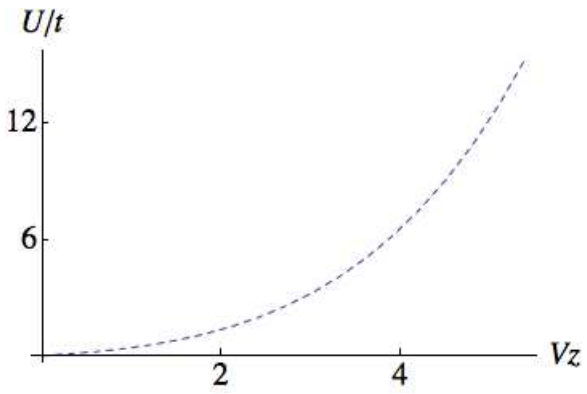

FIGURE C.1: Average interaction U in units of hopping t, as a function of lattice depth V_z in units of recoil energy E_R.

```
(* Joules, meters, Kilograms *)
ħ = 1.054571726×10^-34; m = 39.96399848 *1.660538921×10^-27;
λ = 1030*10^-9; a = λ/2; aB = 5.29*10^-11; (* Bohr Radius *)
a0 = 120.40 aB; a2 = 147.83 aB; a4 = 161.11 aB; a6 = 166.00 aB; a8 = 168.53 aB;
g = 4 π ħ^2/m (a0 + a2 + a4 + a6 + a8) / 5; Er = ħ^2 (π/a)^2 / (2 m); Vxy = 35;
ωxy = √(4 Vxy Er / ħ; ωz[Vz_] := √(4 Vz Er / ħ;
kxy = √(ħ / (m ωxy)) ; kz[Vz_] := √(ħ / (m ωz[Vz])) ;
w[r_, k_] := (1/(√π k))^1/2 Exp[-1/2 (r/k)^2];
w3d[Vz_, rx_, ry_, rz_] := w[rx, kxy]*w[ry, kxy]*w[rz, kz[Vz]];
V[Vz_, rx_, ry_, rz_] := ((π/a)^2 Vxy*(rx^2 + ry^2) + (π/a)^2 Vz*rz^2) Er ;

t[Vz_] :=
  NIntegrate[(w3d[Vz, rx, ry, rz - a])*
    ((-ħ^2/(2 m)) Tr[D[w3d[Vz, rx, ry, rz], {{rx, ry, rz}, 2}]]
      + V[Vz, rx, ry, rz] w3d[Vz, rx, ry, rz]), {rx, -2 a, 2 a}, {ry, -2 a, 2 a},
   {rz, -6 a, 6 a}];
U[Vz_] := g*NIntegrate[w3d[Vz, rx, ry, rz]^4, {rx, -2 a, 2 a}, {ry, -2 a, 2 a},
    {rz, -6 a, 6 a}];

Off[NIntegrate::slwcon];
dat = Table[{Vz, U[Vz] / t[Vz]}, {Vz, 0.00001, 5.5, 6/20}];

ListLinePlot[dat, AxesLabel → {Style["Vz", 20], Style["U/t", 20]},
 PlotStyle → {{Dashed, Bold}, {Dashed, Bold}, {Dashed}},
 Ticks → {{{2, Style["2", 20]}, {4, Style["4", 20]}, {6, Style["6", 20]}},
   {{0, Style["0", 20]}, {6, Style["6", 20]}, {12, Style["12", 20]}}}]
```

FIGURE C.2: Computation of Recoil energy.

C.2 Scattering length

The transformation of scattering length values from total spin to single spin is given by the mapping between Eqs.(1.4) and (1.5), i.e.

$$U_{\mathbf{m},\mathbf{m}'} = \left(\frac{4\pi\hbar^2}{m}\right) \sum_{F=0}^{2S} a_F \sum_{M=-F}^{F} \langle M, F|\mathbf{m}\rangle\langle\mathbf{m}'|F, M\rangle, \tag{C.2}$$

To simplify notation we write $U_{\mathbf{m}}$ when $\mathbf{m} = \mathbf{m}'$ and U_γ for the only case when $\mathbf{m} \neq \mathbf{m}'$. Terms $U_{\mathbf{m}}$ have have multiplicity two. In Fig.C.3 is a calculation in *Mathematica*. Notice we set $\frac{4\pi\hbar^2}{m} \to 1$ and restrict the calculation to the components of the lower multiplet of ^{40}K involved in spin changing collisions, giving rise to the effective 4-component Hamiltonian in Eq.(4.3). Moreover, for fermions the scattering processes with non-vanishing probability are associated to two particle wavefunctions symmetric in space and antisymmetric in spin, i.e. $F + 2S \in odd$.

```
S = 9 / 2;

set = {9 / 2, 7 / 2, 3 / 2, 1 / 2} ;

Print["Spin-9/2: Dynamically relevant components for spin-changing interaction: ",
 set, "."]

STin = Flatten[Table[Abs[(i + j)], {i, set}, {j, set}]];

STstr = {};
For[i = 1, i <= Length[STin], i ++,
  If[OddQ[STin[[i]] + 2 S], FreeQ[STstr, STin[[i]]] && AppendTo[STstr, STin[[i]]]]];

Print["Statistically relevant scattering (Fermions): g[S_T]=",
 Table[a[STstr[[i]]], {i, 1, Length[STstr]}], "."]

c[{σ1_, σ2_}, {ST_, m_}] := ClebschGordan[{S, σ1}, {S, σ2}, {ST, m}];

U[{σ11_, σ12_}, {σ21_, σ22_}] := Module[{val = 0},
   For[j = 1, j <= Length[STstr], j ++,
    ST = STstr[[j]];
    If[(Abs[σ11 + σ12] ≤ ST) && (Abs[σ21 + σ22] ≤ ST),
     val = val + a[ST] * ClebschGordan[{S, σ11}, {S, σ12}, {ST, σ11 + σ12}] *
         ClebschGordan[{S, σ21}, {S, σ22}, {ST, σ21 + σ22}]]];
   val
  ];
```

```
Spin-9/2: Dynamically relevant components for spin-changing interaction: {9/2, 7/2, 3/2, 1/2}.
Statistically relevant scattering (Fermions): g[S_T]={a[8], a[6], a[4], a[2]}.
```

```
Print["U7/2,9/2= ", 2 U[{7 / 2, 9 / 2}, {7 / 2, 9 / 2}]]
Print["U3/2,9/2= ", 2 U[{3 / 2, 9 / 2}, {3 / 2, 9 / 2}]]
Print["U1/2,9/2= ", 2 U[{1 / 2, 9 / 2}, {1 / 2, 9 / 2}]]
Print["U3/2,7/2= ", 2 U[{3 / 2, 7 / 2}, {3 / 2, 7 / 2}]]
Print["U1/2,7/2= ", 2 U[{1 / 2, 7 / 2}, {1 / 2, 7 / 2}]]
```

FIGURE C.3: Computation of scattering lengths.

Appendix D

Strong rung-coupling limit

Here is shown how Eq.(5.15) is derived from Eq.(5.13) in the strong-rung-coupling limit ($J_\perp \gg J_\parallel$) and near the magnetically induced Ising transition ($h \sim J_\perp$). Consider the original basis in Eq.(5.13), where the Dzyaloshinski-Moriya (DM) term is explicit. Consider $\mathcal{P}_j$ to be the projector into the ordered basis $\{|\tilde{\uparrow}\rangle, |\tilde{\downarrow}\rangle\}$, where $|\tilde{\downarrow}\rangle = |RS\rangle$ and $|\tilde{\uparrow}\rangle = |\uparrow\uparrow\rangle$ along the j-th rung. The new onsite terms in the basis: $|RS\rangle \equiv (0,1)^T$ and $|\uparrow\uparrow\rangle \equiv (1,0)^T$, are

$$\mathcal{P}_j(S^x_{1,j}S^x_{2,j}) = \begin{pmatrix} 1/4 & 0 \\ 0 & -1/4 \end{pmatrix}, \tag{D.1a}$$

$$\mathcal{P}_j(S^{y,z}_{1,j}S^{y,z}_{2,j}) = \begin{pmatrix} 0 & 0 \\ 0 & -1/8 \end{pmatrix}, \tag{D.1b}$$

$$\mathcal{P}_j([\mathbf{S}_{1,j}\times\mathbf{S}_{2,j}]^z) = \frac{-1}{\sqrt{2}}\begin{pmatrix} 0 & -i/2 \\ i/2 & 0 \end{pmatrix}. \tag{D.1c}$$

For example,

$$[\mathbf{S}_{1,j}\times\mathbf{S}_{2,j}]^z = S^x_{1,j}S^y_{2,j} - S^y_{1,j}S^x_{2,j}, \tag{D.2a}$$

$$\langle RS|S^x_{1,j}S^y_{2,j}|RS\rangle = \langle\uparrow\uparrow|S^x_{1,j}S^y_{2,j}|\uparrow\uparrow\rangle = 0, \tag{D.2b}$$

$$\begin{aligned}\langle RS|S^x_{1,j}S^y_{2,j}|\uparrow\uparrow\rangle &= \frac{1}{2\sqrt{2}}\langle\downarrow|S^x_{1,j}S^y_{2,j}|\uparrow\rangle \\ &= \frac{1}{4\sqrt{2}}({}_z\langle\uparrow|-{}_z\langle\downarrow|)S^y_{2,j}(|\uparrow\rangle_z+|\downarrow\rangle_z) \\ &= \frac{-i}{4\sqrt{2}} = -\langle RS|S^y_{1,j}S^x_{2,j}|\uparrow\uparrow\rangle,\end{aligned} \tag{D.2c}$$

yields Eq.(D.1c). Assuming $\{|\tilde{\uparrow}\rangle, |\tilde{\downarrow}\rangle\}$ to be the eigenvalues of the pseudo-spin-1/2 operator $\tilde{\tau}_j^x$, one gets

$$\mathcal{P}_j(S_{1,j}^x S_{2,j}^x) \equiv \frac{1}{2}\tau_j^x, \quad \mathcal{P}_j(S_{1,j}^{y,z} S_{2,j}^{y,z}) \equiv \frac{1}{2}\tau_j^x - \frac{1}{4} \quad \text{and} \quad \mathcal{P}_j([\mathbf{S}_{1,j} \times \mathbf{S}_{2,j}]^z) \equiv \frac{1}{\sqrt{2}}\tau_j^y. \quad \text{(D.3)}$$

The latter identification can be confirmed in the well known z-axis basis applying the basis transformation

$$T = \frac{1}{\sqrt{2}} \begin{pmatrix} 1 & 1 \\ 1 & -1 \end{pmatrix} \quad \text{(D.4)}$$

into Eqs.(D.1). The result is a contribution of $-J_\perp cos(2k_0^y a) - J_\perp(1 - cos(2k_0^y a)/4$ to h_x and $h_y = J_\perp sin(2k_0^y a)/\sqrt{2}$. To derive nearest neighbors note that

$$\langle b_{j+1}|\langle a_j|\mathcal{O}_{\alpha,j}\mathcal{O}_{\alpha,j+1}|\tilde{a}_j\rangle|\tilde{b}_{j+1}\rangle = \langle a_j|\mathcal{O}_{\alpha,j}|\tilde{a}_j\rangle\langle b_{j+1}|\mathcal{O}_{\alpha,j+1}|\tilde{b}_{j+1}\rangle \quad \text{(D.5)}$$

the possible states (per rung) being $|RS\rangle$ and $|\uparrow\uparrow\rangle$ for every ladder site. For example,

$$\langle (RS)_j|S_{\alpha,j}^z|(RS)_j\rangle = \langle(\uparrow\uparrow)_j|S_{\alpha,j}^z|(\uparrow\uparrow)_j\rangle = 0, \quad \langle(RS)_j|S_{\alpha,j}^z|(\uparrow\uparrow)_j\rangle = \begin{cases} -\frac{1}{2\sqrt{2}} & \text{if } \alpha = 1; \\ +\frac{1}{2\sqrt{2}} & \text{if } \alpha = 2. \end{cases} \quad \text{(D.6)}$$

Idem for $j+1$. Hence,

$$(\mathcal{P}_j + \mathcal{P}_{j+1})(S_{1,j}^z S_{1,j+1}^z + S_{2,j}^z S_{2,j+1}^z) = \frac{1}{4}\begin{pmatrix} 0 & 0 & 0 & 1 \\ 0 & 0 & 1 & 0 \\ 0 & 1 & 0 & 0 \\ 1 & 0 & 0 & 0 \end{pmatrix} \equiv \tau_j^z \tau_{j+1}^z. \quad \text{(D.7)}$$

Similarly,

$$(\mathcal{P}_j + \mathcal{P}_{j+1})(S_{1,j}^y S_{1,j+1}^y + S_{2,j}^y S_{2,j+1}^y) = \frac{1}{4}\begin{pmatrix} 0 & 0 & 0 & -1 \\ 0 & 0 & 1 & 0 \\ 0 & 1 & 0 & 0 \\ -1 & 0 & 0 & 0 \end{pmatrix} \equiv \tau_j^y \tau_{j+1}^y, \quad \text{(D.8)}$$

and

$$
\begin{aligned}
(\mathcal{P}_j + \mathcal{P}_{j+1})(S^y_{1,j}S^x_{1,j+1} + S^x_{2,j}S^x_{2,j+1}) &= \frac{1}{2}\begin{pmatrix} 1 & 0 & 0 & 0 \\ 0 & 0 & 0 & 0 \\ 0 & 0 & 0 & 0 \\ 0 & 0 & 0 & 0 \end{pmatrix} \\
&\equiv \frac{1}{2}\left(\tau^x_j\tau^x_{j+1} + \frac{1}{2}\tau^x_j + \frac{1}{2}\tau^x_{j+1} + \frac{1}{4}\mathbf{1}_j + \frac{1}{4}\mathbf{1}_{j+1}\right),
\end{aligned}
\tag{D.9}
$$

which explains the remaining terms in Eq.(5.15).

Bibliography

[1] J. S. Krauser, J. Heinze, N. Flaschner, S. Gotze, O. Jurgensen, D. Luhmann, C. Becker, and K. Sengstock. *Nat. Phys.*, pages 813 – 818, 2012.

[2] G. Sun, J. Jaramillo, L. Santos, and T. Vekua. *Phys. Rev. B*, 88, 2013.

[3] M. H. Anderson, J. R. Ensher, M. R. Matthews, C. E. Wieman, and E. A. Cornell. *Science*, 269(5221):198 – 201, 1995.

[4] K. B. Davis, M. O. Mewes, M. R. Andrews, N. J. van Druten, D. S. Durfee, D. M. Kurn, and W. Ketterle. *Phys. Rev. Lett.*, 75:3969 – 3973, 1995.

[5] C. C. Bradley, C. A. Sackett, J. J. Tollett, and R. G. Hulet. *Phys. Rev. Lett.*, 75: 1687 – 1690, 1995.

[6] B. DeMarco and D. S. Jin. *Science*, 285(5434):1703–1703, 1999.

[7] A. G. Truscott, K. E. Strecker, McAlexander W. I., G. B. Patridge, and R. G. Hulet. *Science*, 291(5513):2570–2772, 2001.

[8] W. Hofstetter, J. I. Cirac, P. Zoller, E. Demler, and M. D. Lukin. *Phys. Rev. Lett.*, 89:220407, 2002.

[9] E. Y. Loh, J. E. Gubernatis, R. T. Scalettar, S. R. White, D. J. Scalapino, and R. L. Sugar. *Phys. Rev. B*, 41:9301– 9307, 1990.

[10] Masatoshi Imada, Atsushi Fujimori, and Yoshinori Tokura. *Rev. Mod. Phys.*, 70: 1039 – 1263, 1998.

[11] S. Tomonaga. Remarks on bloch's method of sound waves applied to many fermion problems. *Prog. Theor. Phys.*, 5(544), 1950.

[12] M. P. A. Fisher, P. B. Weichman, G. Grinstein, and D. S. Fisher. *Phys. Rev. B*, 40:546 – 570, 1989.

[13] D. Jaksch, C. Bruder, J. I. Cirac, C. W. Gardiner, and P. Zoller. *Phys. Rev. Lett.*, 81:3108 – 3111, 1998.

[14] M. Greiner, O. Mandel, T. Esslinger, T. W. Hansch, and I. Bloch. *Nature*, 415:39 – 44, 2002.

[15] R. Jordens, N. Strohmaier, K. Gunter, H. Moritz, and T. Esslinger. *Nature*, 455: 204 – 207, 2008.

[16] C. Kollath, U. Schollwöck, and W. Zwerger. Spin-charge separation in cold fermi gases: A real time analysis. *Phys. Rev. Lett.*, 95:176401, 2005.

[17] A. Kleine, C. Kollath, I. P. McCulloch, T. Giamarchi, and U. Schollwöck. *Phys. Rev. A*, 77:013607, 2008.

[18] Tobias Ulbricht, Rafael A. Molina, Ronny Thomale, and Peter Schmitteckert. *Phys. Rev. A*, 82:011603, 2010.

[19] O. M. Auslaender, H. Steinberg, A. Yacoby, Y. Tserkovnyak, B. I. Halperin, K. W. Baldwin, L. N. Pfeiffer, and K. W. West. *Science*, 308(5718):88–92, 2005.

[20] B. J. Kim and *et al. Nat. Phys.*, pages 397 – 401, 2006.

[21] Y. Jompol, C. J. B. Ford, J. P. Griffiths, I. Farrer, G. A. C. Jones, D. Anderson, D. A. Ritchie, T. W. Silk, and A. J. Schofield. *Science*, 325(5940):597–601, 2009.

[22] H. Steinberg, G. Barak, A. Yacoby, L. N. Pfeiffer, K. W. West, I. Halperin, and K. Le Hur. *Nat. Phys.*, pages 116–119, 2008.

[23] Igor Žutić, Jaroslav Fabian, and S. Das Sarma. *Rev. Mod. Phys.*, 76:323 – 410, 2004.

[24] Roberto B. Diener and Tin-Lun Ho. *Phys. Rev. Lett.*, 96:190405, 2006.

[25] R. Barnett, A. Turner, and E. Demler. *Phys. Rev. Lett.*, 97:180412, 2006.

[26] K. Rodríguez, A. Argüelles, M. Colomé-Tatché, T. Vekua, and L. Santos. *Phys. Rev. Lett.*, 105:050402, 2010.

[27] Axel Griesmaier, Jörg Werner, Sven Hensler, Jürgen Stuhler, and Tilman Pfau. *Phys. Rev. Lett.*, 94:160401, 2005.

[28] Fei Zhou and Gordon W. Semenoff. *Phys. Rev. Lett.*, 97:180411, 2006.

[29] A. Artur Widera, Fabrice Gerbier, Simon Flling, Tatjana Gericke, Olaf Mandel, and Immanuel Bloch. *New Journal of Physics*, 8(8):152, 2006.

[30] L. Santos and T. Pfau. *Phys. Rev. Lett.*, 96:190404, 2006.

[31] Ákos Rapp, Gergely Zaránd, Carsten Honerkamp, and Walter Hofstetter. *Phys. Rev. Lett.*, 98:160405, 2007.

[32] P. Lecheminant, P. Azaria, and E. Boulat. *Nuclear Physics B*, 798(3):443 – 469, 2008.

[33] A. Recati, P. O. Fedichev, W. Zwerger, and P. Zoller. *Phys. Rev. Lett.*, 90:020401, 2003.

[34] B. Paredes and J. I. Cirac. *Phys. Rev. Lett.*, 90:150402, 2003.

[35] Ryan Barnett, Dmitry Petrov, Mikhail Lukin, and Eugene Demler. *Phys. Rev. Lett.*, 96:190401, 2006.

[36] K.-K Ni, S. Ospelkaus, M. G. H. de Miranda, A. Pe'er, B. Neyenhuis, J. J. Zirbei, S. Kotochigova, P. S. Julienne, D.S. Jin, and J. Ye. *Science*, 332(5899):231–235, 2008.

[37] Alexey V. Gorshkov, Salvatore R. Manmana, Gang Chen, Jun Ye, Eugene Demler, Mikhail D. Lukin, and Ana Maria Rey. *Phys. Rev. Lett.*, 107:115301, 2011.

[38] C. Wu and S.-C. Zhang. *Phys. Rev. B*, 24:155115, 2005.

[39] C. Wu, J. Hu, and S.-C. Zhang. *Int. J. Mod. Phys. B*, 24(03):311 – 322, 2010.

[40] G. Barcza, E. Szirmai, Ö. Legeza, and J. Sólyom. *Phys. Rev. A*, 86:061602, 2012.

[41] J. Jaramillo, S. Greschner, and T. Vekua. *Phys. Rev. A*, 88:043616, 2013.

[42] Arnaud Koetsier, R. A. Duine, Immanuel Bloch, and H. T. C. Stoof. *Phys. Rev. A*, 77:023623, 2008.

[43] F. Werner, O. Parcollet, A. Georges, and S. R. Hassan. *Phys. Rev. Lett.*, 95: 056401, 2005.

[44] M. Fattori, T. Kock, S. Goetz, A. Griesmaier, S. Hensler, J. Stuhler, and T. Pfau. *Nat. Phys.*, pages 765–768, 2006.

[45] Patrick Medley, David M. Weld, Hirokazu Miyake, David E. Pritchard, and Wolfgang Ketterle. *Phys. Rev. Lett.*, 106:195301, 2011.

[46] M Colomé-Tatché, C Klempt, L Santos, and T Vekua. *New Journal of Physics*, 13(11):113021, 2011.

[47] F. Dalfovo, L. Pitaevskii, and S. Stringari. *J. Res. Natl. Inst. Stand. Technol.*, 101 (4):537, 1996.

[48] L. D. Landau and E. M. Lifshitz. *Quantum Mechanics: Non-relativistic Theory*, volume 3 of *Course of Theoretical Physics*. Butterworth-Heinemann, third edition edition, 2003.

[49] Tin-Lun Ho. *Phys. Rev. Lett.*, 81:742 – 745, 1998.

[50] R. Grimm, M. Weidemöller, and Y. B. Ovchinnikov. In *Optical Dipole Traps for Neutral Atoms*, volume 42 of *Advances In Atomic, Molecular, and Optical Physics*, pages 95 – 170. Academic Press, 2000. arXiv:physics/9902072.

[51] J. Dalibard. Collisional dynamics of ultra-cold atomic gases. In M. Inguscio, S. Stringari, and C. Wieman, editors, *Proceedings of the International School of Physics Enrico Fermi, Course CXL: Bose – Einstein condensation in gases*, Varenna, 1998. www.phys.ens.fr/ dalibard/publications/varenna98.pdf.

[52] J. Dalibard, F. Gerbier, G. Juzeliūnas, and P. Öhberg. *Rev. Mod. Phys.*, 83: 1523–1543, 2011.

[53] C. Chin, R. Grimm, P. Julienne, and E. Tiesinga. *Rev. Mod. Phys.*, 82:1225–1286, 2010.

[54] W. Ketterle and M. W. Zwierlein. *Proceedings of the International School of Physics Enrico Fermi, Course CLXIV: Ultracold Fermi gases*, chapter Making, probing and understanding ultracold Fermi gases. Editors: M. Inguscio, W. Ketterle and C. Salomon, Varenna, 2006. arXiv:0801.2500.

[55] G. Thalhammer, G. Barontini, L. De Sarlo, J. Catani, F. Minardi, and M. Inguscio. *Phys. Rev. Lett.*, 100:210402, 2008.

[56] C. A. Regal, M. Greiner, and D. S. Jin. *Phys. Rev. Lett.*, 92:040403, 2004.

[57] N. Bornemann, P. Hyllus, and L. Santos. *Phys. Rev. Lett.*, 100:205302, 2008.

[58] Eduardo Fradkin. *Field Theories of Condensed Matter Physics*. Cambridge, second edition, 2013.

[59] Frank Göhmann. *The One-Dimensional Hubbard Model*, chapter Yangian symmetry of the Hubbard model. Number 14. University Press, 2005.

[60] Yoshio Kuramoto and Yusuke Kato. *One-Dimensional Quantum Systems*. Cambridge, 2009.

[61] F. Bloch. Bremsvermögen von atomen mit mehreren elektronen. *Z. Phys.*, 81 (363), 1933.

[62] P. Jordan. Lichtquant und neutrino. *Z. Phys.*, 93/98/99/102/105/105 (464/759/109/243/114/229), 1935/1936/1936/1936/1937/1937.

[63] J. Schwinger. *Phys. Rev. Lett.*, 3(296), 1959.

[64] D. C. Mattis and Lieb E. H. Exact solution of a many fermion system and its associated boson field. *J. Math. Phys.*, 6(375), 1965.

[65] S. Coleman. *Phys. Rev. D*, 11(2088), 1975.

[66] S. Mandelstam. *Phys. Rev. D*, 11(3026), 1975.

[67] F. D. M. Haldane. Effective harmonic-fluid approach to low-energy properties of one-dimensional quantum fluids. *Phys. Rev. Lett.*, 47(25):1840, 1981.

[68] F. D. M. Haldane. 'luttinger's theory' of one-dimensional quantum fluids: I. prospects of the luttinger model and their extension to the general 1d interacting spinless fermi gas. *J. Phys. C: Solid State Physics*, 14:2585–2609, 1981.

[69] A. B. Zamolodchikov and Al. B. Zamolodchikov. *Annals of Phys.(NY)*, 120(253), 1979.

[70] A. A. Belavin, A. M. Polyakov, and A. B. Zamolodchikov. *Nucl. Phys. B*, 241 (333), 1984.

[71] D. Bernard and A. LeClair. *Commun. Mah. Phys.*, 142:99–138, 1991.

[72] F. D. M. Haldane. Luttinger's theorem and bosonization of the fermi surface. In R. Broglia and J. R. Schrieffer, editors, *Proceedings of the International School of Physics "Enrico Fermi", Course CXXI: "Perspectives in Many-Particle Physics"*, pages 5–30, 1993. Arxiv:cond-mat/0505529v1.

[73] P. Di Francesco, P. Mathieu, and D. Sénéchal. *Conformal Field Theory*. Springer, 1997.

[74] A. O. Gogolin, A. A. Nersesyan, and A. M. Tsvelik. *Bosonization and Strongly Correlated Systems*. Cambridge, 1998.

[75] A. Luther and I. Peschel. *Phys. Rev. B*, 9:2911–2919, 1974.

[76] V. W. Scarola, L. Pollet, J. Oitmaa, and M. Troyer. *Phys. Rev. Lett.*, 102:135302, 2009.

[77] Shintaro Taie, Rekishu Yamazaki, Seiji Sugawa, and Yoshiro Takahashi. *Nature*, 8:825830, 2012.

[78] Michael Stone, editor. *Bosonization*. World Scientific, 1994.

[79] A. Imambekov, T. L. Schmidt, and L. I. Glazman. One-dimensional quantum liquids: Beyond the luttinger liquid paradigm. *Rev. Mod. Phys.*, 84(3):1253–1306, 2012.

[80] D. B. Gutman, Yuval Gefen, and A. D. Mirlin. *Phys. Rev. B*, 81:085436, 2010.

[81] P. Lecheminant, E. Boulat, and Azaria P. *Phys. Rev. Lett.*, 95(240402), 2005.

[82] B. D. Esry, H. Suno, and C. H Greene. Ultracold three-body recombination of fermionic atoms. In D. E. Pritchard H. R. Sadeghpour and E. J. Heller, editors, *Proceedings of XVIII International Conference on Atomic Physics*, volume Degenerate Fermi Systems. World Scientific.

[83] Congjun Wu, Jiang-ping Hu, and Shou-cheng Zhang. *Phys. Rev. Lett.*, 91:186402, 2003.

[84] Congjun Wu. *Mod. Phys. Lett.*, 20(1707), 2006.

[85] Howard Georgi. *Lie Algebras in Particle Physics: From Isospin to Unified Theories*, volume 54 of *Frontiers in Physics*. Addison-Wesley, 1982.

[86] D. G. Shelton, A. A. Nersesyan, and A. M. Tsvelik. *Phys. Rev. B*, 53:8521–8532, 1996.

[87] I. Affleck. *Phys. Rev. B*, 43(3215), 1991.

[88] J. Jaramillo, S. Greschner, and T. Vekua. *arXiv:1305.0894v1*, 2013.

[89] Congjun Wu. *Phys. Rev. Lett.*, 95:266404, 2005.

[90] F. H. L. Essler and I. Affleck. *J. Stat. Mech.*, P12006.

[91] E. Berg, E. G. Dalla Torre, Giamarchi T., and Altman E. *Phys. Rev. B*, 245119 (77), 2008.

[92] C. L. Kane and E. J. Mele. *Phys. Rev. Lett.*, 95:146802, 2005.

[93] D. L. Campbell, G. Juzeliūnas, and I. B. Spielman. *Phys. Rev. A*, 84, 2011.

[94] Brandon M. Anderson, I. B. Spielman, and Gediminas Juzeliūnas. *Phys. Rev. Lett.*, 111, 2013.

[95] Y.-J. Lin, K. Jimenez-Garcia, and I. B. Spielman. *Nature*, 471:83–86, 2011.

[96] Pengjun Wang, Zeng-Qiang Yu, Zhengkun Fu, Jiao Miao, Lianghui Huang, Shijie Chai, Hui Zhai, and Jing Zhang. *Phys. Rev. Lett.*, 109:095301, 2012.

[97] Lawrence W. Cheuk, Ariel T. Sommer, Zoran Hadzibabic, Tarik Yefsah, Waseem S. Bakr, and Martin W. Zwierlein. *Phys. Rev. Lett.*, 109, 2012.

[98] M. C. et al Beeler. *Nature*, 498:201–204, 2013.

[99] Masaki Oshikawa and Ian Affleck. *Phys. Rev. Lett.*, 79, 1997.

[100] Michele Fabrizio, Alexander O. Gogolin, and Alexander A. Nersesyan. *Phys. Rev. Lett.*, 83, 1999.

[101] A. P. Kampf, M. Sekania, G. I. Japaridze, and P. Brune. *J. Phys.: Condens. Matter*, 15, 2003.

[102] S. R. Manmana, V. Meden, R. M. Noack, and K. Schönhammer. *Phys. Rev. B*, 70, 2004.

[103] F. Mila. *Eur. Phys. J. B*, 6:201–205, 1998.

[104] Karlo Penc, Jean-Baptiste Fouet, Shin Miyahara, Oleg Tchernyshyov, and Frédéric Mila. *Phys. Rev. Lett.*, 99, 2007.

[105] Thierry Giamarchi. *Quantum Physics in One Dimension*. Oxford University Press, 2003.

[106] Y.-J. Wang. *arXiv:cond-mat/0306365*.

Acknowledgements

A mi familia por sostener mi corazón. A mis maestros en Colombia. To Temo Vekua for his guidance and support. To Luis Santos for his enlightened lectures on cold atoms. I'm specially thankful with Alexander Nersesyan for matters of heaven and earth.

I acknowledge the institutional support from QUEST and the physics department at the Leibniz University of Hannover, and to my former institutions: the Abdus Salam International Centre for Theoretical Physics in Trieste and the Universidad del Valle in Colombia.

Curriculum Vitae

Personal Information

Name Juan Diego Jaramillo Salazar
Date of birth March 28th, 1983
Place of birth Tuluá, Colombia
Citizenship Colombian

Education

2010 - 2014 **Ph.D.**
Leibniz Universität Hannover. Hannover, Germany.

2008 - 2009 **Dipl.-Phys.**
Abdus Salam International Centre for Theoretical Physics. Trieste, Italy.

2001 - 2007 **B.Sc.**
Universidad del Valle. Cali, Colombia.

1988 - 2000 Colegio Salesiano San Juan Bosco. Tuluá, Colombia.

List of Publications

1. J. Jaramillo, S. Greschner, and T. Vekua, *Band-to-Mott insulator transformations in four-component alkali-metal fermions at half-filling,* Phys. Rev. A 88, 043616 (2013).

2. G. Sun, J. Jaramillo, L. Santos, and T. Vekua, *Spin-orbit coupled fermions in ladder-like optical lattices at half-filling,* Phys. Rev. B 88, 165101 (2013).

Other publications of the author:

1. Juan D. Jaramillo and John H. Reina, *Temporal Resources for Global Quantum Computing Architectures,* Brazilian Journal of Physics Vol. 38, n.4 (2008).

Selbstsändigkeitsearklärung

Hiermit versichere ich, die vorliegende Doktorarbeit selbstsändig und unter ausschliesslicher Verwendung der angegebenen Hilfsmittel angefertigt zu haben.

Hannover, den 23. April 2014

Juan D. Jaramillo